Electrodialysis in flow injection systems

by

Cornelius Johannes Hattingh

Submitted in partial fulfilment of the requirements of the degree

Philosophiae Doctor

in the Faculty of Science

University of Pretoria

Pretoria

October 1999

Summary

Electrodialysis in flow injection systems

by

Cornelius Johannes Hattingh

Supervisor: Professor JF van Staden

Department of Chemistry

University of Pretoria

Degree: Philosophiae Doctor

Flow injection analysis (FIA) is a continuous flow technique developed in the early 1970's. FIA is based on reproducible sample injection, accurate timing and controlled dispersion. This technique is very versatile due to the control of the variables and can easily be automated. This technique is very suitable for routine laboratory analysis. By introducing various sample modifying techniques in tandem with the FIA system, samples can easily be modified. Some modifying techniques are analyte pre-concentration, sample dilution and sample cleanup. Passive dialysis can be used very successfully for sample dilution and cleanup. Problems arise when samples with low analyte concentration have to be analysed. For this reason an electrodialyser unit, equipped with a passive membrane, was developed. The history, development and theory of membranes and membrane processes are discussed. A study of the movement of ions, in solution and across a passive membrane, under the influence of an applied d.c. electrical potential is given. Passive

membranes were evaluated for use in the proposed system. The following factors influencing the efficiency of electrodialysis in the FI system were studied: The flow rate of the donor and acceptor channels; the applied d.c. electrical potential; injection loop volumes; flow direction in the electrodialyser unit. An investigation was done into on-line analyte pre-concentration and regulated dilution probabilities of the electrodialysis system. Systems that were evaluated are the following: The determination of chloride in water effluents; The determination of copper and zinc in pharmaceuticals; The direct and indirect determination of phosphate in fertilisers. A comparative study between the advantages and disadvantages of the passive dialysis and electrodialysis system is given.

UNIVERSITEIT VAN PRETORIA
UNIVERSITY OF PRETORIA
YUNIBESITHI YA PRETORIA

Elektrodialise in vloei inspuit sisteme

deur

Cornelius Johannes Hattingh

Voorgelê ter vervulling van 'n deel van die vereistes vir die graad

Philosophiae Doctor

in die Fakulteit Natuurwetenskappe

Universiteit van Pretoria

Pretoria

Oktober 1999

Samevatting

Elektrodialise in vloei inspuit sisteme

deur

Cornelius Johannes Hattingh

Studieleier: Professor JF van Staden

Departement Chemie

Universiteit van Pretoria

Graad: Philosophiae Doctor

Vloei inspuit analise (VIA) is 'n kontinue vloeitegniek wat aan die begin van die 1970's ontwikkel is. VIA is gebaseer op herhaaldelike monsterinspuiting, akkurate tydmeting en gekontroleerde dispersie. Hierdie tegniek is baie veelsydig weens die beheer van veranderlikes. Hierdie tegniek kan ook maklik ge-outomatiseer word. Hierdie tegniek is verder baie toepaslik vir gebruik in roetine laboratoria. Deur verskeie monstermodifikasie tegnieke in die VIA sisteem in te sluit kan monsters verander word om die sisteem se toepassing te optimiseer. Somige modifikasietegnieke sluit in die analiet prekonsentrasie, monster verdunning en suiwering van monsters. Passiewe dialise kan met sukses vir monster verdunning en suiwering aangewend word. Probleme onstaan egter indien die analiet konsentrasie reeds laag is. Om hierdie rede is 'n elektrodialiseerder, wat toegerus is met 'n passiewe membraan, ontwikkel. 'n Kort inleiding rakende die onwikkeling van die analitiese proses word gegee. Die geskiedenis, onwikkeling en teorie van membrane en

membraanprosesse is bespreek. 'n Studie van die beweging van ione, in 'n oplossing en oor 'n passiewe membraan, onder die invloed van 'n toegepaste direkte stroom elektriese potensiaal is gedoen. Passiewe membrane vir gebruik in die voorgestelde elektrodialiseerder is ge-evalueer. Die volgende faktore wat die effektiwiteit van elektrodialise in die VI sisteem beïnvloed, is bestudeer: die vloeitempo van die skenker- en ontvangerstrome; die toegepaste direkte stroom spanning; die inspuit volumes; vloeirigting in die elektrodialiseerdereenheid. 'n Ondersoek na analiet prekonsentrasie en beheerbare aanlynverdunnings deur die elektrodialise sisteem is uitgevoer. Die volgende sisteme is ge-evalueer: Die bepaling van chloried in afvloeiwater; die bepaling van koper en sink in farmaseutiese produkte; die direkte en indirekte bepaling van fosfaat in kunsmis. 'n Verglykende studie van voor- en nadele van passiewe en elektrodialise word gegee.

Hierdie werk is opgedra aan my vrou

Elsa

ACKNOWLEDGMENTS

I wish to acknowledge with thanks the significant contributions of the following people:

1. Jesus Christ, since I can do all things through Christ who strengthens me.

2. Prof J F van Staden (supervisor), for his excellent academical leadership, positive criticism and motivation during the project.

3. Mr R Dumas, for his technical assistance with the building of some parts of the instrumentation.

4. Ms Carol du Sautoy and Ms Niam Rampersadh who read parts of the manuscript and offered numerous helpful suggestions and corrections.

5. Ms Karin van der Merwe who helped with the typing of Chapter 3.

6. All my friends at Medunsa, University of Pretoria and the University of the North for their moral support.

7. My parents, Koos and Rina Hattingh, for their support (morally and financially) and motivation, not only during this project, but also during all my previous years of study.

8. To my dear wife, Elsa. Thank you very much for your support, understanding and sense of perseverence which carried me through the last part of my studies.

Electrodialysis in flow injection systems

Chapter 1

Introduction

1.1 The Analytical process.

The analytical process can be defined as the set of operations separating the untreated, unmeasured sample from the results expressed as required in accordance with the "analytical black box". Figure 1.1 indicates the three basic stages of this process. [1]

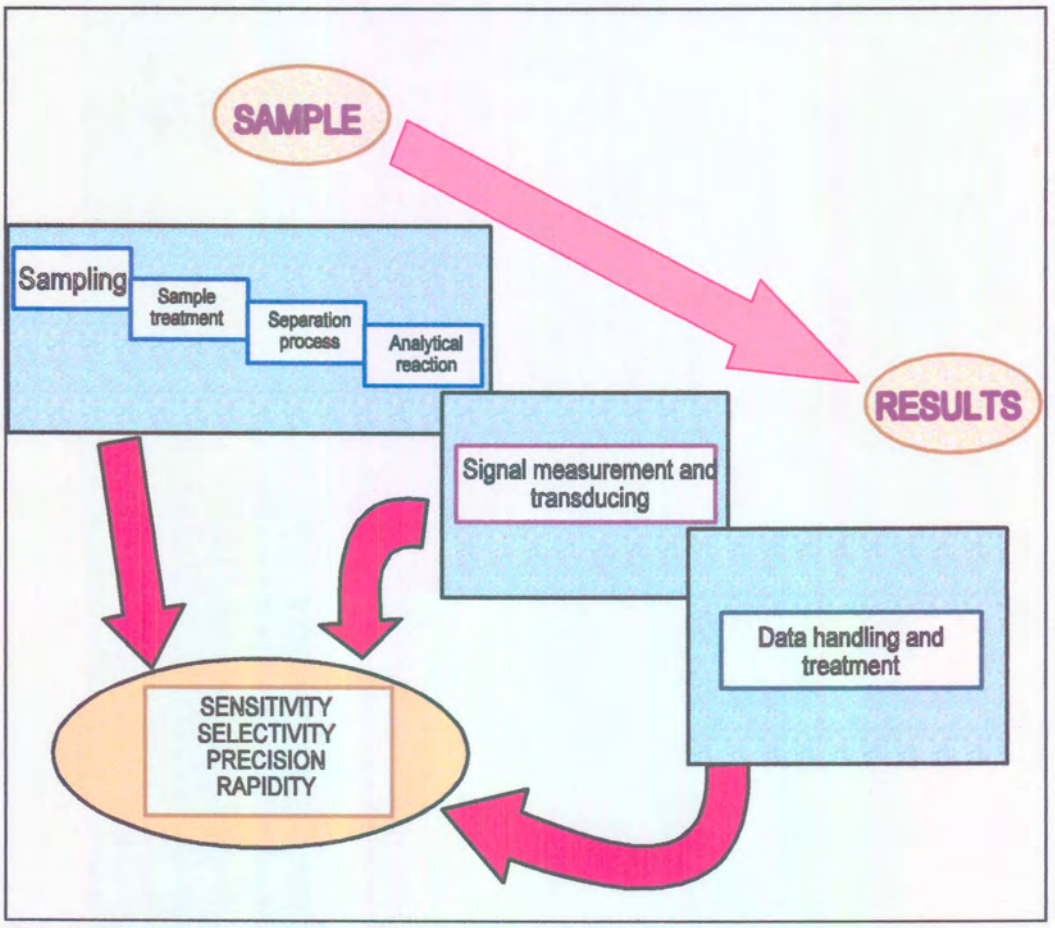

Figure 1.1 General stages of the analytical process.

Notwithstanding the fact that each stage of the analytical process might determine its overall efficiency in every specific situation, the basic features of virtually every analytical methodology are affected by all three stages. [1]

1.2 Analytical chemistry and the need for automation.

Looking back to the not so distant past, it is impossible to mention all the researchers names in the field of instrumental analytical chemistry. Besides the analytical chemistry that developed, there was a need to make analytical chemistry in practice easier and more streamlined. For this reason instrumentation was developed to help the analyst with the number of samples that had to be analysed. Each year the quest for more samples in less time increased and man had to get help from a source which decreased the analysis time and increase the certainty of measurement, and saved on manpower.

Like many other branches of science and technology, analytical chemistry has experienced an enormous expansion in the last few decades of the twentieth century, promoted by scientific advances in general and by the occasionally pressing demands of a permanently, almost frantically changing society. All trends in analytical chemistry have an essential common aim, namely improving on the existing levels of such basic analytical features as sensitivity, selectivity, precision, rapidity, reliability, scope of application, analytical costs, versatility and sample throughput. [1]

The services of the analytical chemist are constantly increasing as more and better analytical tests are developed, particularly in the environmental and clinical laboratories. The analyst often must handle large number of samples and/or process vast amounts of data. Instruments are available that will automatically perform many or all of the steps of an analysis, greatly increasing the load capacity of the laboratory. The data generated can often be processes by the computer techniques; computers may even be interfaced to the analytical instruments. [2]

1.2.1 Flow-based techniques used for analysis

The history of flow-based techniques is well known to most people interested in the field. The concept of injecting a sample directly into a continuous-flow system, and then monitoring it on a continuous base, has been known since 1952. [3, 4] Skeggs's development of the segmented flow system in 1957, which led to the Auto Analyser, was one of the first automated pieces of equipment for general use in clinical and other laboratories. [5] In the late 1960's and early 1970's a new method in flow-based systems, the so called Flow Injection Analysis (FIA) technique, was developed. FIA led to dramatic improvements in the speed and quality of analysis.

Flow injection analysis has established itself nowadays as one of the methods of choice in various fields as an analytical technique which is suitable for automation and increasing sample output in most analytical laboratories. FIA is well documented in more than 5900 papers up to 1997. Since the early 1970's there was a rapid increase in the number of publications up to 1986 whereafter the publications per year stabilised around 500 per year. [6] FIA has been used to automate wet chemical techniques to improve analysis time, and quality and the reproducibility of the analysis.

1.2.2 Separation techniques

Separation and trace enrichment are two of the most fundamental steps in analytical chemistry. With increasing demand for fast and accurate analysis, it is not surprising that the automation of separation processes should play a major role. Separation is performed frequently on soluble species in solution.

Through the ages man has been aware of the importance of separating the valuable from the less valuable in nature's mixtures. This trait has persisted; it is difficult to single out an area of science or a science-based industry where separations do not play an important role. [6]

Separations can be very tedious and can be very labour intensive. For this reason separation, if possible, must be a part of the automation process.

The word separation classically conjures up a model of removing one component or species form a second component. [7] An analytical separation can be described as a process which is responsible for the separation of a mixture into at least two parts of different composition. The purpose of such a separation is to enrich the one fraction with at least one of the components of the mixture in comparison to the other components. To execute such a separation implies that two components must be separated from each other. For this reason transport (removal), which is differential in nature, must be part of the system. [8]

It is worth remembering that separation can only be achieved by exploiting differences between the components of mixtures. These differences may be of a physical nature such as variations in mass, density, size, shape, vapour pressure, or of a chemical nature such as differences in solubility or adsorption characteristics. A separation process may exploit either physical or chemical differences to effect separation, and in some cases a combination of these

factors are used to achieve the desired level of separation. [9]

Sample treatment (of which a separation process can be one of the processes involved) is one of the preliminary steps of the analytical process. It is therefore important to know that analytical separation techniques play a very important role in today's analytical chemistry. Separation techniques are one of three primary ways (the other two are chemical reactivity and signal discrimination) of achieving or enhancing selectivity. (Application of chemometric techniques further enhances selectivity in most instances). [1]

From a more practical view, separation techniques can be classified according to operativeness and efficiency into chromatographic and non-chromatographic techniques. The main thrust of this thesis will be concerned with the non-chromatographic separation techniques. Chromatographic techniques distinguishes itself from the non-chromatographic techniques due to the presence of not only a mobile phase but also a stationary phase for separation of the various analytes. This type of separation is characterised by the occurrence of at least the flow of one of the phases involved in the mass transfer. The implementation of non-chromatographic separation techniques relies on the principles behind, and developments in the field of automatic continuous analysers, both air-segmented and unsegmented. A continuous separation system can give rise to various types of interface across which mass transfer can take place (gas/liquid, liquid/liquid and liquid/solid).

The second phase, which collects the analytes or interferents, can be introduced into the system in a direct fashion (dialysis, liquid-liquid extraction or gas diffusion) or be a part of the separation system (e.g. the active material in a sorption micro column). Also, this second phase can be generated *in situ* by physical change (distillation), chemical change (precipitation) or a combination of the two.

Dynamic separation systems typically use continuous on-line detection systems through which the stream of the phase carrying the analyte are driven after separation.

1.2.2.1 Diaysers in FIA systems acting as sample pretreatment tools

The technique of mass transfer in on-line analytical dialysers has been employed in continuous flow systems with gas-diffusion and dialysis membranes for many years, particularly in routine clinical laboratories. There are a number of thorough and authoritative reviews of the early history of membrane science and all the details are not repeated here. One of the milestones in this regard is a review by Londsdale [11] in the growth of membrane technology up to 1982. Another article worth mentioning is the review article by Van Staden [12], which gives a detailed overview of the use of membranes in FIA systems.

Dialysis is a technique based on a diffusion process which involves the selective separation of sample species through a semi-permeable membrane. The technique can be divided into passive dialysis and active (or Donnan) dialysis. The classification of dialysis processes as passive or active (Donnan) depends on the nature of the membrane [1, 17]. In the passive process a neutral membrane differentiates between separations on a molecular scale with a preciseness of molecular order allowing species within a given range of molecular mass to diffuse across a neutral membrane. In active (Donnan) dialysis (see the definition and a detailed explanation in chapter 2), ions with a given type of charge are transferred across an ion-exchange membrane. Passive dialysis is a highly efficient molecular filter, but was found to be inefficient in terms of solute diffusion rates (0 - 7%) across a semi-permeable membrane. [12, 13].

Active Donnan dialysis is a promising technique for the preconcentration, recovery and speciation of ionic species, but with a limitation in the amount of

mass transfer of species through the membrane. Cox *et al.* [14, 15] have worked for many years on sample preparation on an analytical scale using Donnan dialysis, employing the technique for matrix normalization [14] and sample preconcentration [15].

According to Van Staden [12], the main use of the passive membrane in FIA systems relation is in-line sample dilution. Other methods of in-line sample dilution were also studied but are beyond the scope of this study. [16 - 21] Dilution can be advantageous in the sense of in-line sample preparation but, what about samples with already low analyte concentrations? Work has been done by Van Staden and Hattingh to circumvent the dilution effect and still retain the other advantages of the dialysis system (for example in-line sample cleanup). [22] In this work, a passive dialysis unit was incorporated into a dialysis system and the dialysate was concentrated on an ion-exchange resin. The detection limits decreased dramatically but at the expense of experimental time. This led to the search for a way in which one can lower the detection limit, have a rather short experiment time and at the same time retain all the advantages of the dialyser in the FIA system. Much work has been done on the use of electrodialysers, but most of this work is concerned with the use of ion-exchange membranes and also not as an analytical tool.

As the name implies, electrodialysis (ED) is a dialytic process in which an applied electric field is used to force ions through a membrane [23]. The main driving force which impels ions through the membrane is the potential gradient across the membrane. So far ion separation is affected through the use of selective ion-exchange membranes. In practical ED, many selective membranes are placed perpendicularly in the path of the electrical field. In all the research work reported to date [11, 23 - 26], conventional ED utilized ion-exchange membranes. ED with ion-exchange membranes was also utilized as suppressors in ion chromatography [29, 30] and for electrodialytic neutralization of samples prior to analysis in ion chromatography [29, 30]. The electrodialyser

units described by Cooper et al. [25] were designed with three compartments; a feed solution containing the sample was placed in a channel between a cation exchange membrane on the one side and an anion exchange membrane on the other side. Ions from the sample channel permeate under the influence of an electric field to the respective corresponding acceptor channels.

ED is a membrane-based separation technique that is also appealing because of its capability to deionize one stream while concentrating the electrolytes in another stream. ED therefore produces a purified stream that can either be discharged or reused and a concentrated electrolyte stream that can be disposed of or processed for reclamation of the dissolved salt. In most of these electrodialyser units, cation- and anion-permeable ion-exchange membranes were arranged in an alternating pattern. The series of cells became alternately diluting and concentrating compartments when a direct current was passed through the system. These stacks were mostly employed in desalination systems and industrial applications. Some applications of ED include desalination of brackish waters, desalting of whey and stabilisation of wine, purification of proteins solutions, recovery of metals from plating of rinse waters, recovery of acids, recovery of heavy metals from mining mill processes and the treatment of cooling-tower blowdown for water recovery and effluent volume reduction. [23, 24, 25, 26]

A literature survey showed that, to date, ED has only been exploited to a very limited extent in flow injection systems. ED has been reported for the separation of alanine and aspartic acid [31] and for extraction of ephedrine from spiked plasma [32]. [33] reported an application for the separation of leucine from ketoleucine during flow injection analysis with leucine dehydrogenase. The selectivity for L-amino acids in flow injection analysis was enhanced using ED with amino acid oxidation [30]. Conventional ED configurations [25] using cation- and anion-exchange membranes were employed in all the applications to date.

Although there is a perception in certain circles [29], that passive dialysis through a neutral membrane is a slow process requiring a large volume of sample, it has been reported [1, 12, 34], that membrane separation with passive dialysis is one of the most successful separation techniques in flow analysis. It was thought to combine the advantages of the passive dialysis system with that of the electrodialysis system. To obtain this result, an electrodialyser was designed which consisted of two compartments where a passive neutral membrane is incorporated between two channels (a donor and an acceptor) of the conduits of an FIA system, using the same dialyser configuration as in conventional dialysis. By using this concept it can be possible to enhance the transfer of certain sample components through a passive neutral membrane.

1.3 Objective of the project

From the foregoing paragraph it is obvious that there is an urgent need for the further development of tools to streamline the analytical procedure. Automation is one of the key concepts for the development of such tools. Flow injection analysis (FIA) in general lends itself to a great extent to be automated. One of the means by which FIA was made more streamline, as was mentioned in the previous paragraphs, is the introduction of a tools for in-line sample preparation. The tools of interest include the following;

i. The dialyser unit equipped with a passive membrane for sample dilution and sample cleanup (separation).
ii. Donnan dialysis for sample speciation and preconcentration.
iii. Electrodialysis for the enhanced migration of charged species and the separation thereof.

By building a hybrid of the above mentioned tools, a new tool was envisaged to circumvent the disadvantages of the individual tools and enhance the advantageous points. By introducing a passive membrane into an electrodialyser unit, one should be

able to increase the mass transport of charged species across the membrane, thus a massive increase in the percentage dialysis can be expected. Furthermore a speciation of species due to different charges can be expected. Sample cleanup can be enhanced. It will be possible to remove interfering species to a great extent if there is a charge difference between the analyte and the interfering species. Since the proposed electrodialyser will operate in-line in the FIA system, automation will easily be introduced.

In the experimental chapters to follow, the planning, building, introduction into the FIA system, problems experienced and the solutions thereof will be discussed of the newly developed hybrid dialyser.

1.4 References

1. Valcárcel M., Luque de Castro M.D., (**1991**) Non-chromatographic continuous separation techniques. The Royal Society of Chemistry.
2. Christian G.D., (**1994**) Analytical Chemistry. John Wiley & Sons Inc. NY.
3. Mottola H.A. (**1981**) Anal. Chem. 53: 1313A.
4. Stanley R., (**1984**) J. Autom. Chem. 6(4):175.
5. Snyder L., Levine J., Stoy R., Conetta A. (**1976**) Anal. Chem. 48: 942A.
6. Radu G.L., Tanase I., Baiulescu G.E., (**1998**) Current Trends in Analytical Chemistry, Volume 1. (Invited lecture of J.F. van Staden at the XIVth National Conference on Analytical Chemistry, Piatra Neamţ, Romania, 24-26 September 1998)
7. Perry E.S., (**1968**) Progress in Separation and Purification, Volume 1. Interscience Publishers.
8. Scott K., Hughes R., (**1996**) Industrial Membrane Separation Technology. Blackie Academic & Professional.
9. Miller J.C., Miller J N., (**1988**) Statistics for Analytical Chemistry, Second edition. Ellis Horwood limited.
10. Setford S.J., (**1995**) A Basic Introduction to Separation Science. Rapra Technology Limited.
11. Chen D., (**1991**) Lab. Rob. Autom. 3(3): 125.
12. Lonsdale H.K., (**1982**) J. Membr. Sci. 10: 81.
13. Van Staden J.F., (**1995**) Fresenius J. Anal. Chem. 352: 271.
14. Grimsrud L., Babb A.L., (**1996**) Chem. Eng. Progr. Symp. Ser. 19: 62-66.
15. Cox J.A., Twardowski Z., (**1980**) Anal. Chim. Acta 119: 39.
16. Cox J.A., Dabek-Zlotorynska E., Saari R., Tanaka N., (**1988**) Analyst 113: 1401.
17. Israel Y., Barnes R.M., (**1990**) Analyst. 115: 1411.
18. Jaccintho A.O., Zagatto E.A.G., Reis B.F., Passedena L.C.R., Krug F.J. (**1981**) Anal. Chim. Acta. 130: 361.
19. Růžička J., Hansen E.H. (**1983**) Anal. Chim. Acta. 145: 1.

20. Whitman D.A, Christian G.D. (**1989**) Talanta 36: 205.
21. Tyson J.F., Bysouth S.R. (**1988**) J. Anal. At. Spectrom. 3: 211.
22. Garn M.B., Gisin M., Gross H., King P., Schmidt W., Thommen C. (**1988**) Anal Chim Acta. 207: 225.
23. Van Staden J.F., Hattingh C.J. (**1995**) Anal. Chim. Acta. 308: 214.
24. Schoeman J.J., Steyn A., (**1995**) Evaluation of membrane technology for electroplating effluent treatment. WRC report no 275/1/95.
25. Cooper J.C., Danzer J., Schmidt H.L., (**1993**) Anal. Chim. Acta 282: 369.
26. Spiegler K.S., (**1996**) Principles of Desalination, Academic Press, London.
27. Schoeman J.J., (**1992**) Electrodialysis of salts, acids and bases by electro-osmotic pumping. PhD-thesis, University of Pretoria.
28. Strong D.L., Dasgupta P.K., (**1989**) Anal. Chem. 61: 939.
29. Rabin S., Stillian J., Barreto V., Friedman R., Toofan M., (**1993**) J. Chromatogr. 640 97.
30. Haddad P.R., Laksana S., Simons R.G., (**1993**) J. Chromatogr. 640: 135.
31. Haddad P.R., Laksana S., J. (**1994**) Chromatogr. 671: 131.
32. Strathmann H., Chmiel S., (**1984**) Chem.-Ing.-Tech. 56: 214.
33. Debets A.J.J., Kok W.Th, Hupe K.P., Brinkman U.A.Th., (**1990**) Chromatographia 30: 361.
34. Kittsteiner-Eberle R., Ogbomo I., Schmidt H.L., (**1989**) Biosensors 4 (1989) 75.
35. Fang Z., (**1993**) Flow injection separation and preconcentration, VCH, Weinheim.

Chapter 2

Introduction into Membranes and Membrane processes

2.1 Introduction

Over the past four decades or so the growth of several new industries, based on membrane technology, has observed. It is a highly fragmented technology, covering such wide-ranging applications as reverse osmosis (RO), gas separations, controlled-release pharmaceutical formulations and the artificial kidney. The scientific and engineering disciplines involved are also varied, and include physical and polymer chemistry, electrochemistry and chemical engineering. [1]

2.2 Definition of a Membrane and a Membrane process

Before discussing all the membrane processes in detail, it is imperative that one should have a sound knowledge of what a membrane and a membrane process implies.

As can be seen from paragraph 2.1, there are a wide variety of uses and applications for membranes in general. The difficulty in defining a membrane resides in the variety of uses and applications. The general definition of a membrane was also a problem HK Lonsdale experienced in an issue of *Journal of membrane science*. [2] In this mentioned article, Lonsdale put this question to various groups and individuals who are well established in the membrane field of operation or research. Following are some of comments that he received:

> *"A membrane can be regarded as a phase or group of phases that controls the transport of matter and energy between two essentially uniform phases which separates it."* ***(Patric Meares)***

> *"A membrane is a permeable barrier characterised by flux and selectivity properties that provide functional transport across the partition."* ***(Harvey***

Hoehn)

> *"A membrane is a barrier film that allows selective and specific permeation under conditions appropriate to its function." (**Ashok K Vijh**)*
>
> *"A membrane is an interphase. It has distinct physicochemical properties and it is bounded by two surfaces, each of which joins it to a contiguous bulk phase. Generally it is "thin" in the sense that it has a large ratio of surface area to volume; as its thickness approaches molecular dimensions the interphase becomes an interface. The special separative/barrier/contacting properties of membranes derive from the fact that an interphase can communicate simultaneously with its two adjacent phases; this permits the establishment and maintenance of gradients across the membrane and allows exchange to occur at both surfaces. Thus, when viewed as a contacting device a membrane has an additional degree of freedom over conventional bulk phase operations which have but one bounding surface and it is this feature which is unique to membranes." (**John A Quinn**)*

As can be seen, all the answers given, can be reduced to a basic definition that includes all its applications and uses and it can be given as follows:

> *"A membrane is a thin barrier between two phases which restricts the movement of one or more components of one or both phases across the membrane barrier."* [3]

Membrane processes are an integral part of our every day life, for example: Every day over 20 million litres of brackish water are pumped out of the ground near Jeddah in Saudi Arabia and passed through thin sheets of cellulose acetate in a process known as reverse osmosis before being used as part of the city's water supply. Orange juice can be concentrated by membranes to make a concentrate which retains more of the

flavour than does evaporation. Milk can be concentrated slightly by means of a membrane before making cheese in a process which produces no whey. Gasses rising from the ground in a waste tip can be piped away and the carbon dioxide separated from the methane by a membrane process allowing the methane then to be used as a fuel, simultaneously saving energy and reducing the greenhouse effect since methane is more effective as a greenhouse gas than carbon dioxide. In all of these processes materials are separated by a semi-permeable membrane which allows the passage of one or more of the materials much more readily than the others. [3]

A membrane process requires two bulk phases physically separated by a third phase, the membrane. The *membrane* as the definition implies, is an interphase between two bulk phases which can either be a homogeneous phase or a heterogeneous collection of phases. The membrane phase may either be one or a combination of the following:

- Nonporous solid.
- Microporous or macroporous solid with a fluid (liquid or gas) in the pores.
- A liquid phase with or without the second phase.
- A gel. [4]

Membranes are primary used for separation and membrane processes are generally separation processes. Large scale commercial uses of membrane separations have displaced conventional separation processes. More of these displacements are expected in the future, for one since membrane separation processes are more energy and capital efficient than the conventional separation processes. [3, 4]

The membrane phase (or membrane), interposed between two bulk phases, controls the exchange of mass between the two bulk phases by means of a membrane process. In membrane separation processes the bulk phases are mixtures. One of the species in the mixture is allowed to be exchanged in preference to the others, in other words, the membrane is selective towards one of the species in the mixture. The one bulk

phase is then enriched with this species whilst the other is depleted thereof. *A membrane process thus is the selective and controlled transfer of a species from one bulk phase to the other.* [4]

A membrane may discriminate between two species because of difference in size, shape or chemical structure, and the separation will be achieved only to a *limited* extent. The membrane will *never* be able to separate the mixture completely. The separation of substances which mix spontaneously can be accomplished by some device which consumes energy supplied in the form of heat or mechanical work. The basic principle of any membrane or separation process is that a certain amount of energy is required to accomplish the separation. Two substances will mix spontaneously when the free enthalpy of the mixture is smaller than the sum of the free enthalpies of the pure substances. The minimum amount of energy (W_{min}), necessary to accomplish complete separation is at least equal to or larger than the free enthalpy of mixing. [4]

$$W_{min} \geq \Delta G_m = \Delta H - T\Delta S$$

Before discussing some membrane separation processes in more detail, a short key in the form of a table can serve to distinguish between the different processes (Table 2.1).

Table 2.1 A short key into some membrane processes

Membrane Process	Separation potential for	Driving force	Preferably permeating component
Reverse osmosis	Aqueous low molecular mass solutions	Pressure difference	Solvent
Ultrafiltration	Macromolecular solutions, emulsions	Pressure difference	Solvent
Microfiltration	Suspensions, emulsions	Pressure difference	Continuous phase
Gas permeation	Gas mixtures, water vapour/gas mixtures	Pressure difference	Preferably permeating component
Pervaporation	Aqueous/organic mixtures	Ratio of partial pressure to saturation pressure	Preferably permeating component
Liquid membrane	Aqueous low molecular mass solutions	Concentration difference	Solute
Osmosis	Aqueous solutions	Concentration difference	Solvent
Dialysis	Aqueous solutions	Concentration difference	Solute
Electrodialysis	Aqueous solutions	Electric field	Solute (ions)

2.3 Introduction to some of the membrane processes

There are quite a number of different membrane processes. Since there is no real cut-off point between the different membrane processes, (and the fact that some of them are very closely interrelated [4 -6]) the following very important and related processes will be discussed.

2.3.1 Osmosis

Osmosis, for this project, is most probably the second most important membrane process due to the fact that osmosis it is always accompanied by dialysis in real membranes. (Dialysis cannot take place if osmosis doesn't take place at the same time) [4 - 7]

Osmosis is a natural phenomenon in which water passes through a

semipermeable membrane from the one side with lower solute concentration to the higher solute concentration until equilibrium of solvent chemical potential is restored. At equilibrium the pressure difference between the two sides of the membrane is equal to the osmotic pressure difference. The solvent is transported through the membrane as a result of a difference in trans-membrane concentration. [4 -7]

2.3.2 Pressure driven Membrane Processes

The characteristic of these processes is that the solvent is the continuous phase and that the concentration of the solute is relatively low. Various processes, related to the particle size of the solute and consequently to membrane structure, can be distinguished. These processes are:

- Microfiltration
- Ultrafiltration
- Nanofiltration/Reverse osmosis

The principle of these three processes is illustrated in Figure 2.1.
Due to the driving force, namely applied pressure, the solvent and various solute molecules permeate through the membrane, whereas other molecules or particles are rejected to various extents dependent on the structure of the membrane. Upon comparing the three mentioned processes, in order from microfiltration, ultrafiltration to reverse osmosis,[1] the size (or the molecular mass) of the particles separated, diminishes and consequently the pore sizes (for the separation of these particles) in the membrane must also become smaller. This implies that the resistance of the membranes to mass transfer increases and hence also the applied pressure to obtain the same flux. [5]

---

1. *It should be note that no clear-cut distinction can be drawn between the various pressure driven membrane processes.*

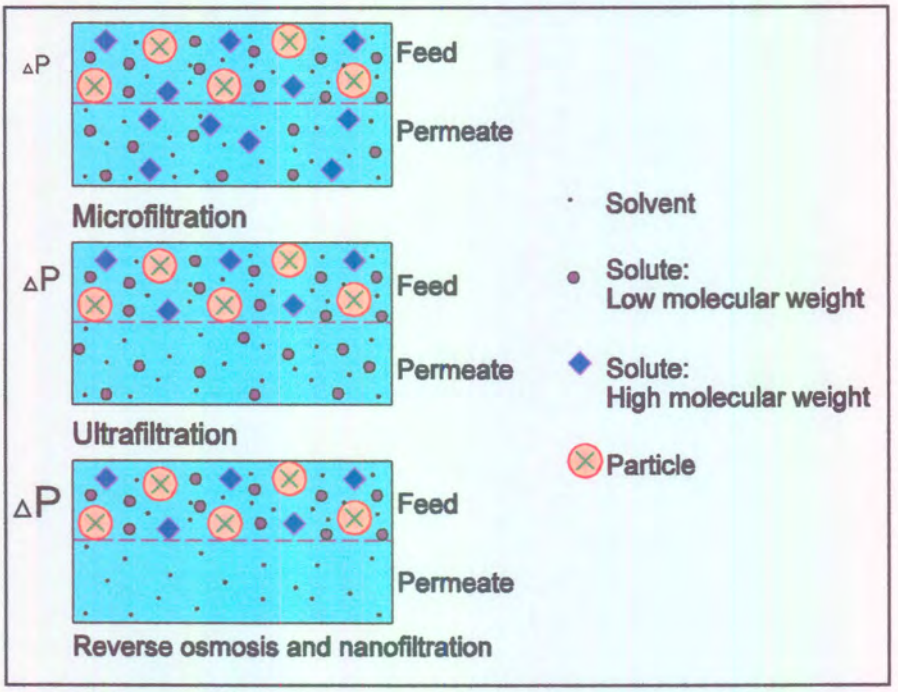

Figure 2.1 *Schematic representation of some pressure driven membrane processes*

2.3.2.1 Microfiltration

Microfiltration is the membrane process which most closely resembles conventional coarse filtration. The pore sizes of microfiltration membranes range from 10 - 0.05 µm, making this process suitable for retaining suspensions and emulsions. [5]

Applications of microfiltration include the following: [6]

- Concentration and /or washing of various colloidal suspensions.
- Separation of emulsions (oil-polluted industrial effluents).
- Pre-treatment for reverse osmosis plants.

2.3.2.2 Ultrafiltration

The nature of ultrafiltration lies between microfiltration and reverse osmosis. The pore size varies between 0.05 µm and 1 nm. Ultrafiltration is typically used to retain macromolecules and colloids from a solution, the lower limit being solutes with molecular weights of a few thousand. For both microfiltration and ultrafiltration, the retention is determined by the size and the shape of the solutes relative to the pore size in the membrane. The transport of the solvent through the membrane is directly proportional to the applied pressure. [5]

The relatively large pores used for ultrafiltration (in comparrison to reverse osmosis) allow both ionic and high molecular weight organic materials to pass through the membrane into the permeate stream. In metal finishing operations, ultrafiltration is typically employed to concentrate emulsified oils from rinses or to recover valuable detergents from cleaning rinse waters. In general osmotic pressure is not a problem when using ultrafiltration and the only energy requirements stems from running a low-pressure pump. Some general applications for ultrafiltration includes the following:

- Cleaners for one-piece steel and aluminum cans.
- Rinses for strip coil coating.
- Cleaning rinses for automobile and aircraft chassis.
- Coolant recovery. [9]

2.3.2.3 Nanofiltration/Reverse Osmosis

The first work in reverse osmosis towards water desalting was undertaken by Reid and his students at the university of Florida in the mid 1950s. This group made use of synthetic polymeric membranes which led to very low fluxes due to the fact that the thinnest these membranes could be cast without any imperfections was about 6 μm. Only in the late 1950s cellulose acetate fibres

were used which had much higher fluxes than the synthetic polymeric membranes. At about the same time Loeb and Sourirajan discovered a way to prepare very thin cellulose acetate membranes. This method is still in use today for the preparation of water desalination reverse osmosis membranes.

The process of reverse osmosis can be explained by Figure 2.2. Applied pressure is used to reverse the "normal" direction of water flow across a semipermeable membrane. If a pressure ($\triangle P$) is applied to the concentrated solution just equal to the osmotic pressure difference between the two solution ($\triangle \pi$), water flow ceases (or there is no nett flow of water) and osmotic equilibrium. At a higher pressure ($\triangle P > \triangle \pi$), water will flow from the concentrated to the dilute solution.

A high-pressure pump forces pure water (permeate/solvent) through the membrane that has the capability to reject salts and organics. As more permeate is removed from the feed stream, the remaining dissolved materials become more concentrated. [9]

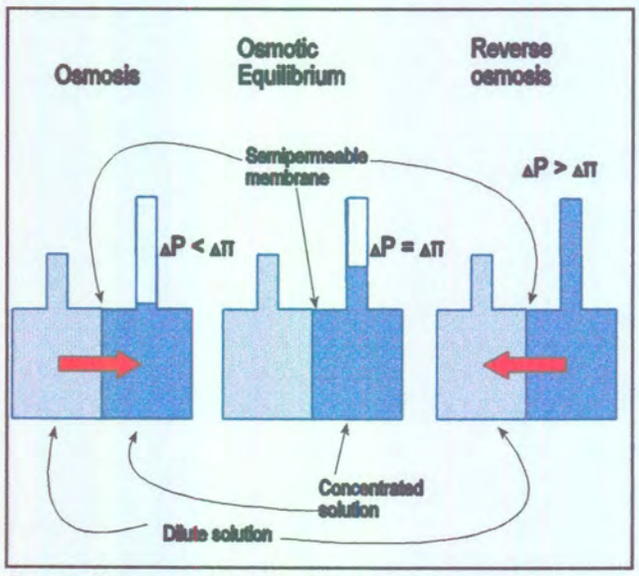

Figure 2.2 Osmotic phenomena.

If a trans-membrane pressure difference greater than that corresponding to osmotic equilibrium is applied to the test cell, then the solvent flux can be reversed so that the solution with the greater concentration is further concentrated. The reversal of the flux then is a direct reason for the name *reverse osmosis.* [6]

Nanofiltration and reverse osmosis are used when low molecular weight solutes such as inorganic salts or small organic molecules such as glucose and sucrose have to be separated from a solvent. Both these processes are considered as one process since the basic principles are the same. The difference between nanofiltration/reverse osmosis and the other pressure driven processes is based upon the difference in size of the solute. Consequently, the membranes required for nanofiltration/reverse osmosis systems are more dense with much higher hydrodynamic resistance. These membranes can be considered as being intermediate between open porous types of membranes (microfiltration and ultrafiltration) and dense non-porous membranes (pervaporation/gas separation). Because of these denser membranes, higher membrane resistance will be experienced and accordingly higher pressures must be applied for the same amount of solvent flux through the membrane. [5]

Reverse osmosis (RO) can be sub-divided into three types: [4]

- High pressure RO, 5.6-10.5 Mpa, (seawater desalination).
- Low pressure RO, 1.4 - 4.2 Mpa, (brackish water desalination).
- Nanofiltration or "loose" RO, 0.3 - 1.4 Mpa

Organic rejection depends on membrane polymer types and structures as well as membrane / solute interactions.

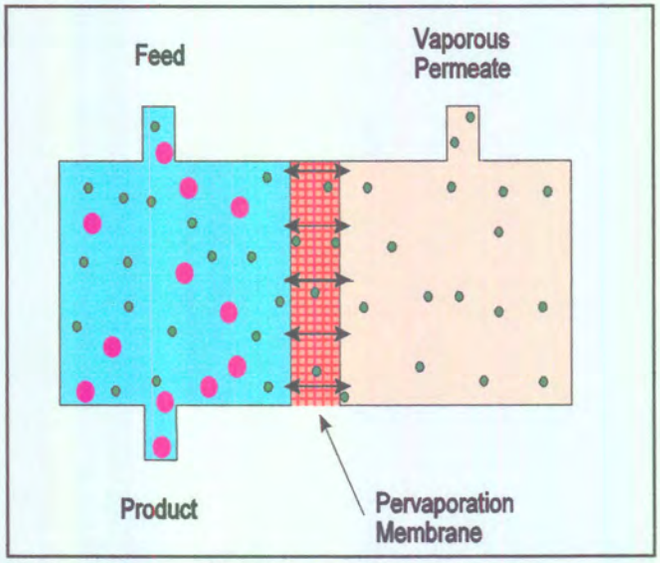

Figure 2.3 The Pervaporation process

2.3.3 Pervaporation

Pervaporation is characterized by the imposition of a barrier (membrane) layer between a liquid and a gaseous phase. [4 - 6] See Figure 2.3.

Pervaporation is distinguished from all other membrane processes by the phase change occurring during mass transfer. The driving force, unlike the applied pressure as discussed previously, is the reduction in activity (reduction of the partial pressure) on the permeate side. Mass transfer across the membrane occurs selectively towards the gas side. Because of the phase change required of the liquid solutes diffusing across the membrane (permselective "evaporation" of the liquid molecules), the process is termed pervaporation. Since different species permeate through the membrane at different rates, a substance at low concentration in the feed stream can be highly enriched in the permeate. Thus separation occurs with the efficacy of the separation effect being determined by the physicochemical structure of the membrane. [4, 6]

The liquid or liquid mixture in the feed side (Figure 2.3) is at atmospheric pressure. The permeate is removed as a vapour because of a low vapour pressure existing on the permeate side. This low (partial) vapour pressure can be achieved by employing a carrier gas or using a vacuum pump. The pervaporation process involves basically three steps namely:

- Selective sorption into the membrane on the feed side.
- Selective diffusion through the membrane.
- Desorption into a vapour phase on the permeate side. [5]

2.3.4 Liquid membranes

Liquid films on porous supports also form solution-diffusion membranes that can be used for gas separations. The liquids, which are held in place by capillary forces, naturally form defect-free layers. This reliance on capillary forces severely limits the allowable trans-membrane pressure difference that can be used. [4]

Two types of liquid membranes can be distinguished namely:

- The liquid film is immobilised within the pores of a porous membrane. This type is the so called Immobilized Liquid Membrane (ILM) or Supported Liquid Membrane (SLM).
- The second type is the so called Emulsion Liquid Membrane (ELM).

Selectivities of liquid membranes are based on the differences in the distribution coefficients of the components of the feed phase with the liquid in the membrane. If the components are similar, these differences are generally not very high. The diffusitivities of components of comparable size are similar so that the selectivity, which is determined by differences in solubility and diffusitivity, will not be high in general. To increase the selectivity, a carrier molecule can be added to the liquid in the membrane. This carrier molecule can have a high affinity for a specific

component in the feed phase and thus will it enhance the transport of this component over the membrane. [5, 10]

2.3.5 Dialysis

Concerning this project, dialysis (passive dialysis) is definitely the most important membrane process. For this reason it will be discussed in more detail than the other processes discussed so far.

2.3.5.1 The history and development of dialysis

Even though dialysis was the first membrane separation process to be discovered and studied, it has never really become industrially important. [1] By far and away the most important application of dialysis is in the medical field: hemodialysis for the treatment of chronic and acute uremia and for the removal of poisons from the bloodstream. Dialysis is not widely used on the industrial separations for the same two reasons membrane separation processes have failed in the past:

- It is a slow process, in part because it is driven by concentration differences, which are usually set by the system. (Time is a crucial factor in industrial processes)
- It is not highly selective, and species that are at all similar in chemistry or molecular size cannot be cleanly separated by dialysis. (Other methods of separation, for example electrodialysis and ion exchange, was much more effective) [1]

In fact, relative to other membrane processes that have come along since (such as reverse osmosis, ultrafiltration and electrodialysis), progress in dialysis has been quite slow.

The first significant application of dialysis occurred in the mid-1930s when

cellophane (regenerated cellulose) was first used to remove salts and other low molecular weight solutes from serum proteins and vaccines. At about the same time it was used for the recovery of caustic soda from hemicellulose solutions in the manufacture of rayon.

The dominant use of dialysis today is in the treatment of patients with kidney failure, to remove urea, uric acid, creatinine and other products of protein metabolism from their blood. In hemodialysis, arterial blood from the patient is passed over one side of the dialysis membrane while a dialysate solution containing a suitable mixture of ions is circulated on the other side. Hemodialysis was first reported by Abel, Rountree and Turner in 1914. However, the first practical unit was not assembled until 1944 by Kolff and Beck in Holland. [1, 11]

In 1950, dialysis membranes became commercially available. The concept of mass-transfer in on-line analytical dialysers was applied for a number of years in continuous flow systems. The use of on-line dialysis in segmented continuous flow systems was reported by Skeggs in 1957. In the mid 1960s, the first, non-segmented continuous flow system with a dialysis application, was introduced by Kadish and Hall. [11,12] In 1975, Růžička introduced the first on-line flow injection dialysis application system.

2.3.5.2 Definition and the process of dialysis

The following definitions of dialysis was obtained:

Dialysis is the flux of dissolved lower molecular mass components through the membrane as a result of a difference in trans-membrane concentration. [5,6]

or in other words

Dialysis is a rate-governed membrane process in which a microsolute is driven across a semi-permeable membrane by means of a concentration gradient. [4]

The microsolute **diffuses** through the membrane at a greater rate than the macrosolutes also present in the feed solution. (Depending on the pore size of the specific membrane, the smaller solutes that will diffuse through the pores with ease, will be classified as micro solutes whereas solutes that have difficulties in diffusing through the pores, will be classified as macrosolutes) If the receiving solution is not continuously renewed, the solute concentrations on both sides of the membrane will tend to equalize, negating the driving force for the separation. A good level of cleanup can be obtained from the process, provided that a concentration gradient can be maintained by continuous removal of the permeating components. Further more it is important to realize that dialysis is always accompanied by osmosis in normal operation. There is thus a reduction of the solute concentration in the feed because of osmosis which can seriously diminish the existing concentration gradient. [4 - 6]

If the feed and the dialysate are composed of the same solvent and differ only slightly in concentration, the assumption is made that the solute concentrations are proportional to their activities. When the feed and dialysate are composed of differing phases, these approximations are no longer valid since the standard states to which the activities are referenced may be different. For exact descriptions of driving forces, estimates of fugasities must be employed. [4]

Even though membrane composition and synthesis will be discussed, it was thought appropriate to give a short introduction into dialysis membranes.

The upper limits of pore dimensions in dialysis membranes are purposely chosen to minimize convective transport. (Convective transport is the transport of solutes due to the mechanical movement of the solution due to stirring, pumping of agitation) Consequently, the solute size that can permeate dialytic membranes has an upper bound determined by the above mentioned factor and by comprises made during membrane fabrication. Dialysis membranes usually have pore radii smaller than 60×10^{-8} cm. Macro molecules for example proteins like albumin, will

to a large extent, be retained. The effective pore size (of synthetic hydrophobic polymer membranes) can be reduced by the adsorption of proteins so that membranes with large pores will, during use in a dialysis system, develop improved protein retention. The hydrogel (celluloses) membranes with rather smaller pore radii (17×10^{-8} cm) do not adsorb the proteins and thus their transport properties will not be effected. To achieve selective mass transport in a dialytic process, one must rely upon a combination of solute and membrane properties. As an initial approximation, two solutes can be separated by dialysis if their diffusion coefficients in the feed differ by at least an order of magnitude. The solute diffusitivity in the continuum within the membrane is an indicator of whether or not, and how fast a solute may permeate the membrane. This diffusitivity is also modified by the matrix structure of the membrane, usually to a smaller value. In the simplest case of a hydrogel membrane, such as regenerated cellulose, the aqueous diffusion coefficient is reduced by a factor of ten for small solutes, with higher reductions for larger solutes. [4]

Many new terms were introduced in paragraph 2.2.5 which can leave the reader somewhat in the dark. This is an introductory description of dialysis and these terms will be explained in the paragraph concerned with membrane syntheses. The theory concerning dialysis and ion movement are discussed in detail in Chapter 3.

A matter which can be a cause of ambiguity, is the difference between normal dialysis and Donnan dialysis. Some disagreement and vagueness was encountered between the different references used. According to Ho and Sirkar [4] and Rautenbach and Albrecht [6], Donnan dialysis differs from other forms of dialysis in that it relies upon an ion-selective membrane to retard the transfer of either a cation or anion across the barrier. According to Mulder [5] normal dialysis is restricted to the diffusion of neutral solutes and that Donnan dialysis is the separation of electrolytes by either a neutral membrane or an ion-selective membrane. For the sake clarity in this thesis, the former of the two definitions will

be used.

2.3.6 Electrodialysis

2.3.6.1 History and development of electrodialysis

Electrodialysis is useful in a number of areas for example:

- Removal of electrolytes from aqueous solutions, e.g. water desalting.
- Concentration of electrolytes.
- Separation of electrolytes from non-electrolytes.
- Oxidation/reduction or acid/base formation.
- Double decomposition reactions.
- Separation of ions of like charge.

The first four of these applications have become substantial industrial applications. The principle application of electrodialysis today is the desalination of brackish water.

The history of electrodialysis dates back to the early 1930s, when aqueous solutions were first desalted in three-compartment cells consisting of an anode compartment, an anion-permeable and cation-permeable membrane forming a middle compartment, and a cathode compartment. Meyer and Strauss were the first to assemble a multicompartment electrodialysis apparatus.

With the advent of commercial reverse osmosis in the early 1970s, there has been considerable competition between electrodialysis and reverse osmosis for the brackish-water desalination market. Electrodialysis has found an important application in desalting foods, as in the removal of salts from cheese whey to produce a milk substitute, and in salt removal from sugar solutions. Another

important application of electrodialysis has been found in Japan, where there is essentially no indigenous supply of table salt. Seawater is treated by electrodialysis to produce a salt solution of about 20 wt % concentration that is then thermally evaporated to dryness.

2.3.6.2 The process of electrodialysis

In this process, electrically charged membranes are used to remove ions from an aqueous solution. A number of cation- and anion-exchange membranes are placed in an alternating pattern between a cathode and an anode. When an ionic feed is pumped through the cell, nothing will happen unless a direct current (dc) is applied. When a dc current is applied, cations and anions will migrate to the cathode and the anode respectively. The cations are obstructed in their migration by the anion-exchange membrane and so also the anions by the cation-exchange membrane. The overall effect is that the ionic concentration increases in alternating compartments accompanied by a simultaneous decrease in ionic concentrations in the other compartments. This principle is well explained in Figure 2.4. [4, 5, 9]

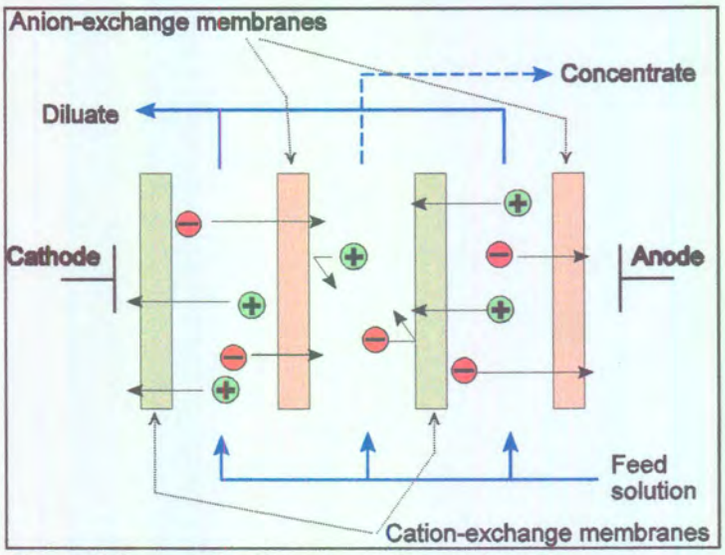

Figure 2.4 The Principle of Electrodialysis

2.4 Characterisation and Structure of Membranes

Membranes can be made of a large number of different materials. A classification of membranes can be divided into two main groups namely biological and synthetic membranes. Biological membranes are essential for life on earth. Every living cell is surrounded by a membrane, but these membranes differ fundamentally in structure, functionality etc. from synthetic organic and inorganic membranes. [5, 8] Synthetic membranes can be divided into organic (polymeric) and inorganic membranes, the most important class of membrane materials being the polymeric membranes. The choice of a given polymer as a membrane material is not arbitrary but based on very specific properties, origination from structural factors. Structural factors determine the chemical, thermal and mechanical properties of the polymer used. Such factors will also influence the permeability of the membrane. [5]

Polymers are high molecular weight components built up from a number of basic units, the monomers. The number of these monomers which link together to form a long chain molecule, will indicate the degree of polymerisation. The molecular weight of a long

chain is dependant on the degree of polymerisation. Basically all polymers can be used as barrier or membrane material but the chemical and physical properties differ so much that only a limited number can be used in practice. [4, 5]

Membranes need to be characterised to ascertain which can be used for specific separations or class of separations. A small change in one of the membrane parameters can change the structure and consequently have a drastic effect on membrane performance. Characterization is necessary to relate structural membrane properties such as pore size, pore size distribution, free volume and crystallinity to membrane separation properties. Membrane characterisation leads to the determination of structural and morphological properties of a given membrane.

Three basic types of membranes[2] can be distinguished based on their structure and separation principles:

- Porous membranes
- Non-porous membranes
- Carrier membranes

A schematic presentation of these various types of membranes is given in Figure 2.5.

2 *Not all membranes and membrane structures are covered by this classification. This approach is used for simplicity so that the basic principles can be understood. Further, there is no distinct transition from one type to the other.*

2.4.1 Porous membranes

Membranes of this type induce separation by discrimination between particle size. High selectivities can be obtained when the solute or particle size is large relative to the pore size. [5]

Porous membranes contain fixed pores. The selectivity is mainly determined by the dimensions of the pores but the choice of material affects phenomena such as adsorption and chemical stability under condition of actual application and membrane cleaning. This implies that the requirements for the polymeric material are not primarily determined by the flux and selectivity but also by the chemical and thermal properties of the material. [4, 5]

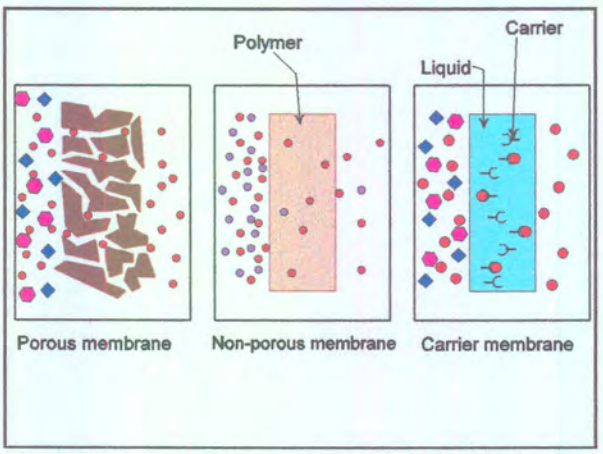

Figure 2.5 *Schematic presentation of the three basic types of membranes*

Even with the pore size and pore distribution determined exactly, the membrane performance is sometimes governed by other parameters such as concentration polarization and fouling. An important and often overlooked parameter is the pore geometry. Some characterisation techniques determine the dimensions of the pore entrance rather than the pore size to obtain information about permeation characteristics. Another important factor is the pore size distribution. The pores

in these membranes do not have the same size but exist as a distribution (Gaussian distribution) of sizes. In this case, the membrane can be characterised as nominal or absolute pore size. With an absolute rating, every particle of this specific size and larger will be retained whereas the nominal rating indicates that a certain percentage of the particles of a specific size or larger will be retained. It should be noted that this definition does not characterise the membrane nor the pores of the membrane, but rather the size of the particles retained by it. Another important factor is the surface porosity. This a very important variable in determining the flux through the membrane, in combination with the thickness of the top layer or the length of the pore.

Two different types of characterisation methods for porous membranes can be distinguished from the above mentioned considerations: [5]

- *Structure related parameters.* The determination of pore size, pore size distribution, top layer thickness and surface porosity.
- *Permeation-related parameters.* Determination of the actual separation parameters using solutes that are more or less retained by the membrane. (The so called cut-off measurements)

It is often very difficult to relate the structure-related parameters directly to the permeation-related parameters because the pore size and shape is not very well defined. The configuration of the pores (cylindrical, packed-spheres) used in simple model descriptions deviate sometimes dramatically from the actual morphology as depicted in Figure 2-6. [4, 5]

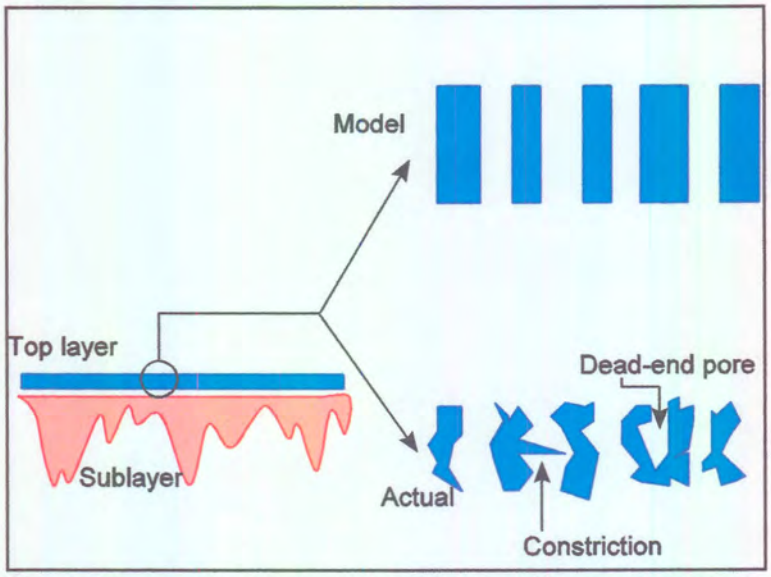

Figure 2.6 *Comparison of an ideal and the actual structure of an Ultrafiltration membrane.*

There are a number of characterisation techniques available for porous media and although both microfiltration and ultrafiltration membranes are porous, different techniques are used for the characterization. [5]

For microfiltration:

- Scanning electron microscopy
- Bubble-point method
- Mercury intrusion porometry
- Permeation measurements

For ultrafiltration: [3]

- Gas adsorption-desorption
- Thermoporometry
- Permporometry
- Liquid displacement
- Rejection measurements

3 The structure is more asymmetrical compared to microfiltration membranes. Such membranes consist of a thin top layer supported by a porous sublayer, with the resistance to mass transfer being almost determined completely by the top layer.

- Transmission electron microscopy

2.4.2 Non-porous membranes

These membranes are commonly used in gas and vapour separation, pervaporation and dialysis. For the abovementioned processes, either composite or asymmetric membranes are used. In this type of membrane the performance permeability and selectivity is determined by the intrinsic properties of the material. The choice of material is determined by the type of application, and the polymer type can range from and elastomer to a glassy material. Membranes in this class are capable of separating species of approximately the same size from each other. Separation takes place through differences in solubility and/or differences in diffusivity. This means that the intrinsic properties of the polymeric material determine the extent of selectivity and permeability. [4]

Nonporous membranes are used to perform separations on a molecular level. However, rather than molecular weight or molecular size, the chemical nature and morphology of the polymeric membrane and the extent of interaction between the polymer and the permeants are the important factors to consider. Transport through nonporous membranes occurs by a solution-diffusion mechanism and separation is achieved either by differences in solubility and/or diffusivity. The determination of the physical properties of these membranes and hence the characterisation of the membrane can be accomplished by one of the following methods:

- Determine the permeability towards gasses and liquids.
- Determine the physical properties of the membrane by means of DSC/DTA methods, density measurements, and XRD.
- Measurement of the thickness of the membrane with plasma etching.
- Surface analysis. [5]

2.4.3 Carrier membranes

In this case, transport is not determined by the membrane or membrane material but by a very specific carrier-molecule which facilitates specific transport. Through the use of specially tailored carriers, extremely high selectivities can be obtained. [4, 5]

2.5 Membrane materials

Hydrophobic materials (see Figure 2.7) such as polytetrafluoroethylene (PTFE), poly(vinylidene fluoride) (PVDF) and isotactic polypropelene (PP) are often used for membranes. PTFE is highly crystalline and exhibits excellent thermal stability. It is not soluble in any common solvent and hence also shows good thermal and chemical resistance. PVDF also shows good thermal and chemical resistance although not as good as PTFE. (It is soluble in aprotic solvents.) PP is also excellent solvent resistant when in the isotactic configuration. (Isotactic: where all the side groups lie on the same side along the main chain). The three polymers PTFE, PVDF and PP cannot be wetted by water spontaneously, i.e. when used in aqueous mixtures have to be pre-wetted. These three materials are commonly used for microfiltration. [5]

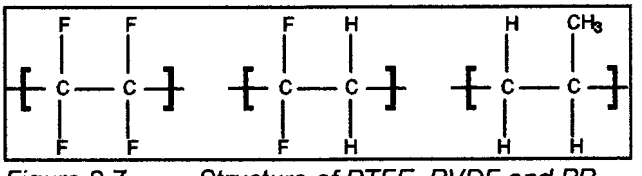

Figure 2.7 Structure of PTFE, PVDF and PP respectively

Cellulose (or regenerated cellulose) is mainly used as a material for dialysis membranes. Cellulose is a polysaccharide that can be obtained from plants. It's molecular weight varies from 500 000 to 1500 000 implying that the number of segments (single carbon chains) is roughly between 3000 and 9000. The glucose segment contains three hydroxyl groups which are very susceptible to chemical reaction by forming esters and ethers. The glucose repeating units in cellulose are connected by β-1,4 glycosidic

linkages (see Figure 2.8). Because of its structure, cellulose is quite crystalline, and although the polymer is very hydrophillic, it is not water soluble. This is due to the crystallinity and intermolecular hydrogen bonding between the hydroxyl groups. Cellulose derivates such as cellulose nitrate and cellulose acetate are used for microfiltration/ultrafiltration applications, whereas cellulose triacetate exhibit good properties as a reverse osmosis membrane in desalination applications. Cellulose esters have got excellent membrane properties but are very sensitive to thermal, chemical and biological degradation. [5]

Another class of membrane polymers are the polyamides. These polymers are characterised by the amide group. Although the aliphatic polyamides comprise a very large class of polymers, the aromatic polyamides are to be preferred as membrane materials because of their outstanding mechanical, thermal, chemical and hydrolytic stability, as well as their permselective properties, particularly in reverse osmosis.

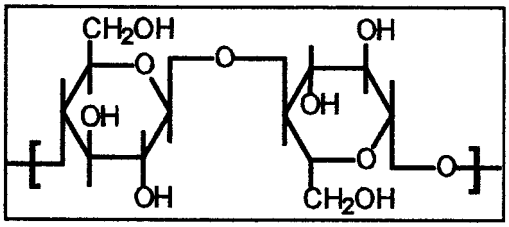

Figure 2.8 *The chemical structure of cellulose*

2.6 References

1. Lonsdale H.K., (**1982**) J. Membr. Sci. 10: 81 -181.
2. Lonsdale H.K., (**1989**) What is a membrane? Part II. J. Membr. Sci. 43:1-3.
3. Regional Courses in Membrane Processes (Module 2).(**1994**) Slovak Technical University , Department of Chemical and Biochemical Engineering. Radlinského Bratislava, Slovakia..
4. Ho W.S.W. and Sirkar K.K.,(**1992**) Membrane Handbook. Chapman & Hall..
5. Mulder M., (**1996**) Basic principles of Membrane Technology, Kluwer Academic publishers.
6. Rautenbach R and Albrecht R, Membrane Processes John Wiley & Sons. 1989
7. Schweitzer PA., (**1979**) Handbook of Separation Techniques for Chemical Engineers, McGraw-Hill book company.
8. Koryta J., (**1982**) Ions, Electrodes and Membranes. John Wiley & Sons..
9. Schoeman J.J. and Steyn A., (**1995**) Evaluation of Membrane Technology for Electroplating Effluent Treatment. Report to the Water Research Commission by the Division of Water Technology, CSIR. WRC report No. 275/1/95.
10. Barnes D.E., (**1993**) Supported Liquid membranes in Flow Systems. PhD dissertation, University of Pretoria.
11. Hattingh C.J., (**1994**) Membraanskeidings met behulp van dialise in vloeisiseme. MSc dissertation, University of Pretoria.
12. Van Staden J.F., (**1993**) LRA 6: 29.

Chapter 3

Theoretical Background to the Movement of Particles in a Solution and across a Membrane

3.1 Introduction.

One of the main objectives of this study was to enhance the mass transfer of particles (analyte) across a passive membrane. It therefore was of utmost importance that one should be equipped with a sound knowledge on the movement of these particles in a solution and across a membrane. This project was based, specifically, on the movement of charged particles (ions) under the influence of an applied potential across a passive membrane. Figure 3.1 is a schematic presentation of a longitudinal cross section of the proposed electrodialyser. In Figure 3.1 the movement of the fluid in the electrodialyser, due to the pumping action of the peristaltic pump, is from left to right. If one considers Figure 3.1, it is clear that there were two categories of movement for the analyte ions namely : (All definitions to follow are based upon analytical and physical chemistry and are not only for Flow Injection Analysis)

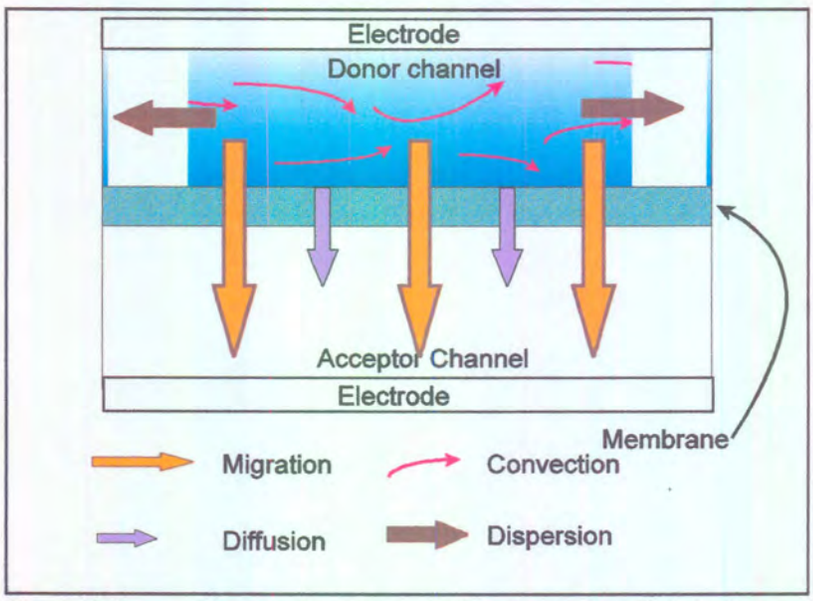

Figure 3.1 *Means of movement of a charged particle in the proposed dialyser unit.*

1. The transport of the ions from the bulk of the solution to the membrane surface.

There are three ways by which an ion can be transported namely: (See Figure 3.1)

1. Dispersion (sample ion distribution in the Flow injection electrodialyser unit): Can be subdivided into convective- (due to the flow of the solvent in the tubing and in the donor channel in the case of Figure 3.1) and diffusional transport (axial and radial concentration gradients that exist due to the form of the injected sample bolus).
2. Diffusion: Ions are transported due to the concentration gradient that exist. (This diffusion must not be confused with the diffusion that do exist due to the form of the sample bolus, but it is rather due to the inhomogeneous composition of the sample bolus.)
3. Migration: Ions are transported due to the influence of the applied potential. [1, 2, 3]

In the bulk of the solution (that is in the donor channel of the dialyser), it is clear that two of these types of transport will predominate namely, the convective transport due to the pumping action through the donor channel and migration due to the applied potential. Diffusion will only be possible as the dispersion process [1], since the analyte solution will be a homogeneous mixture of the analyte ions.

2. The transport of the ions across the membrane.

Various membrane processes (of which electrodialysis and dialysis are the predominant) must be considered. Neutral membranes are used in an electrodialysis system, thus it is not only conventional electrodialysis

across an ion-exchange membrane that was under study but also other membrane processes.

It is clear that this theoretical chapter can be subdivided into the sections as described above. As an introduction into the general theory of ion transport under the influence of an applied potential, it was thought appropriate to make use of the theoretical work as explained by Atkins. [4] Some guidelines are also given by Wesselingh and Krishna. [5] It is furthermore important to note that the Fick's description of mass transfer was used in this theoretical chapter. Mass transfer can also be described by the Maxwell-Stefan relation. [4]

3.2 Ion Transport (the movement of a charged particle under the influence of an applied potential)

In solution, cations move towards a negatively charged electrode (cathode) and anions move towards a positively charged electrode (anode). This migration is a transport process, in principle the same as kinetic theory of gases, with the main differences being the support of the solvent and the drift of ions under the influence of an electrical field. The presence of the field is a simplification, because the average motion of the ions is easy to describe. The presence of the solvent (and the ion-ion interactions) is a complication which is still the subject of current research.

3.2.1 Ion motion : the empirical facts

The conductivity of a solution is determined by measuring its electrical resistance, and the standard method is to incorporate a conductivity cell, of the type shown in Figure 3.2, into one arm of a Wheatstone bridge and to search for the balance point. The main complication is that alternating current must be used because a direct current would lead to electrolysis and to polarisation. The use of alternating current (with a frequency of about 1 kHz) avoids polarisation because

the charging that occurs on one half of the cycle is undone during the second half. By studying the transport of charge through electrolyte solutions it is possible to build up a picture of the events that occur.

The resistance (symbol: R) of a sample increases with its length ℓ and decreases with its cross-sectional area A: $R \propto \ell/A$. The proportionality coefficient is called the resistivity (symbol: ρ), and it can be written as $R = \rho\ell/A$. The conductivity (symbol: κ) is the inverse of the resistivity therefore

$$R = \frac{1}{\kappa}\frac{\ell}{A} \quad \text{or} \quad \kappa = \frac{\ell}{RA} \qquad 3.1$$

Resistance is expressed in ohm (Ω). The reciprocal ohm, Ω^{-1}, is called the siemens (symbol : S, $1\ S = 1\Omega^{-1}$). It follows that the units of conductivity are Sm^{-1} (or $S\ cm^{-1}$). The conductivity of a solution, which is due to contributions from both cations and anions, depends on the number of ions present, and it is normal to introduce the molar conductivity (symbol : Λ_m) defined as

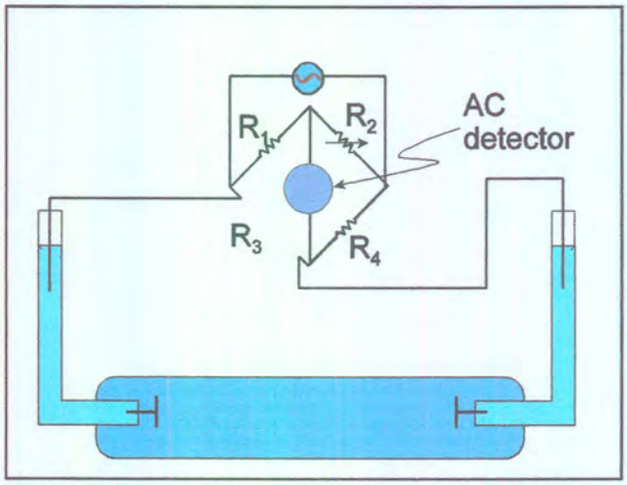

Figure 3.2 *The conductivity of an electrolyte solution is measured by making the cell one arm of a Wheatstone bridge and measuring its resistance.*

$$\Lambda_m = \frac{\kappa}{c} \qquad 3.2$$

with c being the (molar) concentration of the added electrolyte. The equivalent conductivity is also sometimes used. This takes into account the fact that some ions are multiply charged, and so might transport more charge even though they may be moving more slowly. The equivalent conductivity treats all ions as being singly charged. For example, in NaCl (*aq*), each ion carries unit charge in each direction, and the equivalent conductivity is the same as the molar conductivity. In $CuSO_4$ (*aq*), however, each ion transports two units of charge, and the equivalent conductivity is half the molar conductivity.

Molar conductivities depend on the concentration of the electrolyte. (They would be independent of concentration only if the conductivity was exactly proportional to the concentration, and for such strongly interacting particles as ions this is unlikely to be the case.) Measurement of the concentration dependence of molar conductivities shows that there are two classes of electrolyte. In one, the strong electrolytes, the molar conductivity decreases slightly as the concentration is increased (illustrated in Figure 3.3) but the effect is not large. In the other, the weak electrolytes, the molar conductivity is normal at concentrations close to zero, but drops sharply to low values when the concentration departs from zero. (illustrated in Figure 3.3) The classification depends on the solvent employed as well as the solute: lithium chloride, for example, is a strong electrolyte in water,

$$\Lambda_m = \Lambda^0_m - K\sqrt{c} \qquad 3.3$$

This is called Kohlrausch's Law. Λ^0_m is called the limiting molar conductivity and K is a coefficient that is found to depend more on the nature of the electrolyte (i.e. whether it is of the form MA, or M_2A, etc.) than on its specific identity.

Kohlrausch was also able to confirm that the value of Λ^0_m for any electrolyte can be expressed as the sum of contributions from its individual ions. If the molar conductivity of the cations is denoted λ_+, and that of the anions λ_-, then Kohlrausch's Law of the independent migration of ions is

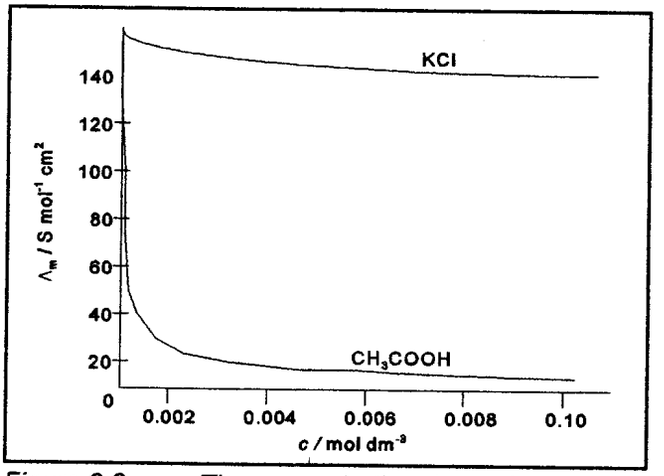

Figure 3.3 *The concentration dependance of the molar conductivities of a strong and weak electrolyte respectively.*

$$\Lambda^0_m = \nu_+\lambda_+ + \nu_-\lambda_- \qquad 3.4$$

where ν_+ and ν_- are the numbers of cations and anions per formula unit of electrolyte (e.g. $\nu_+ = \nu_- = 1$ for HCl, NaCl, and $CuSO_4$, but $\nu_+ = 1$, $\nu_- = 2$ for

$MgCl_2$). This simple result, which can be understood on the grounds that the ions behave independently when the solution is infinitely dilute.

Weak electrolytes are substances that are not fully ionised in solution, and include weak acids and bases. The marked concentration dependence of their conductivities arises from the displacement of the $MA(aq) \rightleftharpoons M^+(aq) + A^-(aq)$ equilibrium towards the right at high dilutions. The conductivity depends on the number of ions in the solution, and therefore on the degree of ionisation, α, of the electrolyte. If the ionisation equilibrium constant of some weak 1:1 electrolyte, MA, is denoted K, then then it is present at a concentration c,

$$K = [M^+(aq)][A^-(aq)] / [MA(aq)] = (a\alpha)(\alpha c) / (1-\alpha)c = \{\alpha^2 / (1-\alpha)\}c \qquad 3.5$$

where a is the activity and c is the concentration. The degree of ionisation when the concentration is c is therefore

$$\alpha = \tfrac{1}{2}(K / c)\left\{\left(1 + 4c / K\right)^{\frac{1}{2}} - 1\right\} \qquad 3.6$$

If the molar conductivity of the hypothetical fully ionised electrolyte is Λ'_m, then since only a fraction α is ionised in the actual solution, the measured molar conductivity (Λ_m) is given by

$$\Lambda_m = \alpha \Lambda'_m \qquad 3.7$$

with a α given by equation 3.6. The value of Λ'_m may be approximated by Λ^0_m, and so, if K is known, equation 3.6 can be used to predict the concentration dependence of the molar conductivity. The dependence agrees quite well with the experimental curve shown in Figure 3.3.

Alternatively, the concentration dependence of Λ_m can be used in measurements

of the limiting molar conductivity. It is quite easy to manipulate the equilibrium constant expression into the form

$$1/\alpha = 1 + \alpha c/K,$$

and so, with

$$\alpha = \Lambda_m / \Lambda^0_m$$

then

$$\frac{1}{\Lambda_m} = \frac{1}{\Lambda^0_m} + \frac{\Lambda_m c}{K\left(\Lambda^0_m\right)^2} \qquad 3.8$$

This is called Ostwald's Dilution Law, and it shows that if $1/\Lambda_m$ is plotted against $c\,\Lambda_m$, the intercept is $1/\Lambda^0_m$.

3.2.2 The mobilities of ions

At this point it is important to become acquainted with some definitions:

The rate of migration of a property (ions in this case, but it can also refer to heat or any other physical property) is measured by its flux (J), which is the quantity passing through unit area per unit time. The flux of a property is usually proportional to the gradient of a related property of a system. (The flux of a species is proportional to its concentration gradient in other words the flux is proportional to a concentration difference times a mass transfer coefficient. [4]) Two kinds of flux can be distinguished namely:

J_z with respect to the (moving) mixture and

N_z with respect to an interface. See Figure 3.4.

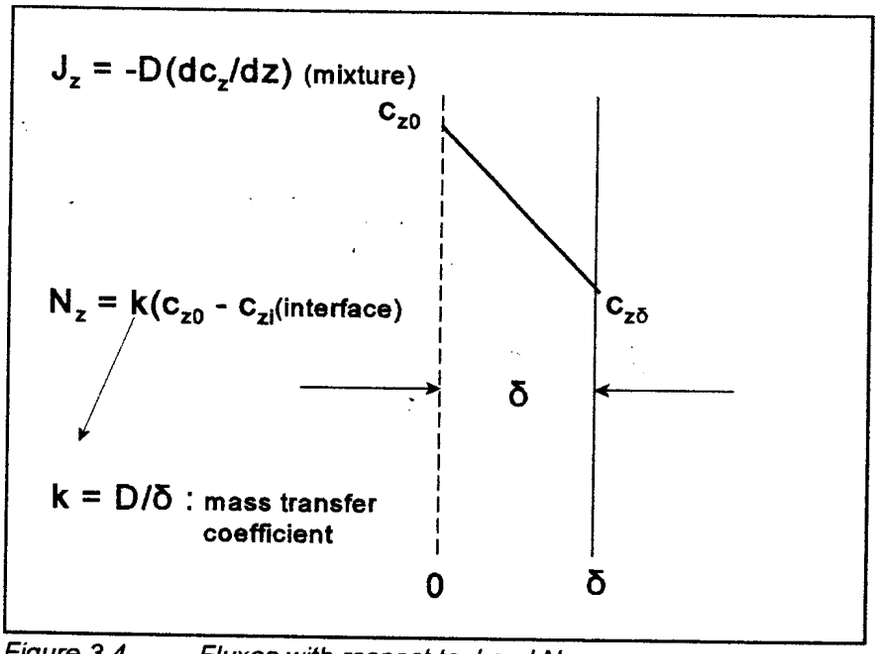

Figure 3.4 Fluxes with respect to J and N.

J is the more fundamental of the two. [4]

The rate of diffusion (the flux of matter) parallel to some axis z (J_z) is found to be proportional to the concentration gradient along that axis, thus

$$J_z \propto dN/dz$$

where N the number density.

J_z is a component of a vector, and the positive sign indicates flow towards increasing z. Matter flow occurs down a concentration gradient and so if dN/dz is negative, J_z is positive. (See Figure 3.5). Therefore, the coefficient of proportionality in the matter flux expression must be negative and it is denoted -D (diffusion coefficient). This leads to Fick's first law of diffusion.

$$J_z = -D\left(dN/dz\right) \qquad 3.9$$

This law will be discussed later in this chapter. Please note that concentration is denoted as c in Figure 3.4 whereas for the same equation (equation 3.9) the number density, N, was used.

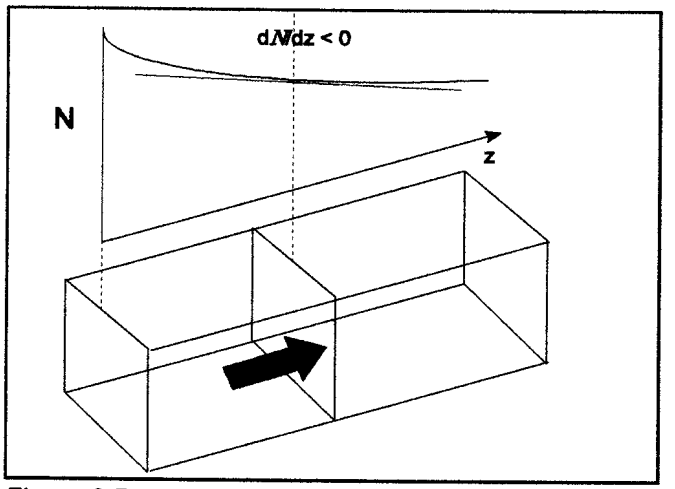

Figure 3.5 *The flux of particles down a concentration gradient.*

Ions in solution are subject to a variety of forces. They experience the random bombardment of the solvent particles, but since these occur in random directions they do not result in net motion if the solution is uniform. In an electric field they also experience an electric force. When two electrodes a distance ℓ apart are at a potential difference $\Delta\phi$, there is a uniform electric field of magnitude $E = \Delta\phi/\ell$ between them. An ion of charge ze experiences a force (Γ) of magnitude.

$$\Gamma = zeE = \frac{ze\Delta\phi}{\lambda} \qquad 3.10$$

With e the elementary charge and z the sign of the charge.

A cation responds by accelerating in the direction of the negative electrode (cathode) and an anion accelerates towards the positive electrode (anode).

As the ion rubs through the solvent a frictional force, Γ', retards it with a strength

that increases with its speed. If we assume that the Stokes formula ($\Gamma' = fs$, $f = 6\pi\eta a$) for a sphere of radius **a**, speed **s** and solvent viscosity η applies even on a microscopic scale, then a terminal speed, called the drift speed, is reached when the accelerating force ($\Gamma = zeE$) is balanced by the viscous drag ($\Gamma'=fs$). This occurs when

$$s = zeE/f \qquad 3.11$$

Where E is the electric field applied and f is the frictional constant.
Since the drift velocity governs the rate at which charge is transported, the conductivity is expected to decrease with increasing solution viscosity and increasing ion size.

Experimental results confirm these predictions for bulky ions (such as R_4N^+ and $RCOO^-$), but not for small ions. For example, the molar conductivities of the alkali metal ions increase from Li^+ to Cs^+, even though the ionic radii increase. The discrepancy is resolved when we realize that the radius in Stokes' formula is the hydrodynamic radius of the ion, its effective radius in the solution taking into account all the solvent molecules it carries. Small ions give rise to stronger electric fields than large ones (it is a result from electrostatics that the electric field at the surface of a sphere of radius R is proportional to ze/R^2, and so the smaller the radius the stronger the field). For this reason small ions are more extensively solvated than big ions. This means that an ion of small ionic radius has a large hydrodynamic radius because it drags many solvent molecules through the solution as it migrates. Therefore, it also has a lower molar conductivity than a bigger ion of the same charge. Friction will be discussed again in paragraph 3.3.

The proton, however, although it is very small, has a very high molar conductivity. This is because it conducts by a mechanism (the Grotthus mechanism) that does not involve its actual motion through the solution. Instead of a single, highly solvated proton moving through the solution, it is believed that there is an effective motion of a proton which involves the rearrangement of bonds through a long chain of water molecules, and the conductivity is governed by the rates at which the water molecules can rotate into orientations in which they can accept or donate protons. (See Figure 3.6)

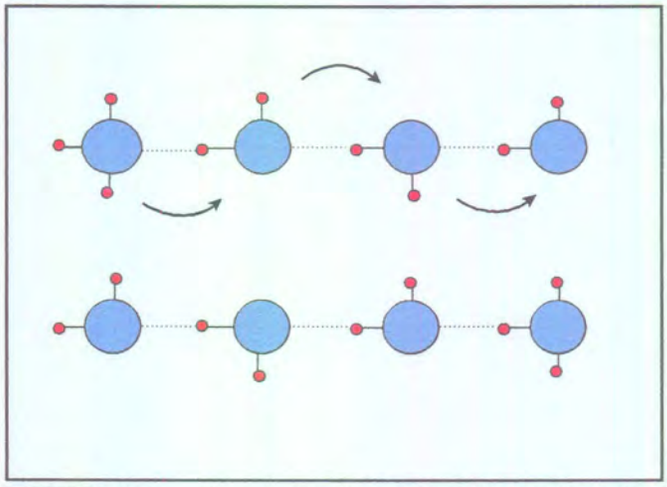

Figure 3.6 The mechanism of conduction in water.

The drift speed is proportional to the strength of the applied field. The coefficient of proportionality is called the mobility of the ion (symbol : u) and we write

$$S = uE \qquad 3.12$$

This means that at a stage in an alternating current (AC) cycle when there is a potential difference of 1 V across a solution of length 1 cm (so that E = 1 V cm^{-1}), the drift speed is typically about 6 x 10^{-4}cm s^{-1}. This might seem slow, but not when expressed on a molecular scale, for it corresponds to an ion passing about 10 000 solvent molecules per second.

The usefulness of ionic mobilities is that they provide a link between measurable and theoretical quantities. As a first step the relation between mobility and conductivity is established. In order to keep the calculation simple, signs are ignored with the concentration being on the magnitude: The direction of flux can always be decided by common sense.

Consider a solution of a strong electrolyte at a concentration c. Let each formula unit give rise to ν_+ cations of charge z_+e and ν_- anions of charge z_-e. The concentration of each type of ion is therefore νc (with $\nu = \nu_+$ or ν_-) and the number density of each type is $\nu c N_A$. (N_A is Avogadro's number) The number of cations that pass through an imaginary window of area A (See Figure 3.7), during and interval Δt is equal to the number within the distance $s_+\Delta t$, and therefore to the number in the volume $s_+\Delta t A$. The number in this volume is equal to $(s_+\Delta t A)(\nu_+ c N_A)$. The number passing through the window per unit area per unit time, the cation flux, is therefore

$$J_{cations} = (s_+ \Delta t A)(\nu_+ c N_A) / \Delta t A = s_+ \nu_+ c N_A$$

Each cation carries a charge z_+e, and so the flux of charge is

$$J(charge) = z_+ s_+ \nu_+ c e N_A = z_+ s_+ \nu_+ c F$$

where $F = eN_A$ is Faraday's constant. Since $s = uE$ this becomes

$$J(charge) = z_+ s_+ \nu_+ c F E.$$

The current through the window due to the cations (I_+) is the charge flux times the area, $I_+ = JA$. The electric field is the potential gradient $\Delta\phi/\ell$. Therefore,

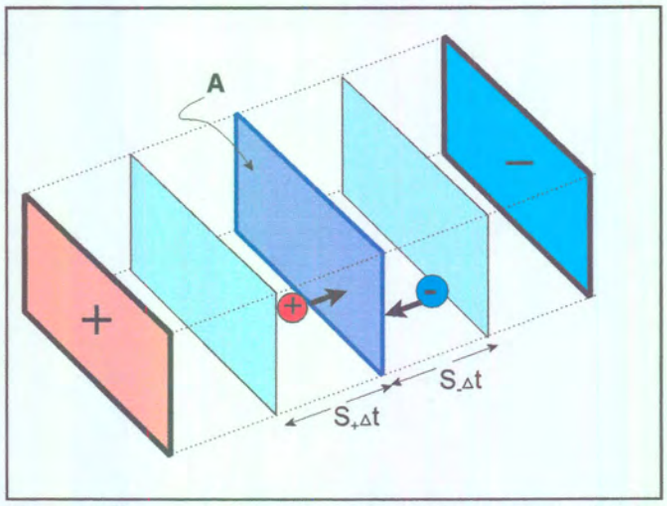

Figure 3.7 *In the calculation of the current, all the cations within a distance $s_{+}\Delta t$ will pass through the area A and likewise for the anions*

$$I_{+} = \frac{z_{+}u_{+}\nu_{+}cFA\Delta\phi}{\ell} \qquad 3.13$$

Current and potential difference are related by Ohm's Law, $I = \Delta\phi/R$, and the resistance R is related to the conductivity by equation 3.1. Therefore, for the cations, $I_{+} = \kappa_{+}(\Delta\phi A/\ell)$. Comparison of this with the last expression gives

$$\kappa_{+} = z_{+}u_{+}\nu_{+}cF,$$

and so the molar ionic conductivity is

$$\lambda_{+} = z_{+}u_{+}F \qquad 3.14$$

Exactly the same argument leads to the corresponding expression for the anion molar conductivity.

$$\lambda_- = z_- u_- F \qquad 3.15$$

It follows that the limiting molar conductivity of a solution is related to the individual ion mobilities by

$$\Lambda_m^0 = \{z_+ u_+ \nu_+ + z_- u_- \nu_-\} F \qquad 3.16$$

In case of a symmetrical z:z electrolyte (e.g. $CuSO_4$), this simplifies to

$$\Lambda_m^0 = z(u_+ + u_-)F \qquad 3.17$$

Ions that are very mobile carry a large fraction of the total current. The transference number or transport number (symbol: t) is defined as the fraction of total current carried by the ions of a specified type. In the case of a solution of two kinds of ion, the cation transport number is defined as

$$t_+ = I_+ / I \qquad 3.18$$

with a similar expression for the anion transport number t_-. Since the total current I is the sum of the cation and anion currents, $t_+ + t_- = 1$. The cation current is related to the cation mobility by equation 3.12, with a similar expression for the anions, and so the relation between the limiting value t^0 and u is

$$t_+^0 = z_+ \nu_+ u_+ / (z_+ \nu_+ u_+ + z_- \nu_- u_-) \qquad 3.19$$

In the case of a symmetrical electrolyte this simplifies to

$$t_+^0 = \frac{u_+}{(u_+ + u_-)} \quad , \quad t_-^0 = \frac{u_-}{(u_+ + u_-)} \qquad 3.20$$

Moreover, since the ionic conductivities are related to the mobilities, from equations 3.13 and 3.14 it follows that

$$t_+^0 = \frac{\nu_+ \lambda_+}{(\nu_+ \lambda_+ + \nu_- \lambda_-)} \quad , \quad t_-^0 = \frac{\nu_- \lambda_-}{(\nu_+ \lambda_+ + \nu_- \lambda_-)} \qquad 3.21$$

and therefore that

$$\nu_+ \lambda_+ = t_+^0 \Lambda_m^0 \quad , \quad \nu_- \lambda_- = t_-^0 \Lambda_m^0 \qquad 3.22$$

Consequently, since there are independent ways of measuring transport numbers of ions, we can determine the individual ionic conductivities and through equations 3.14 and 3.15 the ionic mobilities.

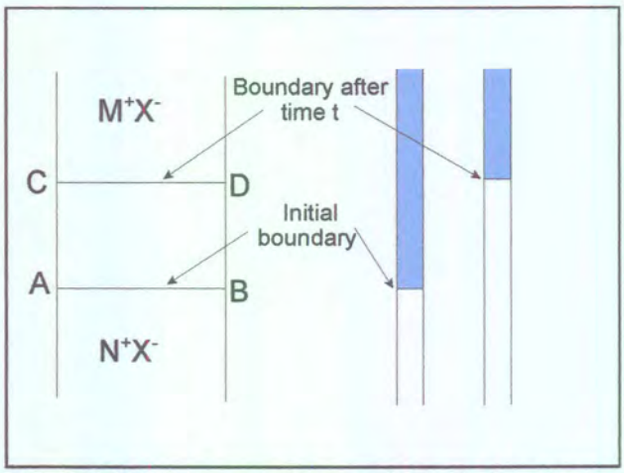

Figure 3.8 *the moving boundary method for the measurement of transference numbers*

3.2.3 The measurement of transport numbers

One of the most accurate methods for measuring transport numbers is the moving boundary method in which the motion of a boundary between two ionic solutions having a common ion is observed as a current flow.

Let MX be the salt of interest and NX (the indicator) a salt giving a denser solution. The indicator solution occupies the lower part of a vertical tube, Figure 3.8, and the MX solution, the leading solution, occupies the upper part with a sharp boundary between them. The indicator solution must be denser than the leading solution, and the mobility of the N ions must be greater than the mobility of the M ions. When a current I is passed for a time t the boundary moves from AB to CD, and so all the M ions in the volume between AB and CD must have passed through CD. That number is cVN_A (where V indicates volume), and so the charge they transfer through the plane is $z_+cVeN_A = z_+cVF$. However, the total quantity of charge transferred when a current I flows for a time t is It. Therefore, the fraction due to the motion of the M ions, which is their transport number, is

$$t_+ = \frac{z_+ cVF}{It} \qquad 3.23$$

Hence, knowing the diameter of the tube and the distance moved by the boundary in the time t, the transport number, and hence the ion conductivity and mobility, may be determined.

In the Hittorf method an electrolytic cell is divided into three compartments and an amount **It** of electricity is passed. An amount It/z_+F of cations are discharged at the cathode but an amount $t_+(It/z_+F)$ of cations migrate into the cathode compartment. The net change in the amount of cations in that compartment is therefore $(t_+ - 1)(It/z_+F)$, or $-t_-(It/z_+F)$. Therefore, by measuring the change of composition in the cathode compartment, t_-, the anion transport number, can be deduced. Likewise, the change in composition of the anions in the anode compartment is $-t_+(It/z_-F)$.

3.2.4 Conductivities and ion-ion interactions

Having accounted for the form of the law of independent migration of ions, the remaining problem is to account for the $c^{½}$ dependence of the Kohlrausch Law, equation 3.1. Note that we have to account for a reduction of the conductivity below its value at zero ionic strength. The activity coefficients of ions also depend on $c^{½}$, and depend on their charge type rather than their specific identities. That was explained in terms of the properties of the ionic atmosphere around each ion, and it is suspected that the same explanation applies here.

When an electric field is applied to a solution of ions and all the ions drift in a definite direction, we have to modify the picture of the ionic atmosphere as being a spherically symmetrical haze of charge around each ion. In the first place, the ions do not adjust to the moving ion infinitely quickly, and the atmosphere is

incompletely formed in front of the moving ion and incompletely decayed in its wake, Figure 3.9. The overall effect is the displacement of the centre of charge of the atmosphere a short distance behind the moving ion. Since the two charges are opposite, the result is a retardation of the moving ion. This reduction of the ions' mobility is called the relaxation effect, because the rearrangement of the ionic atmosphere is a relaxation of the ions into an equilibrium distribution. The electrophoretic effect is a second consequence of the ionic atmosphere. As we have seen, the central ion experiences a viscous drag as it moves through the solution. When the ionic atmosphere is present, this effect is enhanced because the ionic atmosphere moves in an opposite direction to the central ion. The enhanced viscous drag reduces the mobility of the ions, and hence also reduce their conductivities.

The quantitative formulation of these effects is far from simple, but the Debye-Hückel-Onsager theory is an attempt to obtain quantitative expressions at about the same level of sophistication as the Debye-Hückel theory itself. The theory leads to a Kohlrausch-like expression, equation 3.3, with

$$K = A + B_m^0 \qquad 3.24$$

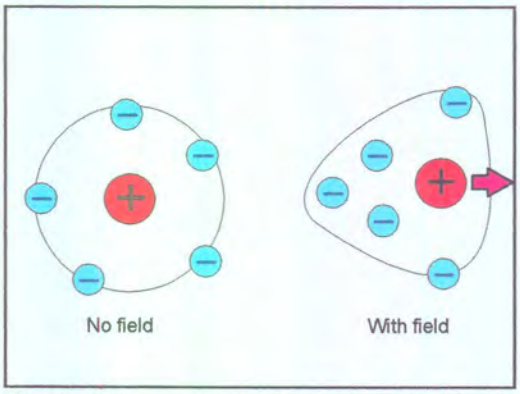

Figure 3.9 *Ionic atmospheres without and with an applied field respectively.*

$$A = \left(\frac{z^2 eF^2}{3\pi\eta}\right)\left(\frac{2}{\varepsilon RT}\right)^{\frac{1}{2}} \quad , \quad B = q\left(\frac{z^3 eF^2}{24\pi\varepsilon RT}\right)\left(\frac{2}{\pi\varepsilon RT}\right)^{\frac{1}{2}} \qquad 3.25$$

where ε is the electric permittivity of the solvent and q = 0.50 for a 1:1 electrolyte. R is the gas constant and T is the temperature. The slopes of the conductivity curves are predicted to depend on the charge type of the electrolyte, as the Kohlrausch measurements require.

The success of the Debye-Hückel-Onsager theory suggests that the model is substantially correct. A further test is to examine what happens when the effects of the ionic atmosphere are eliminated in some way. One way of doing this is to measure the conductivity at very high frequency, for when the central ion moves backwards and forwards very rapidly the retarding effect of the asymmetric atmosphere ought to average to zero. The Debye-Falkenhagen effect is the observation of this increase in conductivity. Another way of eliminating the atmosphere is to cause the ions to move so quickly that they outrun it. The first Wien effect is the observation of higher conductivities at high electric fields, as this predicts. (The second Wien effect is the observation of an increased conductivity as a result of the enhancement of the degree of ionisation of a weak electrolyte when a strong field is applied.)

The simple picture of ions surrounded by a diffuse ionic atmosphere fails at higher concentrations because ions stick together as pairs, triples, and so on. This can be seen from X-ray diffraction by ionic solutions, where peaks in the diffraction pattern can be interpreted in terms of definite ion-ion distances.

3.3 Diffusion and transport

For the discussion of this section, Atkins [4] was used extensively as well as Mulder [6] and Ho and Sirkar [7]

3.3.1 Diffusion: The thermodynamic view

In section 3.2 it was shown that the thermodynamic quantity that governs the direction of spontaneous change under conditions of constant temperature and pressure is the chemical potential . When a unit amount of solute particles moves from a region where their chemical potential is $\mu(1)$ to one where it is $\mu(2)$, the work (w) required is $w = \mu(2)-\mu(1)$. Suppose the chemical potential depends on the position x in the system, then the work required to move material from x to x + dx is

$$dw = \mu(x+dx)-\mu(x)=\{\mu(x)+(d\mu/dx)dx\}-\mu(s)=(d\mu dx)dx \qquad 3.26$$

The derivatives ought to be partial, under the constraints of constant pressure and temperature. In classical mechanics the work required to move an object through a distance dx against a force Γ is $dw = -\Gamma dx$. Therefore, by comparing these expressions, it was found that the slope of the chemical potential is an effective force. It can be written as the thermodynamic force:

$$\Gamma = -\left(\frac{\partial u}{\partial x}\right)_{p,T} \qquad 3.27$$

There is no real force pushing the particles down the slope of the chemical potential, for that is their natural drift as a consequence of the Second Law of thermodynamics and the hunt for maximum entropy. Another point is that the quantity is a molar force, the effective force per unit amount of substance. This will be discussed again in section 3.5

In a solution where the activity of the particles is a, the chemical potential is : $\mu = \mu^{\theta}+RT \ln a$. If the solution is not uniform the activity depends on the position and it can be written as:

$$\Gamma = -(d/dx)\{\mu^{\theta} + RT\ln a\} = RT(\partial \ln a/\partial x)_{p,T}.$$

If the solution is ideal a may be replaced by the concentration c, and so

$$\Gamma = -(RT/c)(\partial c/\partial x)_{p,T} \qquad 3.28$$

because (d/dx) ln c = (1/c) dc/dx. This shows that the thermodynamic force pushes in the direction of decreasing concentration (Γ is positive when dc/dx is negative). (Compare with equation 3.53)

From equation 3.28 it is possible to once again derive Fick's first law of diffusion from a thermodynamic viewpoint. (See also the derivation of equation 3.9) It is supposed that the flux of particles is a response to a thermodynamic force due to the concentration gradient. As a result of the balancing of the force Γ, and the viscous drag on the particles, they settle down to a drift speed s. This drift speed is proportional to the thermodynamic force, and so $s \propto \Gamma$. If the number density of particles is N, the flux of particles through an imaginary window in the fluid is equal to sN. All the particles within a distance $s\Delta t$, and therefore in a volume $s\Delta tA$, pass through the window of area A in the time Δt. (See section 3.2.2 and figures 3.5 and 3.7). Thus, $J = sN = scN_A$. But since s is proportional to Γ, which in turn is proportional to (1/c)(dc/dx), it follows that J is proportional to dc/dx.

Since $J=scN_A$, equation 3.9 can be written as

$$scN_A = -D(dN/dx) = -DN_A(dc/dx).$$

Expressing dc/dx in terms of Γ using equation 3.27 gives

$$s = -\left(\frac{D}{c}\right)\frac{dc}{dx} = \left(\frac{D}{RT}\right)\Gamma \qquad 3.29$$

Therefore, once the effective force and D is known, the drift speed of the particles (and vice versa) can be calculated, and this will be true whatever the origin of the force.

There is one case where we already know the drift speed and the effective force acting on a particle is known: An ion in solution has a drift speed s=uE (equation 3.12) when it experiences a force ezE, so that the force per mole is zFE. Therefore, substituting these known values into equation 3.29 gives

$$uE = \left(\frac{D}{RT}\right)(zeF), \text{ or } u = \frac{ezD}{kT} \qquad 3.30$$

This rearranges into the very important result known as the Einstein relation between the diffusion coefficient and the ionic mobility:

$$D = \frac{ukT}{ez} \qquad 3.31$$

The Einstein relation thus points out the relation between Fick's first law of diffusion and the drift speed of a particle.

The Einstein relation can be developed in two ways. In the first place, it can be used to find the Nernst-Einstein relation between the molar conductivity of an electrolyte and the diffusion coefficients of its ions. First from equation 3.14 it follows that for a cation

$$\lambda_+ = u_+ z_+ F = \frac{e z_+^2 D_+ F}{kT} = \frac{z_+^2 D_+ F^2}{RT} \qquad 3.34$$

and a similar expression for the anion. Then the sum of the two weighted by the numbers of ions from each formula unit, equation 3.30, is the limiting molar conductivity:

$$\Lambda_m^0 = (F^2 / RT)\{\nu_2 z_+^2 D_+ + \nu_- z_-^2 D_-\} \qquad 3.33$$

This is the so called Nernst-Einstein relation. One application of this expression is the determination of ionic diffusion coefficients from conductivity measurements; another is the prediction of conductivities using models of ionic diffusion.

The other development of the Einstein relation leads to the Stokes-Einstein relation between the diffusion coefficient and the viscosity of the solution. By combining the expressions s = iE and s = ezE/f (which comes from equation 3.11), one obtains

$$u = \frac{ez}{f} \qquad 3.34$$

as a relation between an ion's mobility and its hydrodynamic radius. However since u=ezD/kT, it can be written that

$$D = \frac{kT}{f} \qquad 3.35$$

This is the so called Stokes-Einstein relation. Therefore, since $f = 6\pi\eta a$ (see section 3.2.2), and if the hydrodynamic radius (Stokes radius) of the ion is known, the diffusion coefficient of the solution can be calculated from the viscosity of the solution. An important feature of this result, however, is that it is independent of the charge of the diffusing particle. Therefore, it also applies in the limit of a vanishingly small charge; that is, it also applies to neutral particles. This means that viscosity measurements can be used to estimate the diffusion coefficients for molecules in solution.

3.4 Diffusion

The following discussion will concern the time-dependent diffusion processes, where the interest will be in the spreading of inhomogeneities. An example is the concentration distribution in a solvent to which a solute is added.

3.4.1 The diffusion equation

This explanation concentrates on the diffusion of particles, but similar arguments also apply to the diffusion of properties. The aim is to obtain an equation for the rate of change of the concentration of particles in some inhomogeneous region.

Consider a thin slab of cross-sectional area A and extending from x to $x+\Delta x$, Figure 3.10. (Compare with Figures 3.5 and 3.7) Let the number density at x be N at the time t. JA is the number of particles that enter the slab per unit time, and so the increase in concentration inside the slab (which has volume $A\Delta x$) on account of the flux from the left is

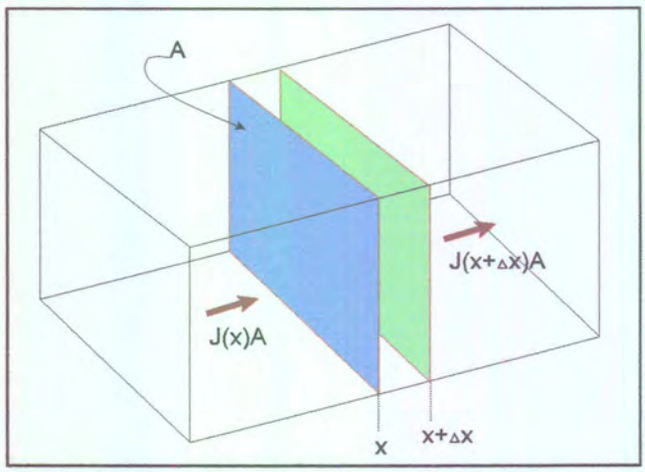

Figure 3.10 *The net flux in a region is the difference between the flux entering the region from a high concentration and the flux leaving to the region of low concentration.*

$$\partial N/\partial t = J(x)\, A/A\Delta x = J(x)/\Delta x.$$

There is also an outflow through the right-hand window. The flux there is $J(x+\Delta x)$, and the change of concentration due to this efflux is

$$\partial N/\partial t = -J(x+\Delta x)\, A/A\Delta x = -J(x+\Delta x)/\Delta x.$$

The net rate of change of concentration is therefore

$$\partial N/\partial t = \{J(x) - J(x+\Delta x)/\Delta x)/\Delta x.$$

The fluxes are proportional to the concentration gradients at the two windows. Using Fick's first law it can be written as:

$$J = (x) - J(x+\Delta x) = -D\left(\frac{\partial N(x)}{\partial x}\right) + D\left(\frac{\partial N(x+Xx)}{\partial x}\right)$$

$$= -D\left(\frac{\partial N}{\partial x}\right) + D\frac{\partial}{\partial x}\left\{N + \left(\frac{\partial N}{\partial x}\right)\Delta x\right\} = D(\partial^2 N / \partial x^2)\Delta x$$

(Unless otherwise specified, N means N(x,t).) Substitution of this relation into the

expression for the rate of change of concentration in the slab leads to the diffusion equation :

$$\partial N / \partial t = D(\partial^2 N / \partial^2 x) \qquad 3.36$$

This is also called Fick's Second Law of Diffusion.

Concerning the diffusion equation (the above mentioned equation) it shows that the rate of change of concentration is proportional to the curvature (more precisely, the second derivative) of the concentration with respect to distance. If the concentration changes sharply from point to point (if the distribution is highly wrinkled) then the concentration changes rapidly with time. If the curvature is zero, then the concentration is constant in time. For example, if the concentration decreases linearly with distance, then the concentration at any point is constant because the inflow of particles is exactly balanced by the outflow. The diffusion equation can be regarded as exactly balanced by the outflow. The diffusion equation can be regarded as a mathematical formulation of the intuitive notion that there is a natural tendency for the wrinkles in a distribution to disappear.

The diffusion equation is a second-order differential equation with respect to space and a first-order differential equation with respect to time. Therefore, in order to arrive at a solution two boundary conditions must be specified for the spatial dependence and a single initial condition for the time-dependence. This can be illustrated by the specific example of a solvent in which the solute is initially coated on one surface (e.g. a layer of sugar on the bottom of a deep beaker of water). The initial condition is that at $t = 0$ all N_0 particles are concentrated on the yz-plane (of area A) at $x = 0$. The boundary conditions are a), that the concentration must everywhere be finite and b), that the total number of particles present is N_0 at all times. The solution of the diffusion equation under these conditions is

$$N = \left\{N_0 / A(\pi Dt)^{\frac{1}{2}}\right\} e^{-x^{2/4Dt}} \qquad 3.37$$

as may be verified by direct substitution. Another solution is for the case of a localised concentration of solution in a three-dimensional solvent (a sugar lump suspended in a large flask of water): The concentration distribution is spherically symmetrical, and at a radius r is

$$N = \left\{N_0 / 8(\pi Dt)^{\frac{3}{2}}\right\} e^{-r^{2/4Dt}} \qquad 3.38$$

The solutions are useful for experimental determinations of diffusion coefficients. In the capillary technique a capillary tube, open at one end and containing a solution, is immersed in a well stirred larger quantity of solvent, and the change of concentration in the tube is measured at a series of times. The solute diffuses from the open end of the capillary at a rate that can be calculated by solving the diffusion equation with the appropriate boundary conditions, and so D may be determined. In the diaphragm technique the diffusion occurs through the capillary pores of a sintered glass diaphragm separating the well-stirred solution and solvent. The concentrations are monitored and then related to the solutions of the diffusion equation corresponding to this arrangement.

3.4.2 Properties of the solutions

The solutions of the diffusion equation, such as those above, can be used to predict the concentration of particles (or the value of some other physical quantity, such as the temperature in a non-uniform system) at any location. The solutions may also be used to calculate the mean distances through which the particle diffuse in a given time.

The number of particles in a slab of thickness dx at x is NAdx, and so the

probability that any of the N_0 particles is there is $NAdx/N_0$. If the particle is there, then it has travelled a distance x form the origin. Therefore, the mean distance travelled by all the particles is the sum of each x weighted by the probability of its occurrence:

$$\langle x \rangle = \int_0^\infty \frac{xNA\,dx}{N_0} = \sqrt{\frac{1}{\pi Dt}} \int_0^\infty x e^{-\frac{x^2}{4Dt}} dx = 2\sqrt{\frac{Dt}{\pi}} \qquad 3.39$$

The average distance of diffusion varies as the square root of the lapsed time. If the Stokes-Einstein relation is used for the diffusion coefficient, the mean distance traveled by particles of radius a in a solvent of viscosity η is

$$\langle x \rangle = (2kT / 3\pi^2 \eta a)^{\frac{1}{2}} \sqrt{t}. \qquad 3.40$$

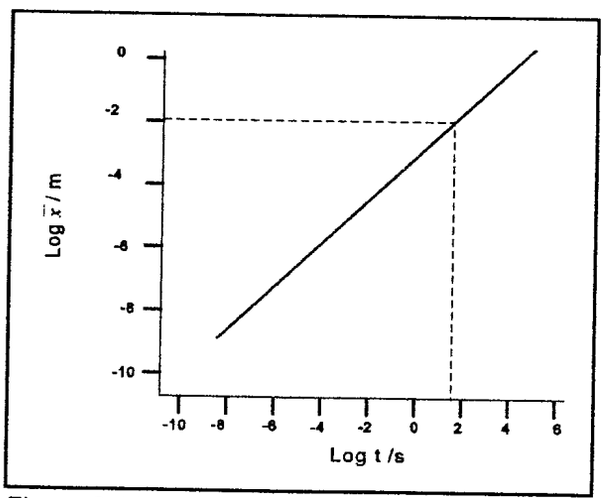

Figure 3.11 *The root mean square distance covered by particles with D = 5 x 10^{-6} cm^2 s^{-1}*

The root mean square distance traveled by diffusing particles is

$$\bar{x} = \left\{ \int_0^\infty x^2 N A dx / N_0 \right\}^{\frac{1}{2}} = (2DT)^{\frac{1}{2}} \qquad 3.41$$

This quantity is a valuable measure of the spread of particles when they can diffuse in both directions from the origin (for then $\langle x \rangle = 0$ at all times). The value of x for particles with a typical diffusion coefficient ($D = 5 \times 10^{-6} cm^2 s^{-1}$) is shown in Figure 3.11: This shows how long it takes for diffusion to increase x to about 1 cm in an unstirred solution: **diffusion is a very slow process**.

The proportion of particles that remain within a distance $\bar{x}$ of the origin is a useful number because it indicates how many particles remain close to their original position. Since the number in the slab at x is NAdx, the total number in all the slabs up to the one at $\bar{x}$ is the sum (integral).

$$N(x \leq x) = \int_0^{\bar{x}} N A dx = 0.68 N_0 \qquad 3.42$$

It follows that the proportion of particles inside the range $0 \leq x \leq \bar{x}$ is 0.68. Therefore, over two-thirds of the particles are still close to the origin and only 32 % have escaped beyond $\bar{x}$ (but do not forget that $\bar{x}$ increases with time). (The 0.68 and 32 % values are determined statistically)

3.4.3 Diffusion with convection

Because diffusion is so slow, reaction vessels are generally stirred and the slow diffusion of particles is dominated by brute-force mixing. The transport of particles arising from the motion of a streaming fluid is called convection. If diffusion is ignored, the flux of particles through an area A in a time Δt when the fluid is streaming at a velocity υ can be calculated in the way we have used

several times before (counting the particles within a distance $\upsilon\Delta t$), and is

$$J = (Na\upsilon\Delta t)/A\Delta t = N\upsilon \qquad 3.43$$

J is called the convective flux. This flux contributes to the concentration of particles in a region, and a calculation similar to the one already done gives the rate of change of concentration in a slab of thickness Δx and area A as

$$\partial N / \partial t = \{AJ(x) - AJ(x+\Delta x)\} / A\Delta x$$
$$= \upsilon\{N - [N + (\partial N / \partial x)\Delta x]\}\Delta x = -\upsilon(\partial N / \partial x) \qquad 3.43$$

Velocity was assumed constant.

When both diffusion and convection are of similar importance the total change of concentration in a region is the sum of the two effects, and so the generalised diffusion equation is

$$\partial N / \partial t = D(\partial^2 N / \partial x^2) - \upsilon(\partial N / \partial x) \qquad 3.45$$

A further important refinement, which is important in chemistry, is the possibility that the concentrations of particles may change as a result of reaction. When this is incorporated into the last equation, a powerful differential equation for discussing the properties of reacting, diffusing, convecting systems: it is the basis of reactor design in chemical industry and of the utilisation of resources in living cells.

3.4.4 The statistical view of diffusion

An intuitive picture of diffusion is that the particles move in a series of small steps and gradually migrate from their original positions. To explore this idea by building a model which assumes that the particles can leap through a distance d in a time τ, so that the distance traveled by a particle in a time t is $(t/\tau)d$. This does not mean that the particle will be found at that distance from the origin. The direction of each step may be different, and the net distance traveled must take this into account. To simplify the discussion allow the particles to travel only along a straight line (the x-axis), and for each step (t the left or the right) to be through the same distance d each time, to obtain the one-dimensional random walk.

When the calculation is carried through, it turns out that the probability of being at a distance x from the origin after an interval t is

$$P = (2\tau / \pi t)^{\frac{1}{2}} e^{-x^{2\tau/2td^2}} \qquad 3.46$$

This has precisely the same form as equation 3.37, the difference of detail arising from the fact that in this calculation the particles can migrate in either direction from the origin and may reside only at discrete points separated by d instead of being anywhere on a continuous line. This suggests that diffusion can indeed be interpreted as the outcome of a large number of steps in random directions. Furthermore, the details of the calculation also show that the diffusion equation is not valid when the particles have had time to take only very few steps.

Comparison of the two exponents in equations 3.37 and 3.46 leads to the Einstein-Smoluchowski relation between the diffusion coefficient and the step length and rate. From the identification $2d^2/\tau=4D$ it follows that:

Einstein-Smoluchowski relation : $D=d^2/2\tau$ 3.47

The Einstein-Smoluchowski relation is the central connection between the microscopic details of particle motion and the macroscopic parameters relating to diffusion (e.g. the diffusion coefficient and, through the Stokes-Einstein relation, the viscosity). It also brings us back full circle to the properties of gases. For if d/τ is interpreted as a mean speed of particles $\bar{c}$, and d is interpreted as a mean free path (λ), then the Einstein-Smoluchowski relation turns into $D = \frac{1}{2}\lambda \bar{c}$, which is the same expression that we obtained from the kinetic theory of gases. This shows that the diffusion of a perfect gas can be interpreted as a random walk with an average step size equal to the mean free path.

3.5 Transport in membranes.

Transport in membranes can be subdivided into two main groups namely transport through porous membranes and transport through non-porous membranes. Some features of the different transport meganisms, for example the driving force, stay the same. For this reason, both porous and non-porous transport were considered and at the end a unified mechanism was investigated.

3.5.1 Introduction

A membrane may be defined as a permselective barrier between two homogeneous phases. A molecule or a particle is transported across the membrane from one phase to the other because a force acts on that molecule or particle. The extent of this force is determined by the gradient in potential, or approximately by the difference in potential, across the membrane (ΔX) divided by the membrane thickness (ℓ), i.e. (also compare the derivation of equation 3.28)

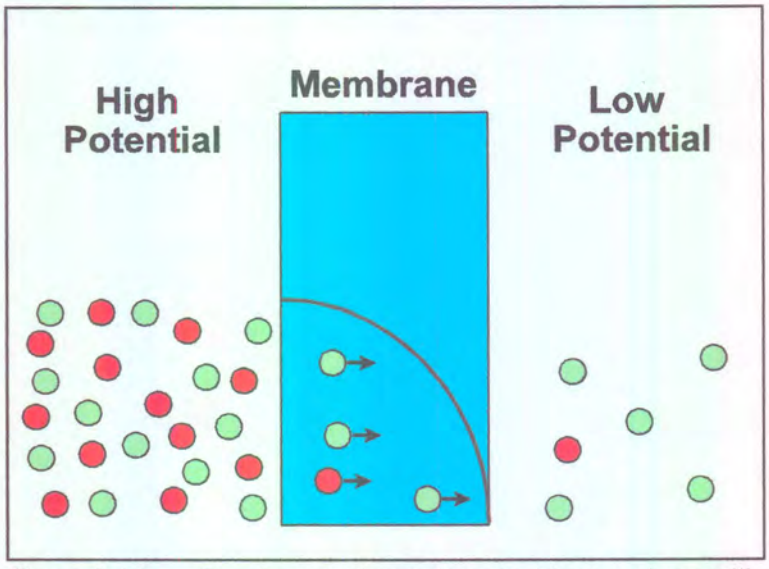

Figure 3.12 *Passive membrane transport from a phase with a high potential to one with a low potential.*

$$\text{driving force} = \frac{\Delta X}{\ell} \qquad 3.48$$

Two main potential differences are important in membrane processes, the chemical potential difference ($\Delta\mu$) and the electrical potential difference (ΔF). (The electro-chemical potential is the sum of the chemical potential and the electrical potential). Other possible forces such as magnetic fields, centrifugal fields and gravity will not be considered.

In passive transport, components or particles are transferred from a high potential to a low potential (See Figure 3.12, section 3.2.2 and section 3.3)

The driving force, in passive transport, is the gradient in potential ($\partial X/\partial x$). Instead of differentials it is often more useful to use differences ($\partial X/\partial x \cong \Delta X/\Delta x$). The average driving force (F_{ave}) is equal to the difference in potential across the membrane divided by the membrane thickness: (Compare with Figure 3.4)

$$F_{ave} = -\frac{\Delta X}{\ell} \qquad 3.49$$

If no external forces are applied to this system, it will reach equilibrium when the potential difference has become zero. When the driving force is kept constant, a constant flow will occur through the membrane after establishment of a steady state. There is a proportionality relationship (A) between the flux (J) and the driving force (X), i.e.

$$J = AX \qquad 3.50$$

The proportionality factor A, determines how fast the component is transported through the membrane or A is a measure of the resistance exerted by the membrane as a diffusion medium. [6, 7]

Another form of passive transport is facilitated or carrier-mediated transport (active transport). Here, transport of a component across a membrane is enhanced by the presence of a carrier. The carrier specifically interacts with one or more specific components in the feed and an additional mechanism (besides free diffusion) results in an increase in transport. It is possible that components can be transported against their chemical potential gradient in carrier-mediated membrane transport. Active transport is mainly found in living cell membranes where the energy is provided by ATP. [6, 8] Facilitated transport however, is beyond the scope of this thesis.

3.5.2 Driving Forces

Transport across a membrane takes place when chemical or electrical potential difference acts on the individual components in the system. The potential differences arises as a result of differences in either pressure, concentration,

temperature or electrical potential. Most transport processes take place because of a difference in chemical potential $\Delta\mu$. Under isothermal conditions (constant temperature), pressure and concentration contribute to the chemical potential of component i according to; (Compare with equation 3.28)

$$\mu_i = \mu_i^\circ + RT \ln a_i + V_i P \qquad 3.51$$

with a_i (which is part of the concentration term) and V_i the activity and molar volumes of component i. P indicates pressure (part of the pressure term). The term μ_i° is a constant.

$$a_i = \gamma_i x_i \qquad 3.52$$

where γ_i is the activity coefficient and x_i the mole fraction. For ideal solutions the activity coefficient $\Rightarrow 1$, and the activity becomes equal to the mole fraction. The chemical potential difference $\Delta\mu_i$ can be subdivided into a difference in composition and a difference in pressure according to

$$\Delta\mu_i = RT\,\Delta \ln a_i + V_i \Delta P \qquad 3.53$$

The composition contribution is equal to the product RT and the logarithm of the composition (activity or mole fraction).

A simple method of comparing driving forces is to make them dimensionless. As shown in Figure 3.12, the driving force is the potential gradient, and the average driving force is the potential difference across the membrane divided by the membrane thickness. (equation 3.48) If the chemical potential and the electrical potential are considered to be the driving forces and assuming ideal conditions,

i.e. $a_i = x_i$ and $\Delta \ln x_i \approx x_i^{-1}$. Equation 3.49 becomes

$$F_{ave} = \frac{RT}{\ell}\frac{\Delta x_i}{x_i} + \frac{z_i \Gamma}{\ell}\Delta E + \frac{V_i}{\ell}\Delta P \qquad 3.54$$

On multiplying equation 3.54 by the factor ℓ/RT (= mol/N), the driving forces become dimensionless:

$$F_{dim} = \frac{\Delta x_i}{x_i} + \frac{z_i \Gamma}{RT}\Delta E + \frac{V_i}{RT}\Delta P \qquad 3.55$$

or

$$F_{dim} = \frac{\Delta x_i}{x_i} + \frac{\Delta E}{E^*} + \frac{\Delta P}{P^*} \qquad 3.56$$

where $P^* = RT/V_i$ and $E^* = RT/(z_i\Gamma)$

The magnitude of the various driving forces being the pressure, electrical potential or the concentration, can easily be compared with each other using equation 3.56. The concentration term $\Delta x_i/x_i$ is often equal to unity, while the pressure term is strongly dependent on the kind of component involvement. The electrical potential depends on the value of z_i. Electrical potential is a very strong driving force in comparison to pressure, which is very weak.

3.5.3 Transport through porous membranes

In porous membranes a large variety of pore geometries are possible. Some possible geometries of porous membranes can be seen in Figure 3.13. In some membranes, such geometries (or structures) exist over the whole membrane

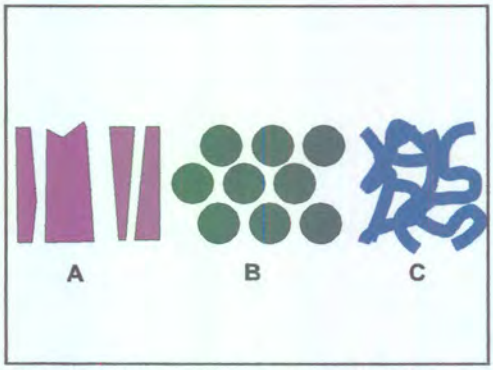

Figure 3. 13 *Some characteristic geometries found in porous membranes.*

thickness and here the resistance is determined by the total membrane thickness. On the other hand, some membranes are asymmetric in their structure. This implies that the resistance is determined only by the porous top layer of the membrane. The existence of these different pore geometries also implies that different models have been developed to describe the transport adequately. [6, 7] The simplest representation is one in which the membrane is considered as a number of parallel cylindrical pores, perpendicular to the membrane surface. (See Figure 3.13 A).

The length of each of the cylindrical pores is equal to the membrane thickness. The volume flux through these pores may be described by the Hagen-Poiseuille equation. Assuming that all the pores have the same radius, it can be written as follows:

$$J = \frac{\varepsilon r^2}{8\eta\tau}\frac{\Delta P}{\Delta x} \qquad 3.57$$

This indicates that the solvent flux is proportional to the driving force (the pressure difference, ΔP), across a membrane of thickness Δx and inversely proportional to the viscosity η. The quantity ε is the surface porosity, which is the fractional pore area. (ε is equal to the ratio of the pore area to the membrane

area A_m multiplied by the number of pores n_p, $\varepsilon = \pi r^2/A_m$), while τ is the pore tortuosity (which for cylindrical perpendicular pores, the value will be equal to unity).

Membranes consisting of the structure depicted in Figure 3.13 B, i.e. a system of closed packed spheres, can be found in organic and inorganic sintered membranes of in phase inversion membranes with a nodular top layer structure. Such membranes can best be described by the Kozeny-Carman relationship:

$$J = \frac{\varepsilon^3}{K\eta S^2(1-\varepsilon)^2}\frac{\Delta P}{\Delta x} \qquad 3.58$$

ε is the volume fraction of the pores, S the internal surface area and K the Kozeny-Carman constant, which depends on the shape of the pores and the tortuosity.

Phase inversion membranes frequently show a sponge-like structure, as schematically depicted in Figure 3.13 C. The volume flux through these membranes are described either by the Hagen-Poiseulle or the Kozeny-Carman relation, although the morphology is completely different.

3.5.4 Transport through nonporous membranes

Even though the following discussion is concerned with the transport of gases, it is imperative to understand the basic meganism of transport across the membrane (which is the same for solute particles), before the process of dialysis will be discussed in more detail.

When the sizes of molecules or particles are in the same order of magnitude, porous membranes cannot affect the separation. In this case nonporous membranes must be used. However, the term nonporous is rather ambiguous

because pores are present on a molecular level in order to allow transport even in such membranes. The existence of these dynamic "molecular pores" can be adequately described in terms of free volume.

Initially transport through these dense membranes will be considered via a somewhat simple approach. Although there are some similarities between gaseous and liquid transport, there are also a number of differences. In general, the affinity of liquids and polymers is much greater than that between gases and polymers (The solubility of a liquid in a polymer is much higher than that of a gas.). A high solubility has a tremendous influence on the diffusitivity, making the polymer chains more flexible and resulting in an increased permeability.

The transport of a gas, liquid of a vapour through a dense, nonporous membrane can be described in terms of a solution-diffusion mechanism:

$$\text{Permeability}(P) = \text{solubility}(S) \bullet \text{Diffusivity}(D) \qquad 3.59$$

Solubility is a thermodynamic parameter and gives a measure of the amount of penetrant sorbed by the membrane under equilibrium conditions. The solubility

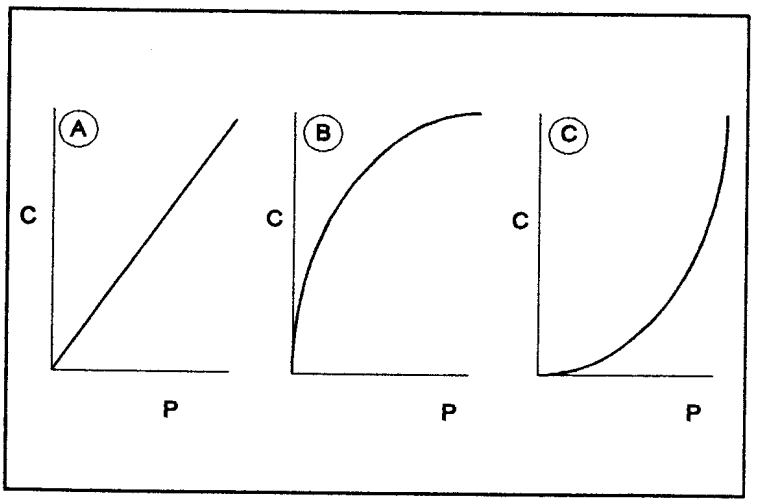

Figure 3.14 *Schematic drawing of sorption isotherms for ideal and non-ideal systems.*

of gases in a polymer is very low and can be described by Henry's law. With vapours and liquids however, the situation is not ideal, and Henry's law does not apply. The diffusivity on the other hand is a kinetic parameter which indicates how fast a penetrant is transported through the membrane. Diffusivity is dependant on the geometry of the penetrant for as the molecular size increases, the diffusion coefficient decreases. However, the diffusion coefficient is concentration dependent with interacting systems and even large molecules, having the ability to swell the polymer, can have large diffusion coefficients.

The solubility of gases in polymers is generally quite low and it is assumed that the gas diffusion coefficient is constant. Such cases can be considered as ideal systems where Fick's first law of diffusion (see equation 3.9) is obeyed. On the other hand, the solubility of liquids and vapours can be relatively high and the diffusion coefficient is now assumed to be concentration dependent, thus the diffusivities increase with increasing concentration.

Two separate cases must therefore be considered, ideal systems where both the diffusivity and the solubility are constant, and concentration-dependent systems where the solubility and the diffusivity are functions of the concentration. (Other cases can be distinguished where the solubility and the diffusivity are functions of other parameters, such as time and place. These phenomena, often termed "anomalous", can be observed in glassy polymers where relaxation phenomena occur or in heterogeneous (porous) types of membranes.

For ideal systems, where the solubility is independent of the concentration, the sorption isotherm is linear (Henry's law), i.e. the concentration inside the polymer is proportional to the applied pressure (Figure 3.14 A). This behaviour is normally observed with gases in elastomers. With glassy polymers the sorption isotherms is generally curved rather than linear (see Figure 3.14 B), whereas such strong interactions occur between organic vapours or liquids and polymer, the sorption isotherm is generally non-linear, especially at high vapour pressures (Figure 3.14

C). Such non-ideal sorption behaviour can be described by free volume models and Flory-Huggins thermodynamics.

The solubility can be obtained from equilibrium measurements in which the volume of gas taken up is determined when the polymer sample is brought into

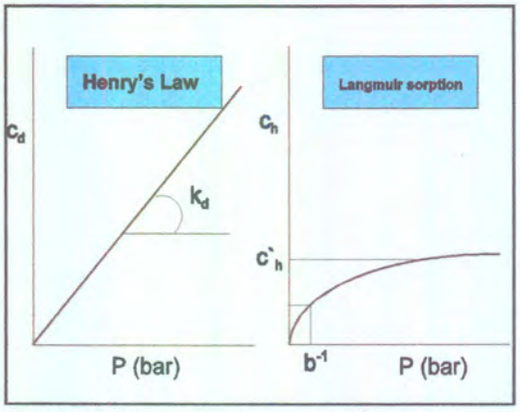

Figure 3.15 *The two contributions in the dual sorption theory.*

contact with a gas at a known applied pressure. For glassy polymers where the solubility of a gas often deviates in the manner shown in Figure 3.14 B, such deviation can be described by the dual sorption theory, in which it is assumed that two sorption mechanisms occur simultaneously, i.e. sorption according to Henry's law and via a Langmuir type sorption. This is shown in Figure 3.15.

In this case, the concentration of gas in the polymer can be given as the sum produced by the two sorption modes

$$c = c_d + c_h \qquad 3.60$$

or

$$c = k_d P + \frac{c'_h bP}{1 + bP} \qquad 3.61$$

where k_d is the Henry's law constant [(k_d]: $cm^3(STP).cm^3.bar^{-1}$ which is equal to the solubility coefficient S, b is the hole affinity constant ([b]: bar^{-1}) and c'_h is the saturation of constant [c'_h]: cm^3 (STP).cm^{-3}). The dual sorption model often gives a good description of observed phenomena and it is very frequently used to describe sorption in glassy polymers. From a physical point of view, however, it is difficult to understand the existence of two different sorption modes for a given membrane which implies the existence of two different types of sorbed gas molecules (the dual sorption theory can also be considered as a three parameter fit).

Permeability is both a function of solubility and diffusivity (see equation 3.58). The simplest way to describe the transport of gases through membranes is via Fick's first law (equation 3.9).

At this point in time it is imperative to once again discuss the diffusion equations which are applicable for transport across membranes. It will be noted that some of these equations were mentioned earlier in section 3.4. It was however thought appropriate to mention them again (sometimes in a different form) to show their applicability to membrane processes.

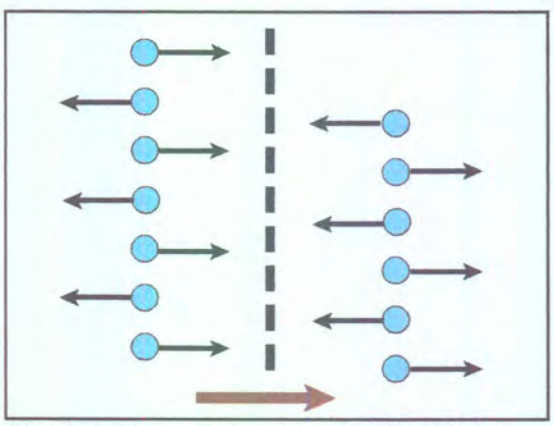

Figure 3.16 *Schematic drawing of diffusion as a result of random molecular motions.*

Diffusion may be considered as statistical molecular transport as a result of the random motion of the molecules. A (macroscopic) mass flux occurs because of a concentration difference. Imagine a plane with more molecules on one side than on the other, then a net mass flux will occur because more molecules move to the right than to the left. (As shown schematically in Figure 3.16 and see also Figure 3.10). Now, consider two planes (e.g. a thin part of a membrane) at the points x and x + δx (Figure 3.17). The quantity of penetrant which enters the plane at x at time δt is equal to J. δt. The quantity of penetrant leaving the plane at x + δx is [J + (∂J/∂x)δx]δt.

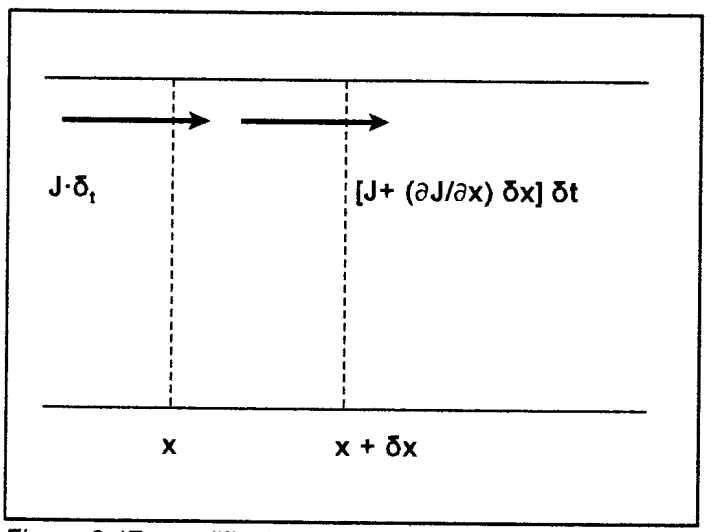

Figure 3.17 *diffusion across two planes situated at the points x and x + δx in the cross section of a membrane.*

The change in concentration (dc) in the volume between x and x + δx is

$$dc = \frac{[J\,\delta t - (J + \left(\frac{\partial J}{\partial x}\right)\delta x)\delta t]}{\delta x} \qquad 3.62$$

which yields

$$dc = -\left(\frac{\partial J}{\partial x}\right)\delta t \qquad 3.63$$

For an infinite small section and an infinite small period of time ($\delta x \Rightarrow 0$, $\delta t \Rightarrow 0$), equation 3.63 becomes

$$\frac{\partial c}{\partial t} = -\frac{\partial J}{\partial x} \qquad 3.64$$

Substitution of equation 3.9 into equation 3.64 yields

$$\frac{\partial c}{\partial t} = -\frac{\partial}{\partial x}\left(D\frac{\partial c}{\partial x}\right) \qquad 3.65$$

If it is assumed that the diffusion coefficient is constant, then

$$\frac{\partial c}{\partial t} = -D\frac{\partial^2 c}{\partial x^2} \qquad 3.66$$

This expression, also known as Fick's second law (compare with equation 3.36), gives the change in concentration as a function of distance and time.

The order of magnitude of the diffusion coefficients of molecules permeating through non-porous membranes depends on the size of the diffusing particles and on the nature of the material through which diffusion occurs. In general, diffusion coefficients decrease as the particle size increases (compare the Stokes-Einstein equation 3.35).

Another example of diffusion being very dependent on the medium through which

it proceeds is shown in Figure 3.17. A schematic representation of the values of the diffusion coefficients in water (or in another low molecular liquid) and in a rubbery polymer as a function of the molecular weight of the diffusing component. In water, the diffusion coefficient decreases only slightly with increasing molecular weight compared to the situation with rubber. This is the normal behaviour when diffusion occurs in non-interacting systems. When concentration-dependent systems are involved, however, the membrane may swell considerably and the diffusing medium may also change significantly. Such strong interactions can have a large impact on diffusion phenomena.

Because of swelling the penetrant concentration inside the polymer will increase. The size will become less important. In general, it can be said that the effect of concentration will increase as the diffusion coefficients decrease at lower swelling values. This is shown schematically in Figure 3.18 (right-hand figure), where the diffusion coefficients of a given low molecular component are plotted versus the degree of swelling. This Figure 3.18 shows clearly that the diffusion coefficients vary by some orders of magnitude with different degrees of swelling, resulting in the occurrence of different types of separation.

Another way of describing diffusion processes is in terms of friction. The penetrant molecules move through the membrane with a velocity v because of a force $\partial\mu/\partial x$ acting on them. This force (the chemical potential gradient) is necessary to maintain the velocity v against the resistance of the membrane. If the frictional resistance is denoted as f, the velocity is then given by

$$v = -\frac{1}{f}\left(\frac{\partial \mu}{\partial x}\right) \qquad 3.67$$

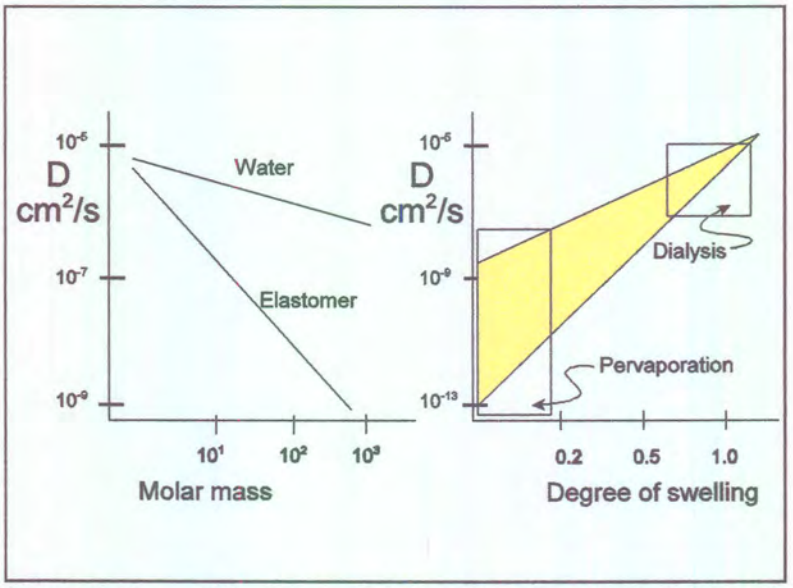

Figure 3.18 *Diffusion coefficients of components in water and in an elastomer membrane as a function of the molar mass and in a polymer as a function of the degree of swelling for a given low molar mass penetrant.*

It can be shown from a frictional model that equation 3.67 can be written as:

$$v = -m\left(\frac{\partial \mu}{\partial x}\right) \qquad 3.68$$

and the quantity of molecules passing through the cross-sectional area per unit time is given by

$$J = v\,c - mc\left(\frac{\partial \mu}{\partial x}\right) \qquad 3.69$$

(Note that the reciprocal of the friction coefficient is the mobility coefficient m.)

The thermodynamic diffusion coefficient D_T is related to the mobility by the relation

$$D_T = m \,.\, RT \qquad 3.70$$

and since the chemical potential μ is given by (see equation 3.28 and 3.51)

$$\mu = \mu^\circ + RT \ln a \qquad 3.71$$

equation 3.69 can be rewritten as

$$\begin{aligned} J &= -\frac{D_T}{RT} c \left(\frac{\partial \ln a}{\partial x}\right) \\ &= -D_T \left(\frac{\partial \ln a}{\partial \ln c}\right)\left(\frac{\partial c}{\partial x}\right) \end{aligned} \qquad 3.72$$

and by comparison with Fick's law the following is obtained

$$D = D_T \left(\frac{d \ln a}{d \ln c}\right) \qquad 3.73$$

Since for ideal systems the activity a is equal to the concentration c and $D = D_T$, equation 3.72 will reduce to Fick's law. However, for non-ideal systems, (organic vapours and liquids) activities must be used rather than concentrations. The fact that D_T changes with the concentration (or activity) indicates that the presence of the penetrant modifies the properties of the membrane.

3.5.5 Transport through membranes. A unified approach.

A number of 'macroscopic' models have been given in the preceding paragraphs in an attempt describe the large differences in the separation principles involved in various membrane processes and membranes, with the extremes being

observed for porous membranes (microfiltration/ultrafiltration) and nonporous membranes (gas separation/pervaporation/dialysis). The model descriptions can be classified as those based on a phenomenological approach and on non-equilibrium thermodynamics, and those mechanistic models such as the pore model and the solution-diffusion model. The phenomenological models are so-called 'black-box' models and provide no information as to how the separation actually occurs. Mechanistic models try to relate separation with structural-related membrane parameters in an attempt to describe mixtures. These latter models also provide information on how separation actually occurs and which factors are important.

The objective is now to unify all the membrane processes under one mode, in order to relate the various membrane processes with each other in terms of driving forces, fluxes and basic separation principles. To do so, the starting point must be a simple model, such as a generalised Fick equation or a generalised Stefan-Maxwell equation (for the use in defining friction coefficients). In order to describe transport through a porous membrane or through a nonporous membrane, two contributions must be taken into account, the diffusional flow (v) and the convective flow (u). The flux of component i through a membrane can be described as the product of velocity and concentration, i.e.

$$J_i = c_i(v_i + u) \text{ (see Figure 3.19)} \qquad 3.74$$

The contribution of convective flow is the main term in any description of transport through porous membranes. In nonporous membranes, however, the convective flow term can be neglected and only diffusional flow contributes to transport. It can be shown by simple calculations that only convective flow contributes to transport in the case of porous membranes (microfiltration). Thus, for a membrane with a thickness of 100 μm, an average pore diameter of 0.1 μm, a tortuosity τ of 1 (capillary membrane) and a porosity ε of 0.6, water flow at 1 bar pressure difference can be calculated from the Poisseuille equation

(convective flow), i.e.

$$J_w = \frac{\varepsilon r^2}{8\eta\tau}\frac{\Delta P}{\Delta x} \approx \frac{0.6\ 0.25\left(10^{-7}\right)10^5}{8\ 10^{-3}\ 10^{-4}} \approx 2\ 10^{-3}\ m/s$$

The driving force for diffusion is the difference in chemical potential, and both the concentration (activity) and the pressure contribute to this driving force. However, it can be assumed that the "concentration" (or activity) on either side of the membrane is equal in microfiltration and hence the pressure difference must be the only driving force. Indeed, diffusive water flow as a result of this driving force is very small, as can be demonstrated as follows. The chemical potential difference can be written as:

$$\Delta\mu_w = v_w.\Delta p = 1.8.10^{-5}.10^5 = 1.8\,J/mol$$

$$J_w = L_p\frac{d\mu}{dx} \approx \frac{D_w}{RT}\frac{\Delta\mu_w}{\Delta x} = \frac{10^{-9}\,2}{2500\ 10^{-4}} \approx 10-8\,m/s$$

and a comparison of the value for the convective and diffusive contributions indicates quite clearly that diffusion can be neglected in this case.

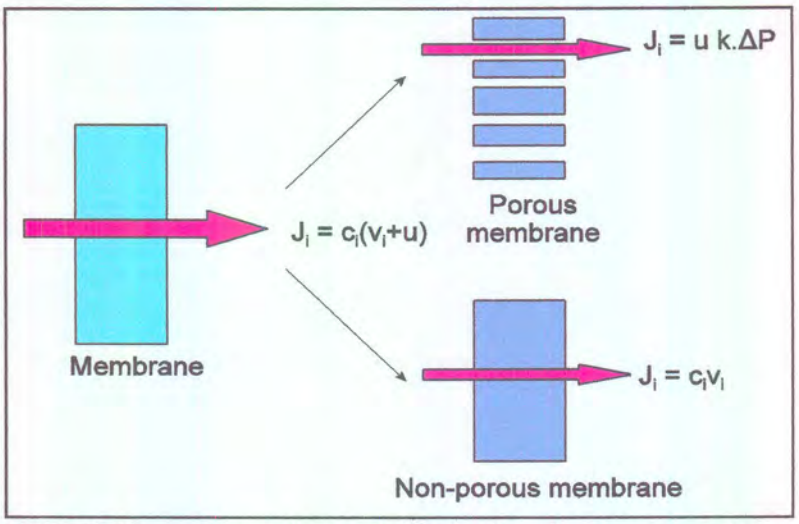

Figure 3.19 *Convective and diffusive flow in a porous and a non-porous membrane.*

Considering only the extreme cases, it can be stated that transport in porous membranes occurs by convection and in nonporous membranes by diffusion. However, in going from porous to nonporous membranes, an intermediate region exists where both contributions have to be taken into account.

The last part of this chapter will be devoted to a comparison of membrane processes where transport occurs through nonporous membranes. A solution-diffusion model will be used where each component dissolves into the membrane and diffuses through the membrane independently. As a result, simple equations will be obtained for the component fluxes involved in the various processes which allows to compare the processes in terms of transport parameters.

The flux of a component through a membrane may be described in terms of the product of the concentration and the velocity, i.e. convective flow makes no contribution (see equation 3.74). Hence,

$$J_i = c_i\ v_i \qquad 3.75$$

The mean velocity of a component in the membrane is determined by the driving force acting on the component and the frictional resistance exerted by the membrane, i.e.

$$v_i = \frac{X_i}{f_i} \qquad 3.76$$

The driving force is given by the gradient $d\mu/dx$. The frictional coefficient can be related to the thermodynamic diffusion coefficient D_T. If ideal conditions are assumed, i.e. if the thermodynamic diffusion coefficient is equal to the observed diffusion coefficient, equation 3.75 then becomes

$$J_i = \frac{D_i c_i}{RT}\frac{d\mu_i}{dx} \qquad 3.77$$

The chemical potential can be written as

$$\mu_i = \mu^\circ_i + RT \ln a_i + V_i.(p - p^\circ)$$

And substitution of equation 3.53 into equation 3.77 gives

$$J_i = \frac{D_i c_i}{RT}\left[RT\frac{d\ln a_i}{dx} + V_i\frac{dP}{dx}\right] \qquad 3.78$$

Figure 3.20 gives a representation of the process conditions necessary for describing transport through nonporous membranes, where the superscripts m and s refer to membrane and feed/permeate side, respectively. If it is assumed

that thermodynamic equilibrium exists at the membrane interfaces, i.e. that the chemical potential of a given component (liquid or gas) at the feed/membrane interface is equal in both the feed and the membrane, and furthermore, that the pressure inside the membrane is equal to the pressure on the feed side, the following equations may be obtained:

at the feed interface (phase 1/membrane):

$$\mu_{i,2^m} = \mu_{i,1^s} \Rightarrow a_{i,1^m} = a_{i,1^s} \qquad 3.79$$

and at the permeate interface (membrane/phase 2):

$$\mu_{i,1}{}^{m} = \mu_{i,2}{}^{s} \Rightarrow a_{i,2}{}^{m} = a_{i,2}{}^{s} e^{\left[\frac{-V_i(P_1 - P_2)}{RT}\right]} \qquad 3.80$$

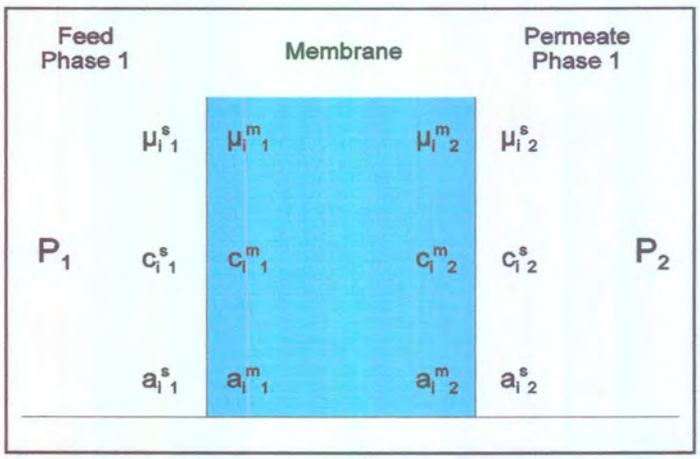

Figure 3.20 *Process conditions for transport through non-porous membranes.*

The activities at the feed interface can be written as

$$c_{i,1}^{m} \cdot \gamma_{i,1}^{m} = c_{i,1}^{s} \cdot \gamma_{i,1}^{s} \qquad 3.81$$

while the activities at the permeate interface are

$$c_{i,1}^{m} \gamma_{i,2}^{m} = c_{i,2}^{s} \gamma_{i,2}^{s} e^{\left[\frac{-V_i(P_1 - P_2)}{RT}\right]} \qquad 3.82$$

If the solubility constant K_i is defined as the ratio of the activity coefficients, we can write:

$$K_{i,1} = \frac{\gamma_{i,1}^{s}}{\gamma_{i,1}^{m}} \text{ and } K_{i,2} = \frac{\gamma_{i,2}^{s}}{\gamma_{i,2}^{m}} \qquad 3.83$$

or

$$c_{i,1}^{m} = K_{i,1}^{s} \text{ and } c_{i,2}^{m} = K_{i,2} \cdot c_{i,2}^{s} \qquad 3.84$$

Furthermore, if it is assumed that the diffusion coefficient is concentration-independent, Fick's law (equation 3.9) can be integrated across the membrane to give

$$J_i = -\frac{D_i}{\ell}(c_{i,2}^{m} - c_{i,1}^{m}) \qquad 3.85$$

After substitution of equations 3.81, 3.82 and 3.83 into equation 3.85 one arrives at

$$J_i = \frac{D_i}{\ell}\left(K_{i,1} c_{i,1}^{\ s} - K_{i,2} c_{i,2}^{\ s} e^{\left[\frac{-V_i(P_1-P_2)}{RT}\right]} \right) \qquad 3.86$$

and if $\alpha_i = K_{i,2} / K_{i,1}$ (i.e. the solubility coefficient are similar at both interphases) and $P_i = K_i.D_i$, then equation 3.86 converts into

$$J_i = \frac{P_i}{\ell}\left(c_{i,1}^{\ s} - \alpha_i c_{i,2}^{\ s} e^{\left[\frac{-V_i(P_1-P_2)}{RT}\right]} \right) \qquad 3.87$$

Equation 3.87 is the basic equation used to compare various membrane processes when transport occurs by diffusion. The phases involved in such processes are summarised in table 4.1.

Table 4.1 Phases involved in diffusion controlled membrane processes (L = Liquid, G = Gas)

Process	Phase 1	Phase 2
reverse osmosis	L	L
dialysis	L	L
gas separation	G	G
pervaporation	L	G

3.5.5.1 Reverse osmosis

Reverse osmosis is normally used with aqueous solutions containing a low molecular weight solute, which is often a salt. It can also be used for aqueous solutions containing very small amounts of organic solutes. This process involves the application of pressure to the liquid feed mixture as driving force, the total flux being given by the sum of the water flux J_w and the solute flux J_s. However, since this project is more concerned with the flux of ions across a

dialysis membrane, this section will not be discussed in detail.

3.5.5.2 Dialysis [7]

In general, the driving force for mass transfer is the potential gradient across the membrane thickness. Phenominological models used to describe mass transfer processes are concerned with the relationship between the driving force and the resulting flux. In dialysis, the primary flux is that due to diffusion, which is driven by the concentration gradient component of a gradient in chemical potential. While other driving forces may exist, (migration or pressure gradient component of chemical potential causing bulk flow) dialysis is fundamentally a diffusive process and is modelled as such by solution-diffusion theory. The cornerstone of this theory of course is Fick's first law of diffusion. This law is a simple phenomenological model that describes the potential/flux relationship for diffusive mass transfer. It states that the diffusive flux is proportional to the gradient in concentration, mole fraction or chemical potential at constant pressure. In the strictest sense, a system consisting of solute, solvent, and membrane is ternary rather than binary. However, a pseudobinary approach can be taken in which solute A diffuses through component B, where B can be defined as both the membrane and the solvent. The molar flux can be described by the following general form of Fick's first law of diffusion:

$$J_{Ay} = x_A(J_{Ay} + J_{By}) - c_t D_{AB}\frac{dx_A}{dy} \qquad 3.88$$

where J_{ay} and J_{by} are the molar fluxes of A and B in thy y-direction, x_A is the mole fraction of solute A, c_t is the total concentration of A and B, and D_{AB} is the binary diffusion coefficient. The first term on the right represents bulk flow resulting from unequal counter diffusion of A and B, whereas the second term gives the diffusive flux. In reasonably dilute solutions, the bulk flow term may be neglected

and the total molar concentration, c_t may be considered constant. Now equation 3.88 can be simplified to

$$J_{Ay} = -D_{AB}\frac{dc_A}{dy} \qquad 3.89$$

which is similar to equation 3.9. In dialysis, liquid phases containing the same solvent are present on both sides of the membrane in the absence of a pressure difference. The pressure terms can therefore be neglected and the following equation may be obtained from equation 3.87 if $\alpha_i = 1$. Assuming a linear concentration gradient and integrating equation 3.89 across the membrane,

$$J_{Ay} = \frac{D_{AB}(c_{1m} - c_{2m})}{\ell} \qquad 3.90$$

where c_{1m} and c_{2m} are concentrations within the membrane at each of its interfaces and ℓ is the membrane thickness.

A partition coefficient K can be defined as the ratio between membrane and external solution concentrations at equilibrium:

$$K = \frac{c_{1m}}{c_{1s}} = \frac{c_{2m}}{c_{2s}} \qquad 3.91$$

which is similar to the partition coefficient in general chromatography. Combining equations 3.90 and 3.91 and simplifying by eliminating the subscripts:

$$J = \frac{KD\Delta c}{\ell} \qquad 3.92$$

Since separation on a membrane is determined by the permeability, it is essential to once again illuminate this principle. The permeability can be defined as

$$P = \frac{KD}{\ell} \text{ and } R = \frac{\ell}{KD} \qquad 3.93$$

with R the membrane mass transfer resistance. Equation 3.92 can now be written as

$$J = P\Delta c = \frac{\Delta c}{R} \qquad 3.94$$

This simple equation describe the solute flux in dialysis indicating that it is proportional to the concentration difference. Separation arises from differences in permeability coefficients: thus macromolecules have much lower diffusion coefficients and distribution coefficients than low molecular weight components.

3.5.5.3 Gas permeation

In gas permeation or vapour permeation, both the upstream and downstream sides of a membrane consist of a gas or a vapour. However, once again this is not relevant to the membrane processes of interest.

3.5.5.4 Pervaporation

Pervaporation is a membrane process in which the feed side is a liquid while the permeate side is a vapour as a result of applying a very low pressure downstream.

3.5.5.5 Electrodialysis [6,7]

As discussed in paragraph 3.5.5.2, the concentration gradient of the solute species across the membrane is the driving force for solute transport across the membrane. Due to this reason, the extent of solute transfer in dialysis is limited by the condition of zero concentration gradient, at which time dialytic transfer stops. In electrodialysis, the continuous supply of electrical energy ensures a positive driving force. In classical electrodialysis electrolytes are usually transported from low concentrations to high concentrations. The practical requirements for ion (electrolyte) transfer can be described as follows:

The total electrical potential drop across an electrodialysis cell consist only partly of the concentration potential. The other part is to overcome the ohmic resistance of the cell. This ohmic resistance is caused by the friction of various ions with the membranes and water while being transferred from one solution to the other, resulting in an irreversible energy dissipation in the form of heat generation. The technical feasibility of electrodialysis as a mass separation process, that is its ability to separate certain ions from a given mixture, is mainly determined by the membranes used in the system. In a cation-exchange membrane, the fixed anions are in electrical equilibrium with the mobile cations in the interstices of the polymer. In contrast the mobile anions (co-ions) are more or less completely excluded from the polymer matrix because of their electrical charge which is identical to the fixed ions. This type of exclusion is called the Donnan exclusion.

3.6 References

1. Bard A.J., Faulkner L.R. (**1980**), Electrochemical Methods, Fundamentals and Applications. John Wiley & Sons, Inc.
2. Skoog D.A., Leary J.J., (**1992**), Principles of Instrumental Analysis, fourth edition, Saunders college publishing.
3. Valcarcel M., Luque de Castro M.D., (**1987**), Flow injection analysis. Principles and Applications. Ellis Horwood, Chichester.
4. Atkins P.W., (**1987**), Physical Chemistry, third edition. Oxford University Press.
5. Wesselingh J.A., Krishna R., (**1991**), Mass Transfer. Ellis Horwood.
6. Mulder M., (**1996**), Basic Principles of Membrane Technology, second edition. Kluwer Academic Publishers.
7. Ho W.S.W., Sirkar K.K., (**1992**), Membrane Handbook. Chapman & Hall.
8. Koryta J., (**1982**), Ions, Electrodes and Membranes. John Wiley & Sons.

Chapter 4

The evaluation of passive membranes for use in electrodialysis systems: Determination of chloride.

4.1 Introduction

As is evident from chapter 1, the use of an electrodialysis (ED) system as an analytical application is a rather rare and unexploited device. The use of ion-exchange membranes in the electrodialyser system as part of a water purification system was the norm for use in ED systems. A new dimension in analysis was opened with the introduction of the ED into the conduits of the FIA (Flow Injection Analysis) system. ED (equipped with an ion-exchange membrane) had been reported for the separation of alanine and aspartic acid by Strathmann and Chmiel. [1] Debets *et al.* [2] reported on the extraction of ephedrine from spiked plasma by also making use of an ED system equipped with an ion-exchange membrane. An application for the separation of leucine from ketoleucine in a flow injection system was reported by Kittsteiner-Eberle et al. [3] The latter group, however, was the first group to use an ED/FIA system equipped with a passive membrane instead of the usual ion-exchange membrane. This group, however, did not evaluate the ED/FIA system but was rather concerned with the separation of the amino acids.

The use of passive membranes in an ED/FIA system was thus going through its growing pains. To ascertain the right of existence of the use of an ED system equipped with a passive membrane, the system was evaluated bearing in mind the following points:

- The main thrust in the initial stages of this investigation was to ascertain whether or not there will be an increase in the mass transfer across the passive membrane with the introduction of the applied potential across the passive membrane.

- The next important part of the investigation was to establish if a change in the applied potential would lead to an improvement in the enhanced mass transfer (if any).
- Another important aspect that had to be considered was if there was, to be an increase in the mass transfer across the passive membrane, how would different membranes react to such an applied potential.

Since the evaluation of the ED/FIA system was a priority at this stage of the investigation, a suitable analyte had to be found. The main prerequisite for the analyte chosen was that the FIA system used for its analysis must be simple, pose few as possible interferences and the electrodialyser must be easily introduced into this FIA system.

The determination of chloride was studied extensively in various FIA systems by making use of quite a number of possible detection methods. Potentiometric detectors were used rather extensively for the determination of chloride in FIA systems. Linear relationships were found to vary considerably depending on the application. Potentiometric methods were applied for the analysis of bottled water [5], natural water [6, 7], electroplating baths [8] and wine [9], just to name a few. Another very popular method was the indirect determination of chloride by the spectrophotometric measurement of the coloured $Fe(SCN)^{2+}$ complex (the mercuric thiocyanate method). [11, 12]. Other spectrophotometric methods include the liberated chlorinilate ions [13] and the phenolphthalein reaction [14]. Methods, other than spectrophotometry and potentiometry, included precipitation (indirect method) [15] and FIA titration methods [16].

Initially an ISE (Ion Selective Electrode) was preferred (as described by Van Staden [17]) since this FIA system was very simple to use. However, tremendous problems were encountered with this detection system. Massive baseline drift occurred the moment the potential was applied across the membrane and distorted peaks were observed no matter how well the electrodialyser and other equipment were grounded.

For this reason electroanalytical methods combined with the ED/FIA system were avoided. The next most suitable detection method was the spectrophotometric determination of chloride using the mercuric thiocyanide colour reaction. [11,12]

Dialysis was employed quite often in the determination of chloride in FIA systems. [18 - 23]. The percentage dialysis max of 7% obtained in all the abovementioned references confirms the values mentioned by Van Staden in a review article on membranes. [24] Slight deviations were observed from the micro dialysis system that was described by Sundqvist [25]. It was thus crucial to confirm that there would be an increase of mass transport across the membrane (a percentage dialysis of higher than 7%) with the applied potential to confirm the credibility of the proposed ED system.

4.2 Experimental

4.2.1 Reagents and solutions

All reagents were prepared from analytical grade chemicals unless otherwise specified. Deionized water from a Modulab system (Continental Water Systems, San Antionio, TX) was used for dilution. The water was tested for traces of chloride before use. All solutions were degassed before measurement with a water vacuum pump system. The main solutions were prepared as follows:

4.2.1.1 Standard chloride solution

A standard stock chloride solution containing 10 000 mg ℓ^{-1} was prepared by dissolving 32.97 g of dried sodium chloride in water and diluting to 2ℓ with de-ionized water. Working standard solutions were prepared by appropriate dilutions to cover the working ranges as discussed in the text.

4.2.1.2 Colour reagent

The colour reagent was prepared by dissolving 1.26 g of mercury(II)thiocyanate in 300 ml of methanol, 1ℓ of de-ionized water was added and shaken to mix well. 10 ml concentrated nitric acid (specific gravity 1.42) and 31g ferric nitrate nona hydrate ($Fe(NO_3)_3 \cdot 9H_2O$) were added, dissolved and diluted to 2 ℓ with de-ionized water. The colour reagent was filtered if necessary. The reagent was found to be stable for several months at room temperature if stored in a dark bottle.

4.2.2 Instrumentation

The FIA system (Figure 4.1) used in this work, was composed from the following components: a six-roller Cenco peristaltic pump rotating at 10 rpm, a Valco (Houston, Texas) 10-port electrically actuated injection valve with a sample loop of 70 μℓ, reaction manifold system and a laboratory-made electrodialyser. The electrodialyser used (see Figures 4.2 and 4.3) was a slightly modified version of the dialyser unit as desribed by Van Staden [26, 27]. The dialyser unit consisted of two, mirror image, PVC blocks. Embedded into each of these blocks were graphite electrodes which acted as the anode (acceptor side) and the cathode (donor side) respectively. Placed onto each of the PVC blocks was a 0.6 mm thick Perspex spacer. Into each of the Perspex blades, a groove of 0.6 mm diameter and 300 mm length was cut so as to form a channel when placed onto each of the PVC blocks respectively. The PVC blocks were then fitted onto each other in such a way that the Perspex blades facing each other and the grooves in the respective Perspex blades coincided with each other. The membrane was then sandwiched between the two Perspex blades as the only separation between the two tubes so formed. The walls of the tubes that were formed thus consisted of, at the far end, the graphite (which was embedded into the PVC blocks), the side walls of Perspex and the common wall, the membrane. A Leader LPS 156 potentiostat was used to apply the d.c. potential. Two different passive membranes were used namely, a Spectrapore membrane (MW cut-off

6000-8000, pore size 2.5-4 nm, thickness 0.031 mm) and a Technicon type C membrane (pore size 4-6 nm, thickness 0.015mm). Tygon tubing (0.76 mm id) was used to construct the manifold system. For current and potential measurements a Prema 5000 intergrating multimeter was used. The detector used was a Unicam 8625 UV/VIS spectrophotometer equipped with a 10 mm Hellma-type flow-through cell (volume 80 µℓ). The spectrophotometer and the injection valve were coupled to a personal computer equipped with the FlowTEK program [28].

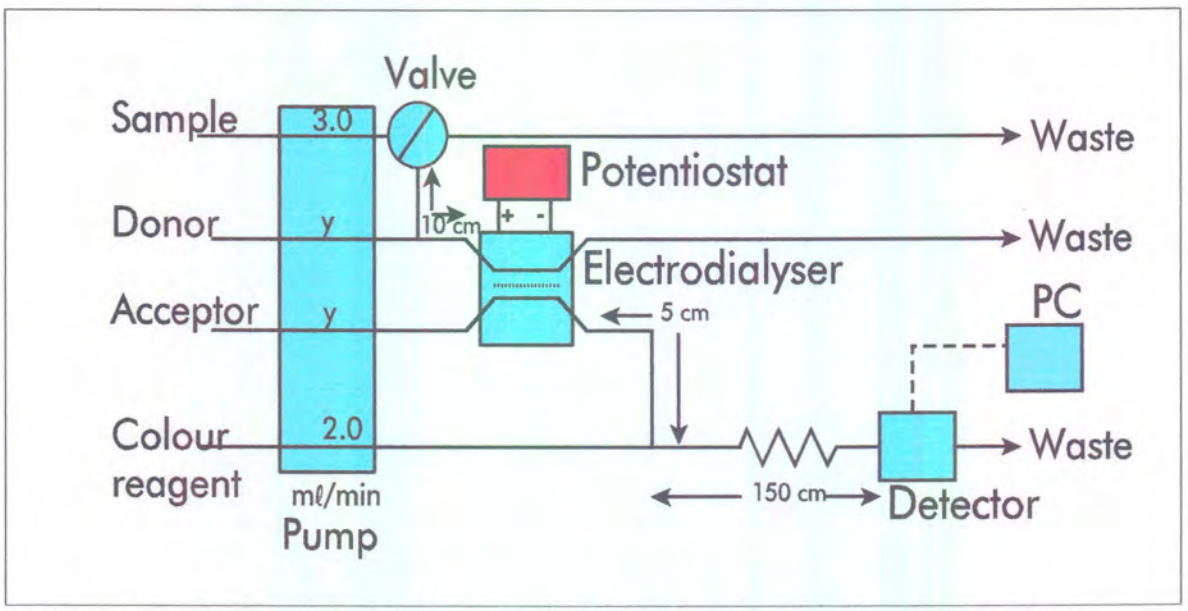

Figure 4.1 *Schematic flow diagram of the electrodialyser/flow injection system for the determination of chloride.*

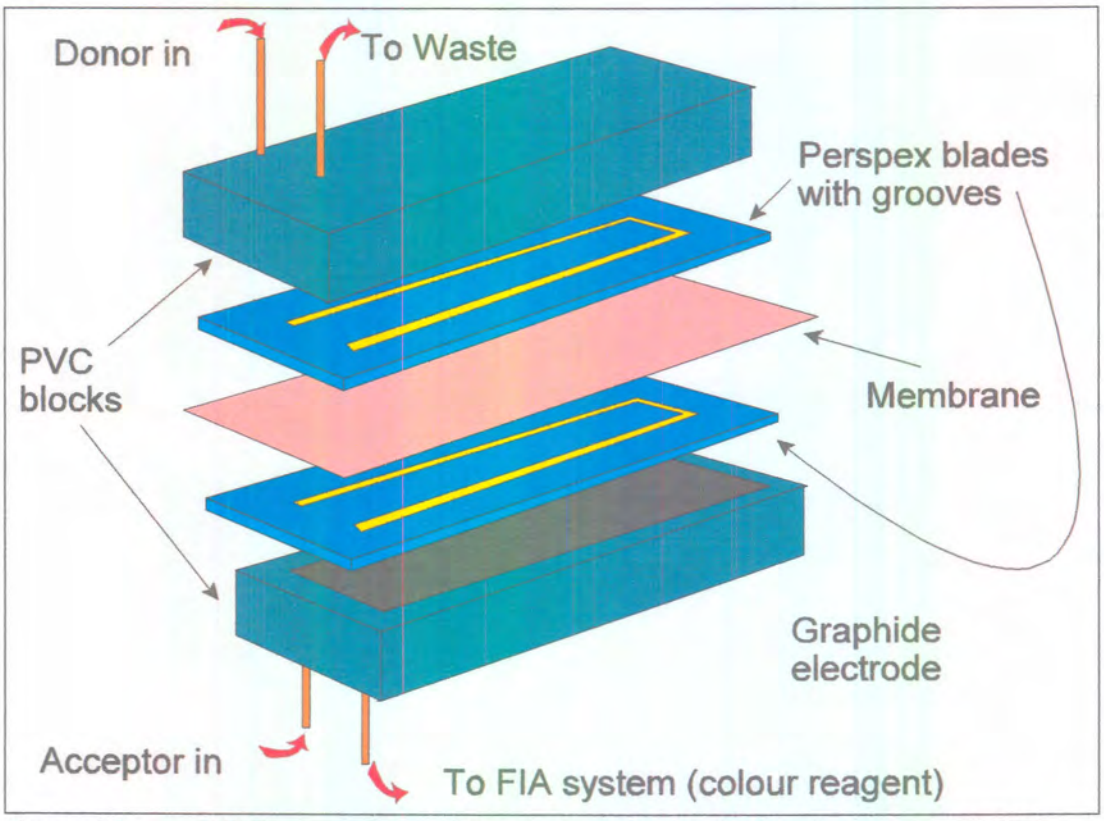

Figure 4.2 *3-D Representation of the electrodialyser indicating the placement of the different components.*

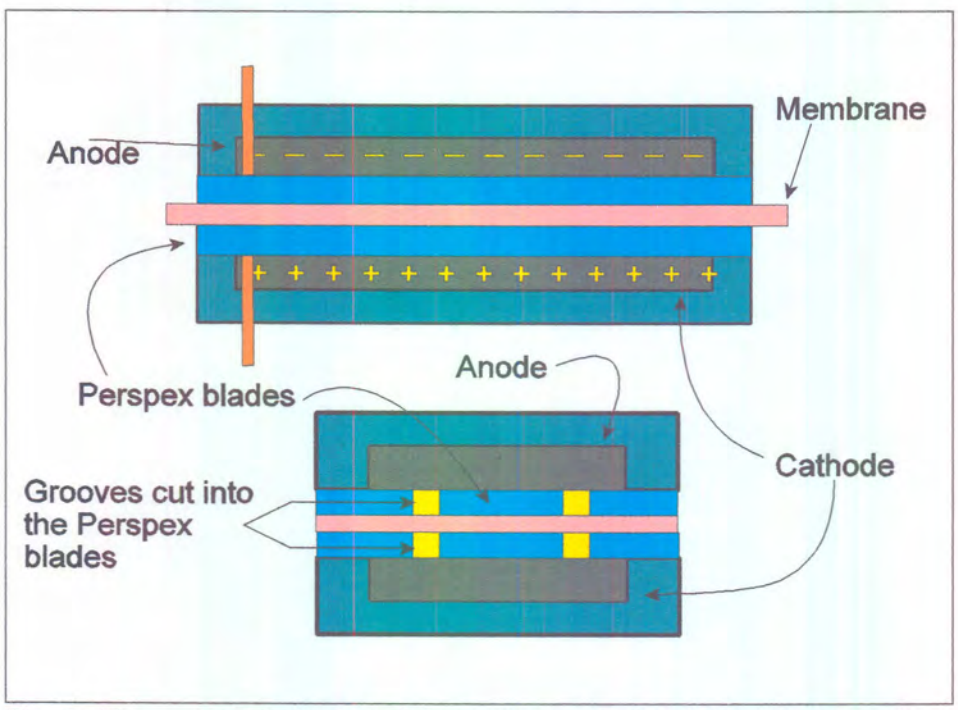

Figure 4.3 *Longitudinal- and diagonal cross sections of the dialyser unit indicating the fitting of the different components.*

4.2.3 Flow system

The flow system used is depicted in Figure 4.1. Sample solutions were drawn up into a 70 µℓ sample loop of the Valco valve from where it was injected into the carrier donor stream and transported into the electrodialyser. Analytes in the sample donor stream were electrodialysed under the influence of an applied d.c. potential through the passive neutral membrane to the acceptor channel. The electrodialysate ions were swept from the electrodialyser unit and mixed with iron(III)/mercury(II)thiocyanate chromogenic reagent in the reaction manifold system. The following reactions took place:

With the addition of the analyte (chloride) ions, which have a larger affinity for the mercury than the thiocyanide ions, the thiocyanide ions were displaced from the mercury/thiocyanide complex in amounts proportional to the added analyte chloride ions:

$$Hg(SCN)_2\ (aq) + 2\ Cl^-\ (aq) \rightarrow HgCl_2\ (aq) + 2\ SCN^-\ (aq)$$

The displaced thiocyanide ions were then free to react with the Fe^{3+} ions to form the $FeSCN^{2+}$ complex which has an absorption maximum at a wavelength of 480 nm.

$$SCN^-\ (aq) + Fe^{3+}\ (aq) \rightarrow\ FeSCN^{2+}\ (aq)$$

Some higher order ferric/thiocyanide complexes may also form, but at low concentrations of thiocyanide, the major species will be $FeSCN^{2+}$. The displacement of the thiocyanide and therefore the initial concentration of the thiocyanide (that is the concentration before the commencement of the second reaction) was very low since the volume (70 µℓ) and concentration (200 - 3200 mg ℓ^{-1}) of the analyte chloride ions injected was very low. For this reason,

according to Lewin and Wagner [29], the major ferric/thiocyanide complex that would form, would be $FeSCN^{2+}$.

This coloured reaction product was transported to the spectrophotometer for measurement at a wavelength of 480 nm.

Data acquisition and device control were achieved using a PC30-B interface board (Eagle Electric, Cape Town, South Africa) and an assembled distribution board (MINTEK, Randburg, South Africa). The FlowTEK [28] software package (obtainable from MINTEK) for computer aided flow-analysis was used throughout for device control and data acquisition. All the data given (mean height values) are the average of 10 replications.

4.3 Results and discussion

In order to enhance the mass transfer of chloride anions through the passive neutral membrane as an accurate and precise measurable product, optimum system conditions were of critical importance in the design and operation of the electrodialyser/flow injection system. The first main target of the optimisation was to ensure that the maximum amount of chloride ions were drawn across the neutral membrane into the conduits of the acceptor channel by applying a d.c. potential gradient across the two sides of the membrane. The second goal was to prevent any gas evolving reactions that might occur at the anode. Since rather high potentials were used (5 - 27 V), most oxidizable species that migrated to the anode would have reacted. Any of the gas evolving anode reactions had to be avoided at all costs since the debubblers developed up to this stage of the investigation were not very effective for the removal of the gaseous products that ended up in the FIA system. This was done by optimising the acceptor stream flow rate so that the dialysate analyte ions would be rushed out of the acceptor channel into the reaction manifold before the ions could come in contact with the anode. Thus it was essential to optimise flow rates of the donor and acceptor

channels and the applied potential over the membrane. Initially therefore, this part of the project concentrated on the design of the ED system.

4.3.1 Applied potential

The sensitivity and reproducibility of the electrodialysed chloride analyte sample plugs in the electrodialyser unit depended on the potential gradient applied on the system. The applied potential was therefore evaluated using the detector signal for response and %RSD as indicators. The d.c. potential was varied between 0 and 27 V for both membranes, while the flow rates in the donor and acceptor streams were kept constant at 1.6 mℓ min^{-1}. The results in Figure 4.4 revealed that the precision at low applied potentials was poor (%RSD > 8% for the Technicon membrane and > 13 % for the Spectrapore membrane), indicating that the contribution of detectable chloride ions drawn through the neutral membrane was unstable. As the applied voltage was increased to 6.8 V, the %RSD decreased significantly, reaching an optimum value of 2.8% for the Spectrapore membrane and 1.9% for the Technicon membrane. It can be assumed that the majority of electrodialysate chloride ions were drawn into the core of the acceptor stream and that the anode electrode had a minor influence at the applied potential of 6.8 V. It is furthermore apparent that there is a slight increase of the %RSD from very low voltages (6.8 V) to higher voltages (27 V) in both the membranes. This is probably due to the stronger attraction forces exerted on the chloride anions from the anode resulting in a loss of anions from the main acceptor stream and also to possible electrode reactions. A rather sharp increase in the %RSD is observed from 20 V and higher. This was due to the formation of gas at the anode. From equation 3.10 , it is evident that with an increase in the applied potential there should be an increase in the movement of the ions in solution, and thus the chloride ions should reach the anode in a shorter period of time. The precision of the Spectrapore membrane deteriorated faster than the precision of the Technicon membrane with the increase of applied voltage above 6.8 V. The influence of applied potential on the peak height is depicted in Figure

4.5. The results in Figure 4.5 show an increase in peak height when the applied potential was increased from 0 to 24 V. The results in Figure 4.5 reveal that the peak height of the Technicon membrane increased faster than the peak height of the Spectrapore membrane when the applied potential was increased from 0 to 24 V. This is probably due to the larger pore size and smaller thickness of the Technicon membrane. The increase in peak height of the Technicon membrane flattened off for applied potentials larger than 24 V.

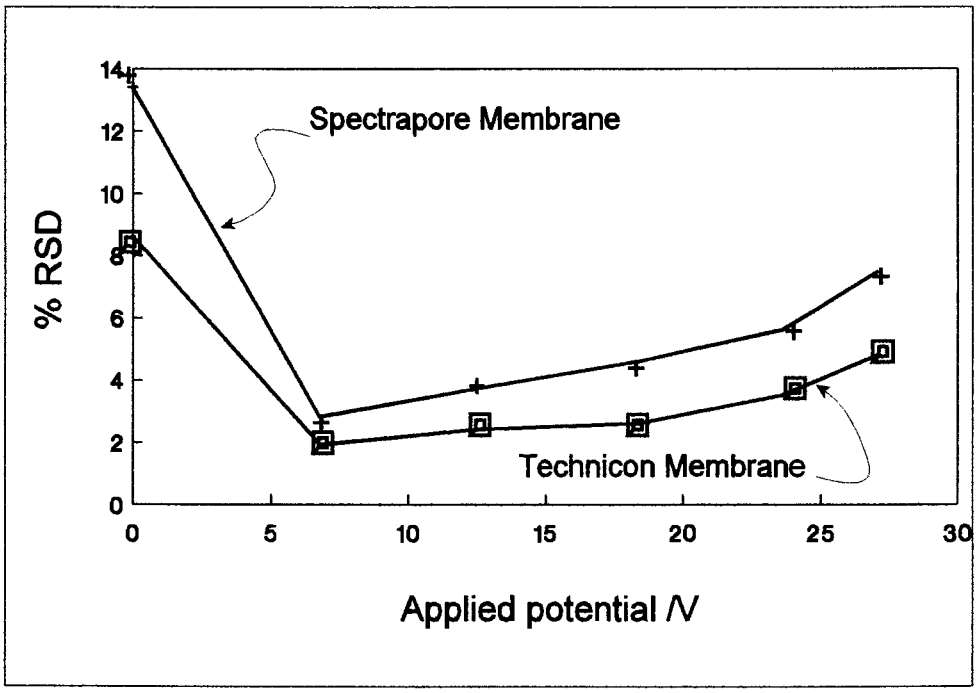

Figure 4.4 *Evaluation of relative standard deviation as a function of applied potential.*

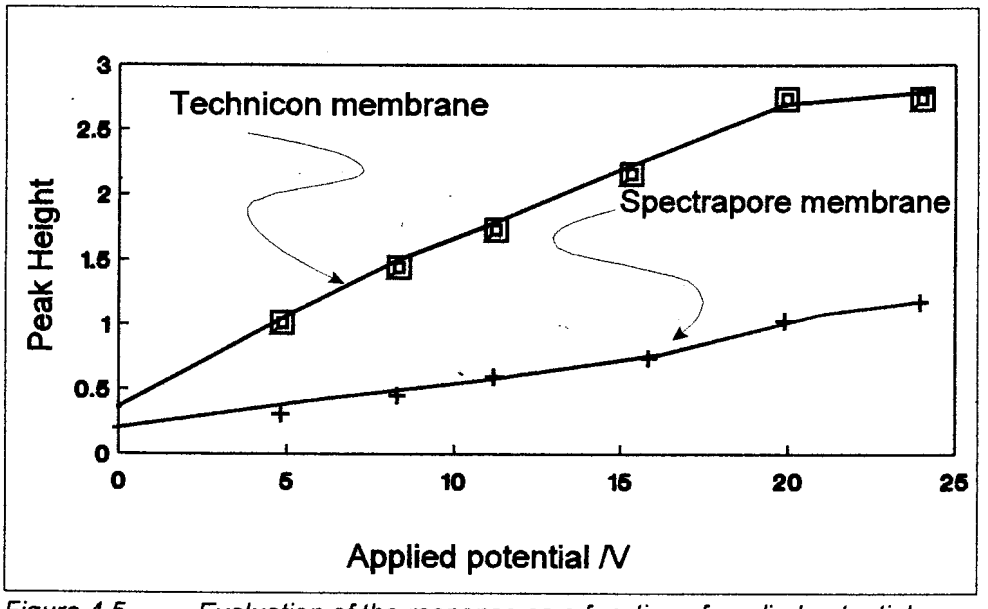

Figure 4.5 *Evaluation of the response as a function of applied potential.*

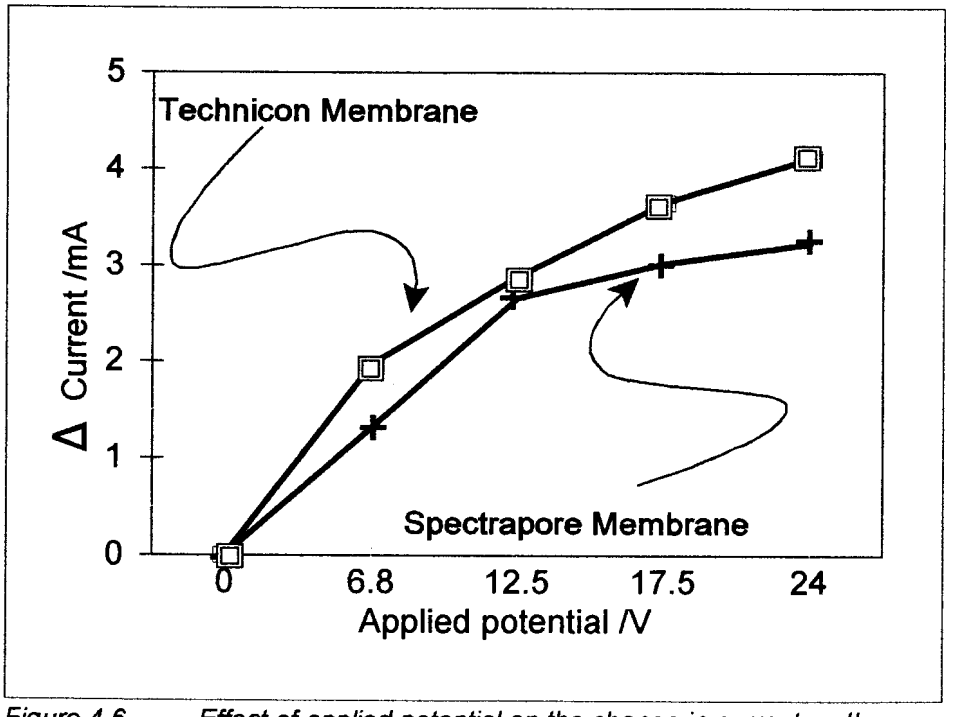

Figure 4.6 *Effect of applied potential on the change in current on the acceptor channel indicating the flux of ions through the passive membrane .*

From Figure 4.6 it is evident that there was a definite increase in the current across the membrane, for both membranes, with an application of a dc potential. The change in current was negligible at an applied potential of 0 V. The current however increased dramatically, for both membranes, with increasing applied potential. For the Technicon membrane this increase flattened off only slightly with increasing applied potential. For the Spectrapore membrane however there was a definite flatting in the curve after potential was increased above 12.5 V. This phenomenon, most probably, was due to the increased membrane thickness of the Spectrapore membrane in comparison to the thickness of the Technicon membrane.

4.3.2 Flow rates of the donor and acceptor streams

The main purpose of flow rate of the acceptor stream was to flush the dialysate chloride anions immediately, as they emerged from the membrane, to the reaction manifold to prevent any anions to reach the surface of the anode. Evaluation of the flow rates of both the donor and acceptor streams revealed that the best results were obtained with the flow rates of both streams in the same direction when applied in the continuous mode. Sensitivity and precision were used as indicators in the optimisation of the flow rates. In all the experimental work done, the same flow rate was applied for both the donor and acceptor streams. The reason for this is that previous studies indicated that the best precision and sensitivity was obtained when the same flow rate was used in both the donor and the acceptor channels. [21] During these experiments the applied potential was kept constant at 15 V while the flow rates of the donor and acceptor streams were varied. The influence of the flow rates, for both membranes, was first compared on the basis of %RSD, as illustrated in Figure 4.7. It is clear from the results that the precision deteriorated remarkably for flow rates below 1.4 mℓ min^{-1} for the Spectrapore membrane and for the flow rates below 1.6 mℓ min^{-1} for

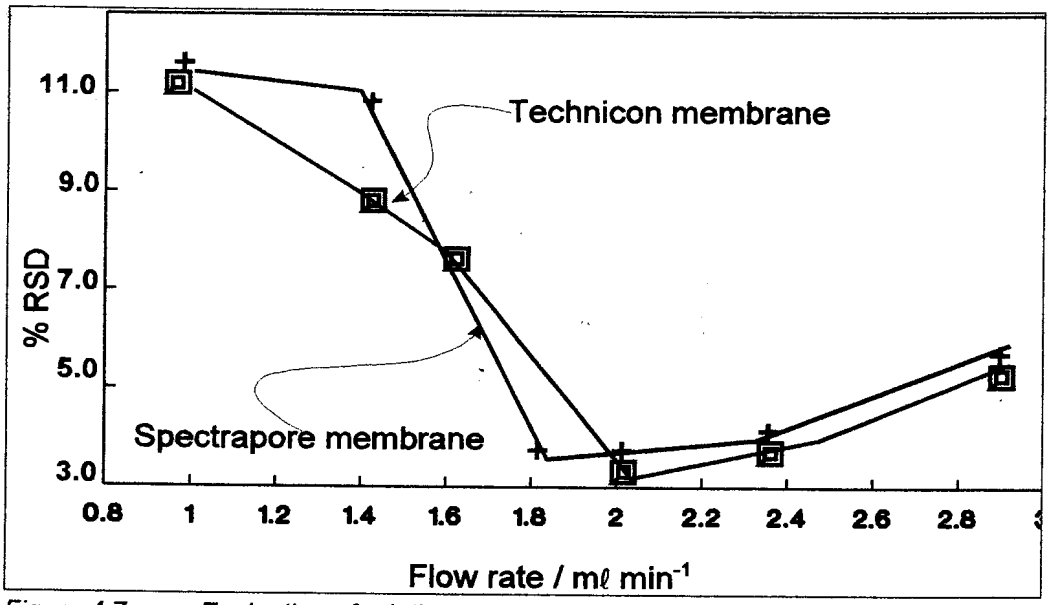

Figure 4.7 *Evaluation of relative standard deviation as a function of the flow rate of both membranes.*

the Technicon membrane. It is obvious that at low flow rates the dialysate chloride ions tended to move through the core of the acceptor stream and were able to reach the anode where possible electrode reactions could cause sufficient disturbance to increase the %RSD. Another contribution to this increase is the

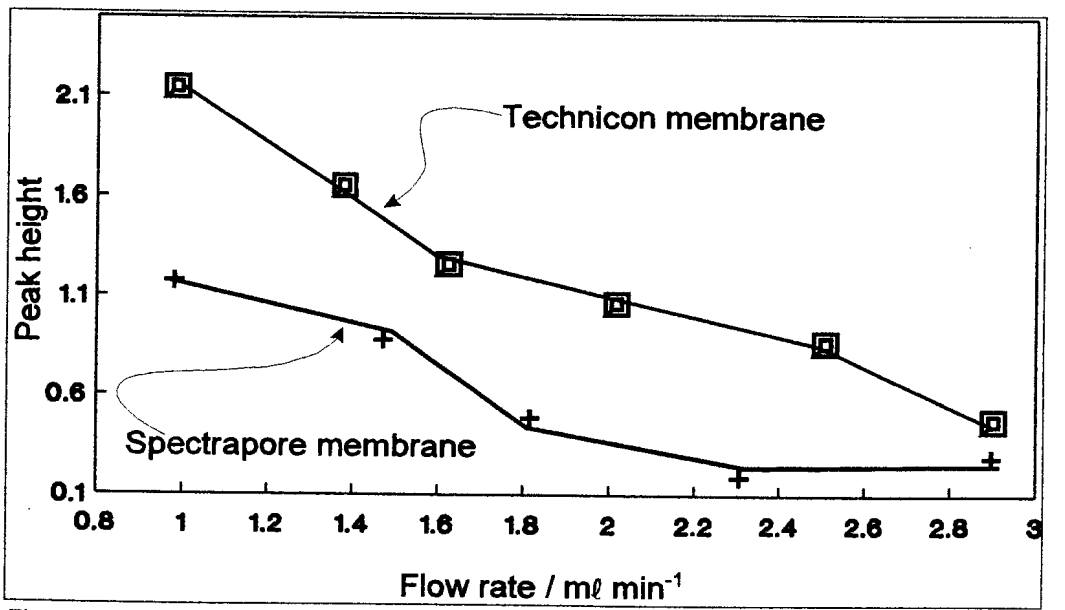

Figure 4.8 *Evaluation of response as a function of the flow rate of both membranes.*

irregular flow patterns at lower flow rates. The precision improved at higher flow rates with the best precision obtained at a flow rate of 2 mℓ min^{-1} for both membranes. If one considers the peak height versus the flow rate (Figure 4.8), the best response was obtained with flow rates of 1 mℓ min^{-1} for both membranes. A possible explanation for the decrease in sensitivity with higher flow rates was that although the flux of ions across the neutral membrane under the influence of the applied electric field remained the same, it could not match the influence of the higher flow rate with dilution effect on the dialysate anions in the acceptor channel of the FIA system. The best compromise between sensitivity and precision for employment of the proposed electrodialyser/FIA system was obtained with a flow rate of 1.6 mℓ min^{-1} for the Technicon membrane and 2.0 mℓ min^{-1} for the Spectrapore membrane. The proposed electrodialyser/FIA system is, however, very flexible and it is therefore possible to use the influence of donor and acceptor stream flow rates to apply the system in other analyte concentration ranges when required.

4.3.3 Interferences

The ions, Br^-, I^- and NH_4^+ were found to have an influence on the response of chloride ions in the ED/FIA system. It was found that bromide and iodide ions interfered positively with the determination of chloride, starting at levels as low as the detection limit for chloride. An evaluation revealed that the bromide and the iodide interfered whether they were injected into the donor or the acceptor streams. The conclusion of this was that the bromide and iodide being anions, experienced the same driving force exerted by the applied potential as the chloride ions. Additionally, however the main interference was that the bromide and iodide ions also reacted with iron(III)/mercury(II)thiocyanate chromogenic reagent to give coloured reaction products absorbing at the same wavelength as the colour product from the chloride ions. The influence of ammonia/ammonium

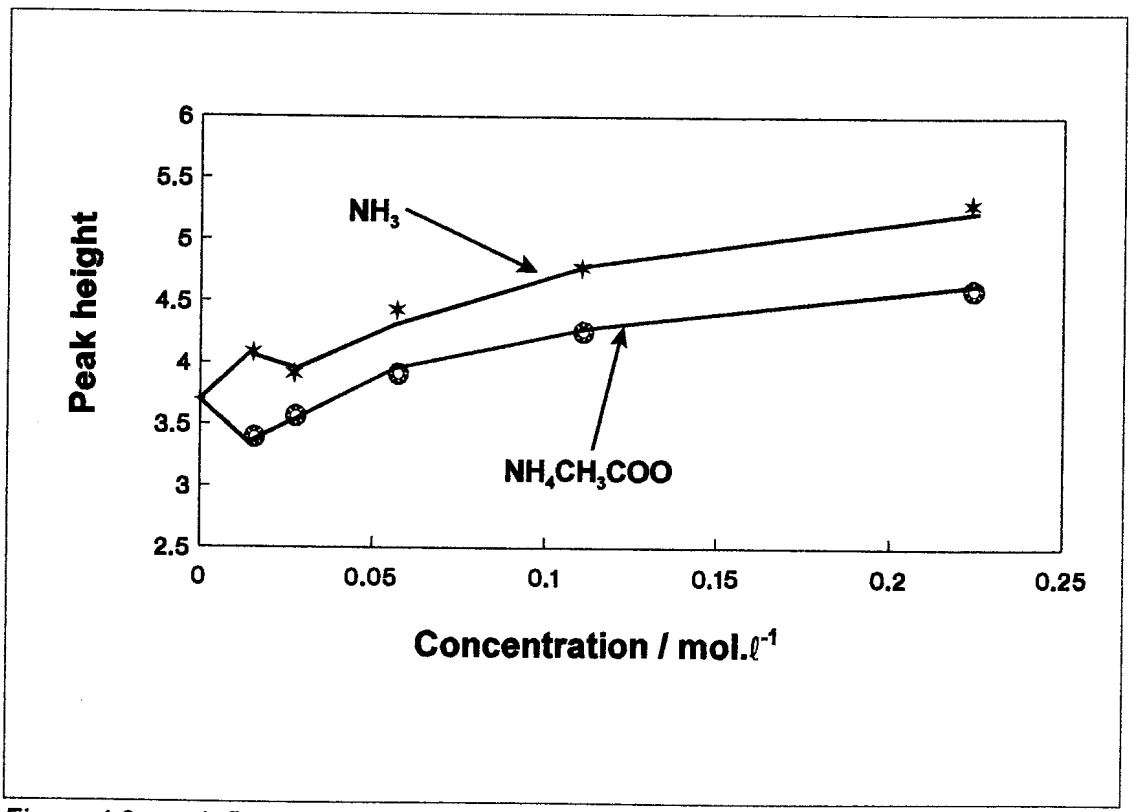

Figure 4.9 Influence of interferences: Technicon membrane.

ion is illustrated in Figure 4.9. The interference of ammonia depends on the type of compound used. When ammonium hydroxide was used as the primary source of ammonia, interference occured when very low concentrations of the ammonia salt were injected into the donor stream of Technicon membrane as seen from Figure 4.9. Interference also started at a concentration of 0.011 mol ℓ^{-1} when the Spectrapore membrane (Figure 4.10) was used. Gas and molecular diffusion was probably the main cause for this interference as the ammonium cations were not able to reach the anode. Two factors contributed to this: the total effective cross-sectional area of pores available for gas and molecular diffusion were big enough to allow for the ammonia/ammonium ions to diffuse through the passive neutral membranes. Secondly, the thinner Technicon membrane dimensions were probably responsible for the ability of the ammonium acetate to diffuse through the membrane, whereas the Spectrapore membrane was just thick enough to prevent diffusion through the membrane even at higher concentrations, as is evident in Figure 4.10. The ammonia/ammonium ion that diffused through both membranes had a buffer effect on the acidic colour reagent. The influence of the buffer effect was reduced by increasing the amount of HNO_3 used in the colour reagent about five to ten fold.

4.3.4 Calibration and comparison of the Spectrapore and Technicon membranes

A comparison between the performances of Spectrapore and Technicon membranes in the electrodialyser/flow injection system is outlined in table 3. 1. The linearity of the ED/FIA system for the determination of chloride was evaluated under optimum running conditions for both membranes (2.0 mℓ min^{-1} and 1.6 mℓ min^{-1} for the Spectrapore and Technicon membranes respectively with an applied potential of 15 V for both membranes). As can be seen from table 3.1, the linear range for the Spectrapore membrane was between 400 and 3200 mg ℓ^{-1} with the straight line equation y = 0.002039x-0.8556 and r^2=0.9974. The linear range for Technicon membrane was found to be between 200 and 1200 mg ℓ^{-1} with the equation for the straight line y = 0.003975x - 0.2557 and

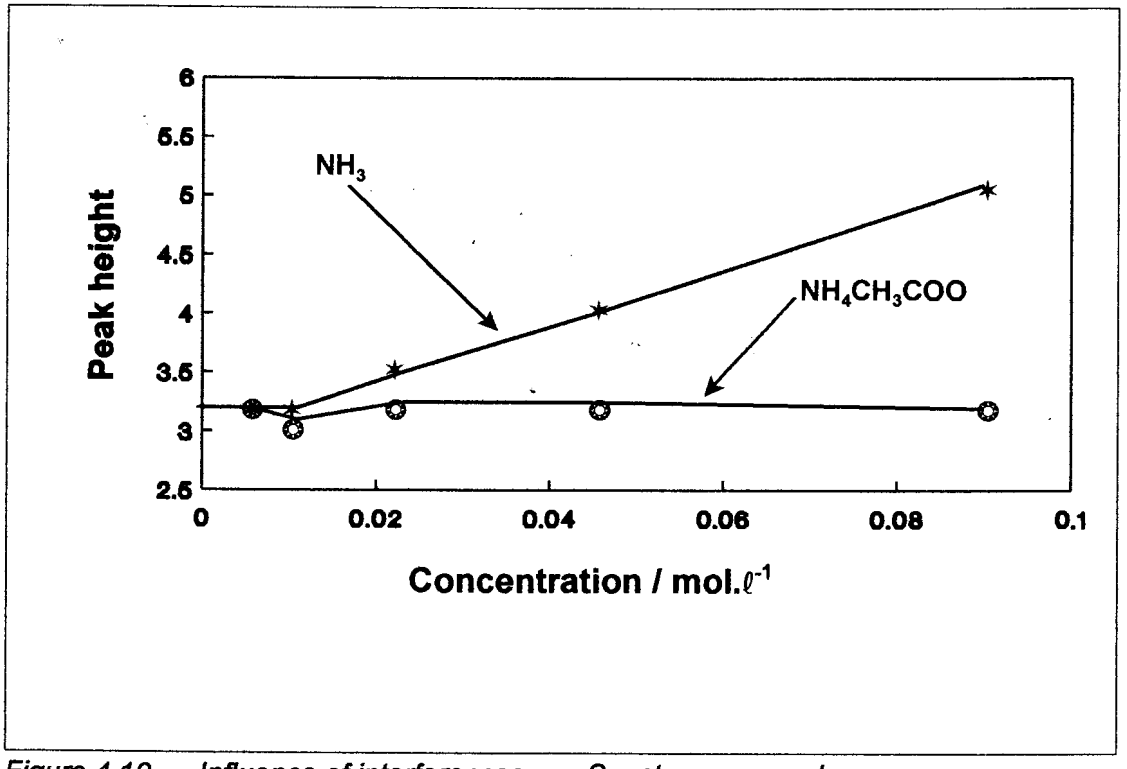

Figure 4.10 Influence of interferences: Spectrapore membrane.

r^2 = 0.9941. The mass transfer was increased to 10% and 37% for the Spectrapore and Technicon membrane respectively, which was a remarkable improvement on the values possible with conventional dialysis. Sample interaction was 0.23% for the Spectrapore membrane and 0.32% for the Technicon membrane at sample frequencies of 26 and 23 samples per hour respectively. These sample interactions are negligible.

Table 4.1 *Comparison of the performance of the Spectrapore and Technicon membranes in the electrodialyser/flow injection system.*

Parameter	Spectrapore Membrane	Technicon Membrane
% Electrodialysis	10	37
Runs h^{-1}	26	23
Experimental time (s)	140	160
Sample interaction (%)	0.23	0.32
Linear range (mg ℓ^{-1})	400 - 3200	200 - 1200
Applied potential (V)	15	15
Flow rate (mℓ min^{-1})	2	1.6

Note should be taken that the percentage dialysis at an applied potential of 0 V could not be detected. Reason for this was the high flow rates. As was mentioned previously, the expected percentage dialysis is 0 -7 % [24] at optimal conditions. Higher than optimum flow rates were used in both membrane systems and consequently percentage dialysis will be extremely low. For this reason the concentration of the analyte in the acceptor stream, without the applied dc potential, will nearer zero concentration.

4.3.5 Samples

Real samples from industrial effluents were analysed with the proposed ED/FIA system. The results obtained for both membranes were compared with the results obtained from a standard titration method for the determination of chloride. The results, as shown in Table 2, revealed a good correlation between the ED/FIA system and the standard titration procedure.

Table 4.2 *Comparison of the results of a number of samples as determined with the Spectrapore and Technicon membranes in the electrodialyser/flow injection system and a standard titration procedure.*

Sample	Spectrapore membrane	Technicon membrane	Standard titration procedure
1	1054	1060	1063
2	435	444	439
3	2004	2007[a]	1997

[a] Diluted to fall within the linear range.

4.4 Conclusion

The aim of the project was to investigate the viability of ED in the enhancement of mass transfer over passive neutral membranes in FIA systems. Chloride anions were selected to evaluate the electrodialyser/FIA system. The system proved to be very successful and it was possible to retain all the advantages of passive dialysis in flow systems, but at the same time, increase mass transfer through the membrane. The flexibility of the ED/FIA system is also shown by variation in the working range to fit a specific application, a commodity that was possible with alternation in the applied voltage and flow rates of the donor and acceptor streams.

To return to the points of evaluation mentioned in paragraph 4.1: Will there be an increase in the mass transfer across the membrane? The answer is undoubtedly yes. There was a massive increase in the % dialysis, especially in the case of the Technicon membrane and to a lesser extent also in the case of the Spectrapore membrane. The reasons why the Technicon membrane performed better than the Spectrapore membrane can be one of, or a combination of the following:

The Spectrapore membrane is thicker than the Technicon membrane thus the value of ℓ in equation 3.92 is higher for the Spectrapore membrane than for the Technicon membrane. Since the flux, J, is inversely proportional to the membrane thickness, ℓ, ($J \propto \ell^{-1}$), the flux is expected to decrease with increasing membrane thickness.

The pore diameter of the Technicon membrane is slightly larger than those of the Spectrapore membrane. Considering equation 3.57, it is clear that the flux is directly proportional to the surface porosity. ($J \propto \varepsilon$) Thus the flux will increase with increasing pore size.

The optimum flow rate for the Spectrapore membrane is slightly higher than for the Technicon membrane . This led to a higher dilution factor in the acceptor channel of the Spectrapore membrane.

Even though the NH_3/NH_4^+ had less influence on the signal in the case of the Spectrapore membrane, the influence in the Technicon membrane was easily circumvented by the addition of more nitric acid to the colour reagent mixture. For this specific FIA system, the Technicon membrane was found to suit the system better than the Spectrapore membrane.

This newly developed ED/FIA system is of great value for the determination of any charged species. The main problem encountered with this system was the formation of gaseous products at the anode (acceptor channel of the dialyser) as a result of anode reactions. The detection system used was very sensitive towards bubbles in the flow system. For this reason rather high flow rates through the dialyser unit was used to prevent the dialysate chloride ions (or any species that will oxidise at the anode) from reaching the anode. This procedure however, limited the time the sample bolus spent in the dialyser unit and thus reducing the time available for movement of the analyte across the membrane. It is therefore recommended that for ED/FIA systems which make use of the same type of detector, some kind of de-bubbler must be incorporated into the flowing stream before the dialysate ions reach the detector.

4.5 References

1. Strathmann H., Chmiel H. (**1984**) Chem. Ing. Tech. 56: 214.
2. Debets A.J.J., Kok W.Th., Hupe K.P., Brinkman U.A.Th., (**1990**) Chromatographia 30: 361.
3. Kittsteiner-Eberle R., Ogbomo I., Schmidt H.L., (**1989**) Biosensors 4: 75.
4. Brody T., (**1996**) Nutritional Biochemistry. Academic press.
5. Abdennabi A.M.S., Koken M.E., Khaled M.M., (**1998**) Anal. Chim. Acta. 360:195.
6. Alvares-Ribeiro L.M.B.C., Machado A.A.S.C., (**1998**) Analyst. 123: 653.
7. Ylasov Yu.G., Ermolenko Yu.E., Popov I.A., El'Marug S.Yu., Kihoroshev V.G., (**1997**) J. Anal. Chem. 52: 81.
8. Etxebarria M.B., Lima J.L.F.C., Montenegro M.C.B.S.M., Perez-Olmos R., (**1997**) Anal. Sci. 13: 89.
9. Couto C.M.C.M., Lima J.L.F.C., Montenegro M.C.B.S.M., (**1998**) Analusis. 26: 182.
10. Chalk S.J., Tyson J.F., (**1998**) Anal. Chim. Acta. 366: 147.
11. Jones E.A., (**1985**) Rep. MINTEK. M200, Pp. 65
12. Tyson J.F., Fogg A.G., Wang X., (**1989**) Quim. Anal. 8: 179.
13. Eremina I.D., Shpigun L.K., Zolotov Yu.A., (**1989**) Zh. Anal. Khim. 44: 399.
14. Toei J., Baba., (**1986**) Bunseki Kagaku. 35: 832.
15. Martinez-Jimenez P., Gallego M., Varcarcel M., (**1987**) Anal. Chem. 59(1): 69.
16. Alegret S., Alonso J., Bartroli J., Garcia-Raurich J., Martinez-Fabregas E., Sanchez-Rodrigues J., (**1995**) Quim. Anal. 14(2): 121.
17. Van Staden J.F., (**1986**) Anal. Chim. Acta. 179: 407.
18. Van Staden J.F. (**1986**) Anal. Lett. 19(13-14): 1407.
19. Chang Q., Meyerhoff M.E., (**1986**) Anal. Chim. Acta. 186: 81.
20. Lapa R.A.S., Lima J.L.F.C., Barrado E., Vela H., (**1997**) Farmaco. 52(2): 127.
21. Van Staden J.F., Van Rensburg A., (**1990**) Frezenius'. Z. Anal. Chem. 337(4): 393.
22. Van Staden J.F., (**1991**) Frezenius'. Z. Anal. Chem. 340(7): 415.

23. Van Staden J.F., (**1991**) Talanta. 38(9): 1033.
24. Van Staden J.F., (**1995**) Frezenius'. Z. Anal. Chem. 352: 271.
25. Sundqvist U., (**1988**) Frezenius'. Z. Anal. Chem. 329(6): 688.
26. Van Staden J.F., Van Rensburg A., (**1990**) Analyst. 115: 1049.
27. Van Staden J.F., (**1992**) Anal. Chim. Acta. 261: 453.
28. Marshall G.D., Van Staden J.F., (**1992**) Anal. Instr. 20 79.
29. Lewin S.Z., Wagner R.S., (**1953**) J. Chem. Ed. 30: 445.

Chapter 5

Determination of Copper (II) ions in multivitamin tablets after enhancement of mass transfer across the neutral membrane and the preconcentration of the dialysate ions.

5.1 Introduction

In chapter 4, the right of existence of the use of an electrodialyser (ED), equipped with a neutral, passive membrane, was established for use in an anion, flow injection analysis (FIA) system. The aim of the investigation was expanded to include the use of the above mentioned ED system for use in a cation FIA system. The main objective of this part of the study was to evaluate the use of the ED system incorporated into an FIA system for the analysis of a cation. A prerequisite for the detector used was its compatibility with the ED/FIA system, the detection limit and also the rate at which the sample could be analysed.

Various methods of determination of copper ions in FIA systems have been exploited. Most commonly used method was the direct determination of the copper ions by means of spectroscopic methods. Atomic spectrometry is one of the most sophisticated and elegant methods for direct assay of cations. [1] Flame atomic absorption spectrophotometry (FAAS) is used extensively in FIA systems. [2-14] The graphite furnace [15 -17] and the Inductively Coupled Plasma (ICP) [18 - 21] as a means of detection was also often used. Other methods used includes electrochemical methods [22 - 25], and also the reactions of copper ions with a colour reagent and detection of the coloured product with a UV/Vis spectrophotometer [36 - 30].

The obvious choice was the use of the FAAS detector. It gave a direct and fast determination of the copper ions with very few interferences. [1] Direct determination (without sample pretreatment) could give a sampling rate of as high as 150 samples per hour. [1] The use of a colour reagent gave a lower sampling rate (due to the reaction

that had to take place) but higher detection limits than the FAAS. [31] The use of electrochemical detectors were not advised due to the interference of the ED system on the detector (as was also experienced in chapter 4).

The use of flow injection (FI) techniques for the preparation of solutions prior to their aspiration into atomic spectrometry systems forms the basis of interfaced flow injection-atomic spectrometry. Although FI has become a well-known name to most chemists over the past two decades, the real success of practical instrumental FI analysers in routine analytical laboratories and process analysers depended on the type of basic components used, and the construction thereof into a working FI system. It is apparent, from the above mentioned FAAS literature, that a very wide variety of different on-line manipulations of samples and standards had been carried out by FI techniques and that the combination with conventional FAAS enhanced the performance of an analytical method. The most prominent example of such on-line sample pretreatment was the preconcentration of the analyte on an ion-exchange column built into the conduits of the FIA system as was illustrated by Hirata *et al* [3], Purohit and Devi [4], Naghmush *et al* [7], Burguera *et al* and Van Staden and Hattingh [13]. Other very effective ways of preconcentration (not necessarily used in FIA/FAAS systems) were the use of immobilised micro organisms (which was done by Elmahadi and Greenway [9] and Maquieira *et al* [10, 11, 32]), solvent extraction as illustrated by Kuban *et al* [2] and precipitation by Zhuang *et al* [16] and Esmadi *et al* [33].

Active or Donnan dialysis is a promising technique for the preconcentration, recovery and speciation of ionic species, but with a limitation in the amount of mass transfer of species through the membrane. Cox and co-workers [34 - 36] worked for many years on sample preparation on an analytical scale using Donnan dialysis, employing the technique for matrix normalization [34] and sample preconcentration. [35, 36] Active dialysis was also used as a preconcentrating technique by Koropchak and co-workers. [37, 38]

In the case of passive dialysis, very little work was done to circumvent the

disadvantages of the dilution of the analyte during its passage over the neutral membrane. It is evident, from the experimental work mentioned in chapter 4, that there was a substantial increase in the percentage dialysis with the incorporation of the electrodialyser. Still there is a massive dilution factor since, at its best, the percentage dialysis was found to be only 37 %. The preconcentration methods, described earlier in this chapter, can of course be used with great success by preconcentrating the dialysate ions before detection in the FI system. Kuban et al. [39] used solvent extraction to preconcentrate copper in an FI manifold before detection with FAAS, although normally ion-exchange resins are used for on-line preconcentration in FI systems. Carbonell et al. [40] compared various cation-exchange resins which are commercially available. Using liquid chromatography (LC), Turnell and Cooper [41, 42] first dialysed the sample after which it was derivatized or preconcentrated before injection into the LC system. Preconcentration, using an ion-exchange column after dialysis in an FI system was also employed by Van Staden and Hattingh. [13] The detection limit was decreased dramatically, although most of the analyte ions in solution were lost due to the low efficiency in mass transfer over the neutral membrane. There was no improvement in the percentage dialysis.

The properties of electrodialysis make it potentially applicable to quantification of trace ions in samples which require a prior separation and/or enrichment step and this was evaluated by Cox and Carlson [43] as an active preconcentration method. These workers demonstrated that electrodialysis can be employed for ion enrichment and also that, compared with Donnan dialysis, higher enrichment factors are attained. However, for enrichment of trace ions in samples, the quantification procedure is not straightforward and for very low analyte concentrations internal standard an/or ionic strength normalization methods were required in order to obtain reasonable precision. Van Staden and Hattingh [48] not only encountered the same problem when employing active dialysis membranes as part of their electrodialyser-FI system, but also found that the ion-exchange properties of the Donnan ion-exchange membrane became predominant and the main hindrance to obtaining a reasonable accuracy and precision.

5.2 Experimental

5.2.1 Reagents and solutions

All reagents were prepared from analytical-reagent grade chemicals unless specified otherwise. De-ionised water from a Modulab system (Continental Water Systems, San Antonio, TX, USA) was used for dilution. All solutions were de-gassed with a vacuum pump system before measurement. The solutions were prepared as follows:

A stock standard solution containing 10 000 mg ℓ^{-1} copper(II) ion was prepared by dissolving 78.585 g of copper sulfate pentahydrate in de-ionised water and diluting to 2000 mℓ with de-ionised water.

A 1.0 mol ℓ^{-1} HNO_3 solution was prepared by diluting 42.3 mℓ of a 11.7 mol ℓ^{-1} HNO_3 solution (sp. gr. 1.34) to 500.0 mℓ.

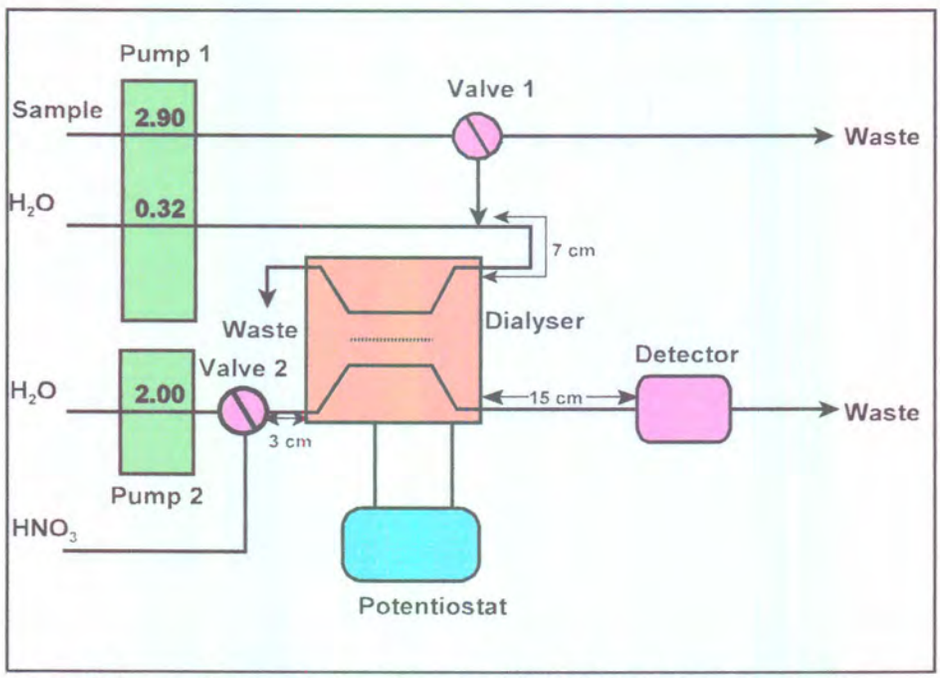

Figure 5.1 Schematic flow diagram of the ED-FI-AAS system for the determination of copper.

5.2.2 Instrumentation

The FI system (Figure 5.1) used was composed of the following components:

1. Two six-roller Cenco peristaltic pumps (rotating at 10 rev min^{-1}). The first pump, P1, was used to draw up sample and flow in the donor stream. This pump was never switched off during the analysis. The second pump, P2, was used for the flow of the deionised water in the acceptor stream. The HNO_3 stream was not transported by a pump, but was drawn up by the Atomic Absorption Spectrometer (AAS) burner.
2. Two Valco (Houston, TX, USA) 10-port electrically actuated injection valves. The first Valco valve, with a sample loop of 80 µℓ, was used to inject the sample into the donor stream whereas the

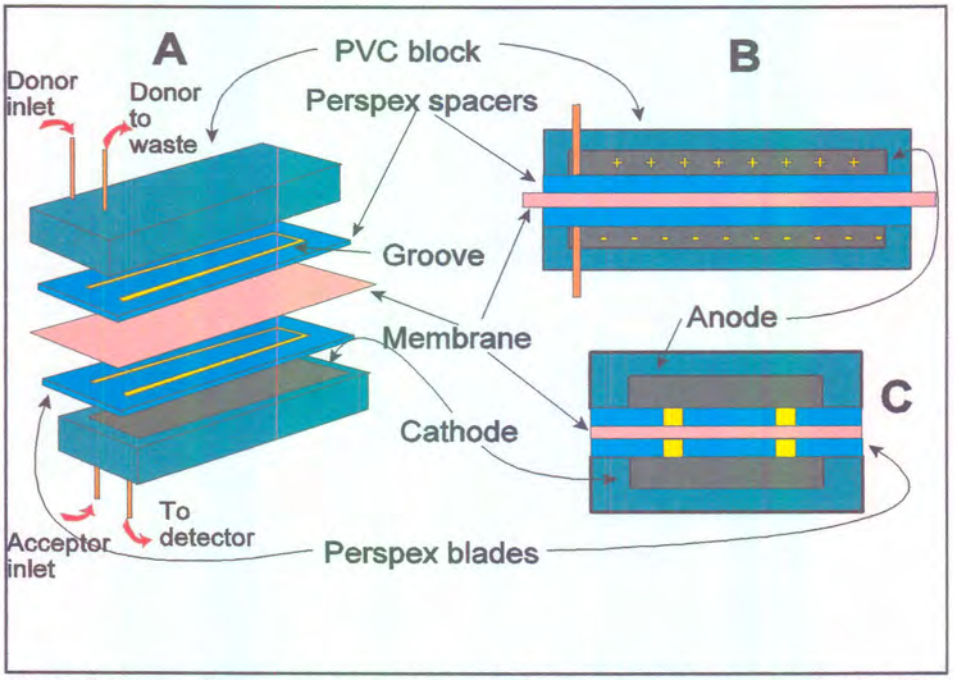

Figure 5.2 *Schematic presentation of the Electrodialyser unit. A - the 3D presentation, B - a longitudinal cross-section and C - a diagonal cross-section.*

second Valco valve was used to select between the H_2O stream from pump 2 and the HNO_3 stream, which was used to flush the acceptor stream.

3. The manifold consisted of Tygon tubing, with an id of 0.76 mm, cut into the required lengths and wound around glass tubes with an od of 10 mm.

4. The electrodialyser unit used (Figure 5.2) was a slightly modified version of the dialyser previously described by van Staden and van Rensburg [45] and modified into an electrodialyser unit. It is similar to the one used in chapter 4 for the determination of chloride with the only difference that the polarity on the electrodes were swopped so that the anode was situated in the donor channel and the cathode in the acceptor channel. The dialyser unit consisted of two, mirror image, PVC blocks. Embedded into each of these blocks were graphite electrodes which acted as the anode (acceptor side) and the cathode (donor side) respectively. Placed onto each of the PVC blocks was a 0.6 mm thick Perspex blade. Into each of the Perspex blades, a groove of 0.6 mm width and 300 mm length was cut so as to form a channel when placed onto each of the PVC blocks respectively. The PVC blocks were then fitted onto each other in such a way that the Perspex blades facing each other and the grooves in the respective Perspex blades coincided with each other. The membrane was then sandwiched between the two Perspex blades as the only separation between the two channels so formed. The walls of the channels that were formed thus consisted of, at the far end, the graphite (which was embedded into the PVC blocks), the side walls of Perspex and the common wall, the membrane. A Spectrapore passive (MW cut-off 6000-8000, pore size 2.5 - 4 nm, thickness 0.031 mm) was used

in the dialyser unit.

5. A Leader LPS 156 potentiostat was used to apply the dc potential.

6. For current and potential measurements a Prema 5000 integrating multimeter was used.

7. The detector used was a Varian (Palo Alto, CA, USA) AA-1275 atomic absorption spectrometer. A Varian Techtron Cu hollow cathode lamp, with a current of 10 mA, was used to give a monochromatic light ray in the detector. A wavelength of 324.7 nm and a spectral bandpass of 0.2 mm was used. A lean (oxidising) air-acetylene flame was used.

8. The AAS detector, the pumps and the valves were coupled to a personal computer equipped with the FlowTEK program. [48]

5.2.3 Flow system

The flow system used is depicted in Figure 5.1. The sample solution was drawn up into an 80 µℓ sample loop of the Valco valve 1 from where it was injected into the carrier donor stream and transported to the electrodialyser. Analytes in the sample donor stream were electrodialysed under the influence of an applied potential through the passive neutral membrane to the acceptor channel, which was stagnant at this time. The dialysed copper ions in the acceptor stream were further plated onto the cathode under the influence of the dc potential. After a certain fixed period of electrodialysis, the acceptor channel was flushed with the HNO_3 stream, dissolving the plated copper metal zone on the cathode, and transporting it directly to the AAS detector. The direction of flushing of the acceptor channel was countercurrent to the flow in the donor channel. Data acquisition and device control were achieved using a PC30-B interface board (Eagle Electric, Cape Town, South Africa) and an assembled distribution board

(MINTEK, Randburg, South Africa). The FlowTEK [48] software package for computer-aided flow analysis was used throughout for device control and data acquisition. All the data given (mean peak area values) are the average of 11 repetitions.

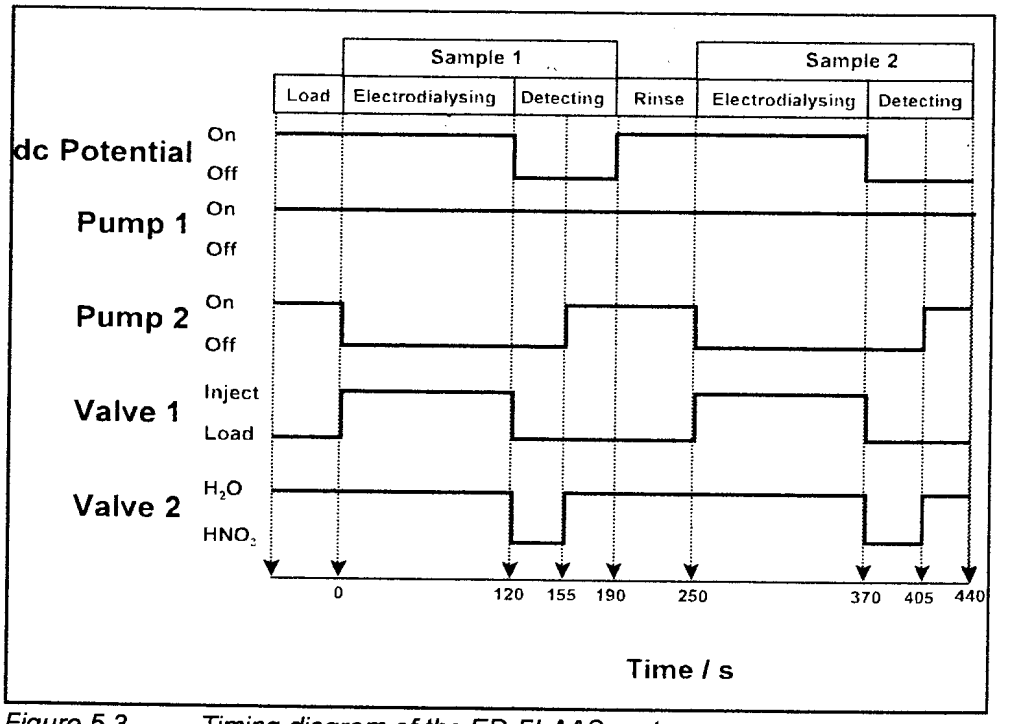

Figure 5.3 Timing diagram of the ED-FI-AAS system

5.2.4 Procedure

The configuration of the FI system is shown in Figure 5.1. The pump and valves operated as described below.

5.2.4.1 Operation of pump and valves

Pumps where either in operation or switched off. Pump P1 (Figure 5.1) was never switched to the "off" position during the analysis. Pump P2 (Figure 5.1) was switched between the "on" and "off" positions at certain intervals. Two types

was used to channel either the HNO_3 solution or de-ionised water through the acceptor stream of the dialyser. A Valco 10-port electrically actuated injection valve (V1 in Figure 5.1) was arranged in such a way that it served as a sampling valve with a sample loop of 81 µℓ. In the "load" position, sample was aspirated through the sample loop to waste filling the whole sample loop. Upon switching to the "inject" position (which was time-regulated with pump P2), part of the donor stream was interrupted and the full sample loop was placed into the donor stream. A Valco 10-port electrically actuated valve (V2 in Figure 5.1) was arranged in such a way that it could be switched between the H_2O and HNO_3 channels feeding the acceptor channel of the electrodialyser at certain intervals (see Figure 5.3).

The timing diagram for treating the samples is outlined in Figure 5.3. The system was switched on and allowed to run for about 10 min in order to equilibrate the flow dynamics of all parts of the system. The computer was then actuated and the timing sequence started in the "load" position which was only used at the beginning of the analysis. The following timing sequences were followed with time regulation from the FlowTEK [48] program:

i. *Starting of the system (Loading)*

Pumps: Pumps P1 and P2 were switched to the "on" position. Pump P1 pumped H_2O through the donor channel at a rate of 0.32 mℓ min^{-1} and the aspirated sample (sample 1) into the sample loop at 2.90 mℓ min^{-1}.

Valves: Valve V1 was in the "load" position and valve V2 directed H_2O at a flow rate of 2.00 mℓ min^{-1} through the acceptor channel of the ED.

Potentiostat: Potentiostat was set to "on" position at 15 V (see Figure 5.1)

ii. *Electrodialysis*

At time T = 0, pump P1 was kept in the "on" position and pump P2 was switched to the "off" position. For the whole duration of the electrodialysis period the flow in the acceptor channel was stopped. Valve V1 was switched to the "inject" position and the whole sample in the loop was inserted into the donor stream. This whole sample plug was then pumped through the donor stream of the dialyser at a flow rate of 0.32 mℓ min^{-1} where electrodialysis occurred. The applied potential over the membrane was kept at 15 V for the duration of the electrodialysing step.

iii. *Detection*

At time T = 120 s, the applied potential was switched off and valve V2 switched to the HNO_3 stream, allowing the detector to draw the HNO_3 with the electrodialysed dissolved copper(II) ion zone through the acceptor channel. The computer also started to read the signal coming from the detector. At time T = 155 s, valve V2 was again switched to H_2O and pump P2 actuated to pump the remaining dissolved analyte to the detector at a flow rate of 2.00 mℓ min^{-1}.

iv *Completion of a run*

At time T = 190 s, the computer stopped measuring the signal from the detector. The potentiostat was again switched on at 15 V. The donor and acceptor channels were rinsed and the next sample was aspirated into the sample loop. At T = 250 s, sample 2 was injected and the analysis of sample 2 started.

5.3 Results and discussion

Van Staden and Hattingh [46] previously tried to use anion-exchange membranes with the electrodialyser-FI system for the determination of chloride, but experienced the same problems as Cox and Carlson. [47] The ion-exchange properties of the Donnan ion-exchange membrane became predominant and a main hindrance to obtaining a reasonable accuracy and precision. They again tried cation-exchange membranes with the electrodialyser-FI-AAS system for the determination of copper(II) ions, but unfortunately, were not very successful, for the same reasons mentioned above. It was then decided to keep to the passive neutral membranes used previously (as was described in Chapter 4) and to try to improve on the performance.

In order to enhance the mass transfer of the copper cations over the passive neutral membrane as an accurate and precise measurable product, optimum system conditions were of the utmost importance in the design and operation of the electrodialyser-FI-AAS system. The first aim of this investigation was to draw the maximum amount of copper ions across the neutral membrane into the conduits of the acceptor channel by applying a dc potential gradient across the two sides of the membrane at optimum flow rates. The second goal was to allow the copper ions to accumulate in the acceptor channel where the copper was preconcentrated into a smaller zone before it was transported to the detector. To evaluate and optimise the preconcentration of the copper, a knowledge of the form in which the copper was concentrated in the acceptor stream was needed. Experimental work confirmed that copper metal was plated onto the cathode. (Confirmation was done by rinsing the acceptor channel of the dialyser unit extensively with de-ionised water. The water was then tested for traces of copper ions. Hereafter the acceptor channel of the dialyser unit was rinsed with a solution of nitric acid. It was found that the nitric acid solution contained copper ions after the rinsing of the acceptor channel)

Hereafter, the remainder of the system was optimised in as far as the following points were concerned: (i) flow rate of the donor channel, (ii) applied potential over the membrane, (iii) injection loop volume, (iv) flow direction of the donor and acceptor channels and (v) interferences.

5.3.1 Flow rate of the donor stream

The flow rate of the donor stream was an important parameter which had an influence on the electrodialysis efficiency. High flow rates prevented the transfer of the bulk of copper ions through the membrane to the cathode, while low flow rates resulted in a decrease in sample frequency. The applied dc potential was kept constant at 10 V during the optimisation of the donor flow rate. The acceptor channel flow was also stopped during the time set aside for the electrodialysis process to take place (Figure 5.3). The flow rate of the donor channel was varied between 0.10 and 0.60 mℓ min^{-1}. The influence of the flow rate of the donor stream was evaluated on the basis of the %RSD and peak area as illustrated in Figure 5.4. From Figure 5.4A it follows that the lowest %RSD was obtained at a flow rate of 0.32 mℓ min^{-1}. It is also apparent from Figure 5.4B that the lower the flow rate, the higher the peak area. It is evident from Figure 5.4B that there was a drastic decrease in peak area when the flow rate increased above 0.35 mℓ min^{-1}. The best compromise between the sensitivity and reproducibility was found at a flow rate of 0.32 mℓ min^{-1}.

5.3.2 Applied potential

The applied potential was evaluated using the detector signal for response (or the percentage electrodialysis) and the %RSD as indicators. The applied dc potential was a very important factor that determined the oxidation state into which the copper was preconcentrated in the acceptor stream. The applied dc potential was varied between 0 and 20 V, while the flow rate of the donor stream was kept constant at 0.32 mℓ min^{-1}. Figure 5.5 clearly indicates the state of the copper in the acceptor stream at different applied dc potentials. Figure 5.5 was obtained from the detector reading in the detection step in Figure 5.3. The moment the acceptor stream is allowed to be rinsed, all the Cu^{2+} ions would be transported towards the detector. (Since during the preconcentration step, only de-ionised water is present in the acceptor channel.) The copper that was plated on the cathode however, will lag behind since it had to be dissolved by the HNO_3 that was used to rinse the acceptor channel. For this reason at lower applied dc potentials not all of the copper ions were plated onto the cathode. The redox

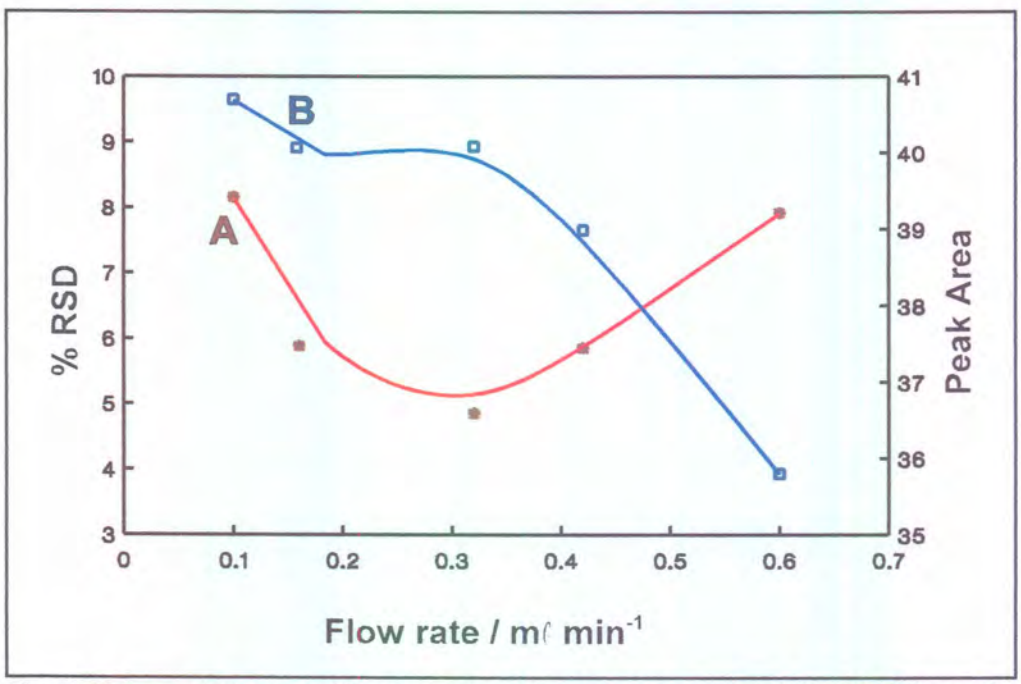

Figure 5.4 *Influence of the flow rate of the donor stream on* A *the %RSD and* B *the peak area.*

reaction for the plating of the copper is the following:

$$Cu^{2+}\ (aq) + 2\ e^- \rightarrow Cu\ (s) \quad E^\circ = 0.337\ V \text{ (at standard conditions)}$$

It is obvious that the applied potential (in Figure 5.5) would have been more than ample for the copper ions to be plated onto the cathode. It is evident from Figure 5.5 that at 5 and 10 V, the copper was in the Cu^0 and in the Cu^{2+} states. At these potentials not all the ions were plated since the migration rate at these potentials was too low for the ions to came into contact with the cathode. At a potential of 15 V however, all the copper ions were converted to the Cu^0 state. For this reason it was advisable always to work at applied potentials of 15 V and higher. The results in Figure 5.6A revealed that the precision increased with an increasing dc potential from 0 to 20 V. The reason for the sharp decrease in the %RSD at a dc potential higher than 10 V is because the bulk of the copper(II) is reduced to Cu(s) at higher dc potentials, whereas some copper is still in the Cu^{2+} oxidation state at lower dc potentials. When looking at the % electrodialysis

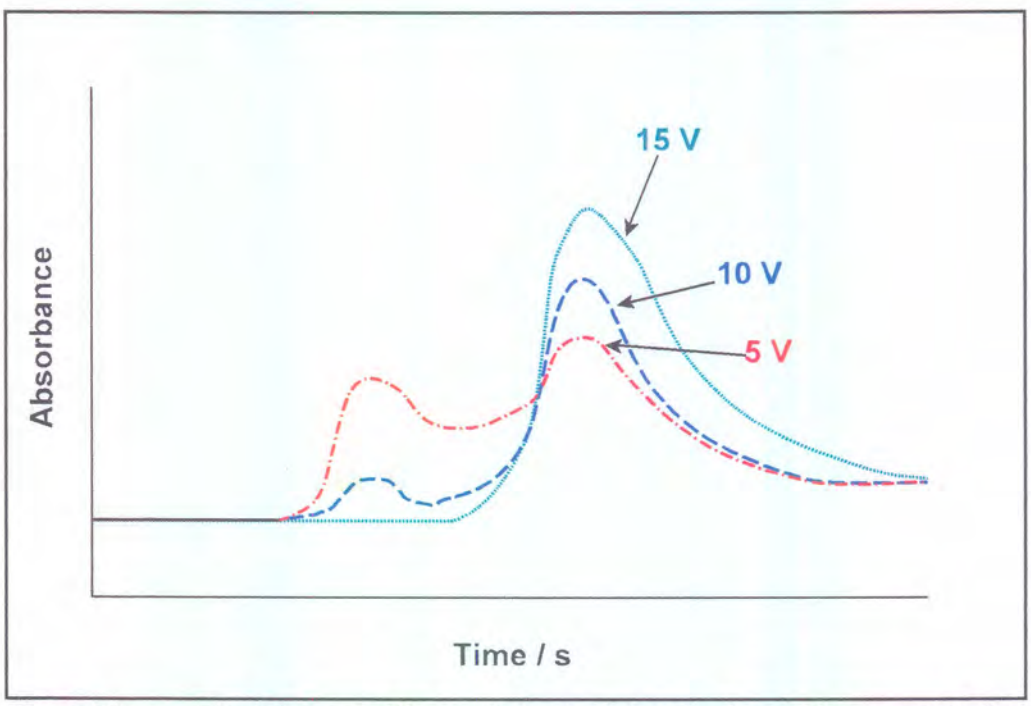

Figure 5.5 *The influence of the applied potential on the form of the copper in the acceptor channel.*

versus the applied dc potential (Figure 5.6B), it is apparent that the optimum dc potential is at 10 V. A further increase in the applied dc potential did not increase the percentage electrodialysis significantly. To compensate, however, for the better precision obtained at the higher applied dc potential and to ensure that all the copper was in the Cu^0 state, a value of 15 V was selected as the optimum.

The optimisation of the applied potential can also be influenced by the membrane potential and the flux of the analyte ions through the membrane. The membrane potential is an indication of the degree of fouling of the membrane as previously described Schoeman and co-workers [51 - 53]. This property was not investigated any further since problems with fouling were not encountered. The flux of the ions over the membrane is, however, also closely related to the applied potential and can therefore also be used as an indicator for choosing the optimum applied dc potential. The results obtained in Figure 5.7 (applied potential *versus* change in current) showed a sharp change in current when the applied potential was increased from 5 to 15 V, which indicated an increase in the flux of analyte ions through the membrane. There was a tendency for the change in current to drop above an applied potential of 15 V, which confirmed that a definite optimum was reached at 15 V.

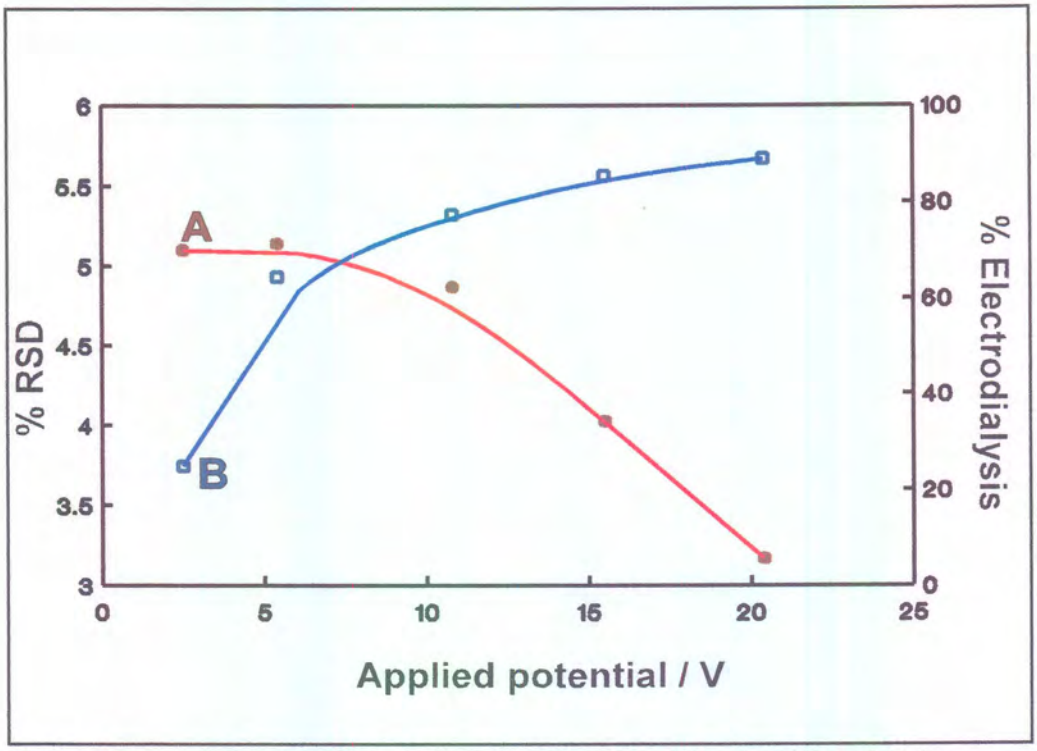

Figure 5.6 *Influence of the applied dc potential on A the % RSD and B the percentage electrodialysis.*

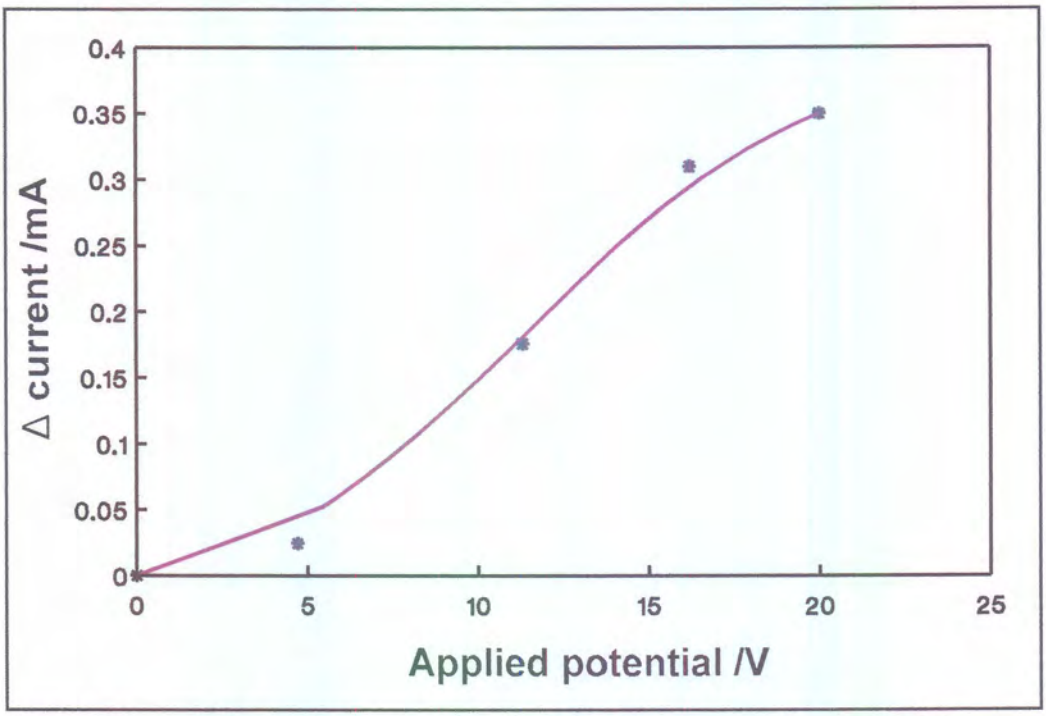

Figure 5.7 *Effect of the applied dc potential on the change of current in the acceptor channel indicating the flux of ions through the passive neutral membrane.*

5.3.3 Injection loop volume

The purpose in the evaluation of the volume of the injection loop was to find a sensitive method in the minimum time period involved for each run. It is evident from Figure 5.8 that the sensitivity of the system increased steadily with an increase in the volume of the injection loop. Thus by increasing the injection loop volume, the detection limit could be altered to fit a specific application. Unfortunately, the time involved for each run also increased with the increase in the volume of the injection loop. Thus, depending on the application, a compromise had to be found between the timing of each run and the sensitivity of the method. A sample loop volume of 80 µℓ gave ample sensitivity for the proposed system for the specific application and samples to be analysed and was, therefore, chosen for further work.

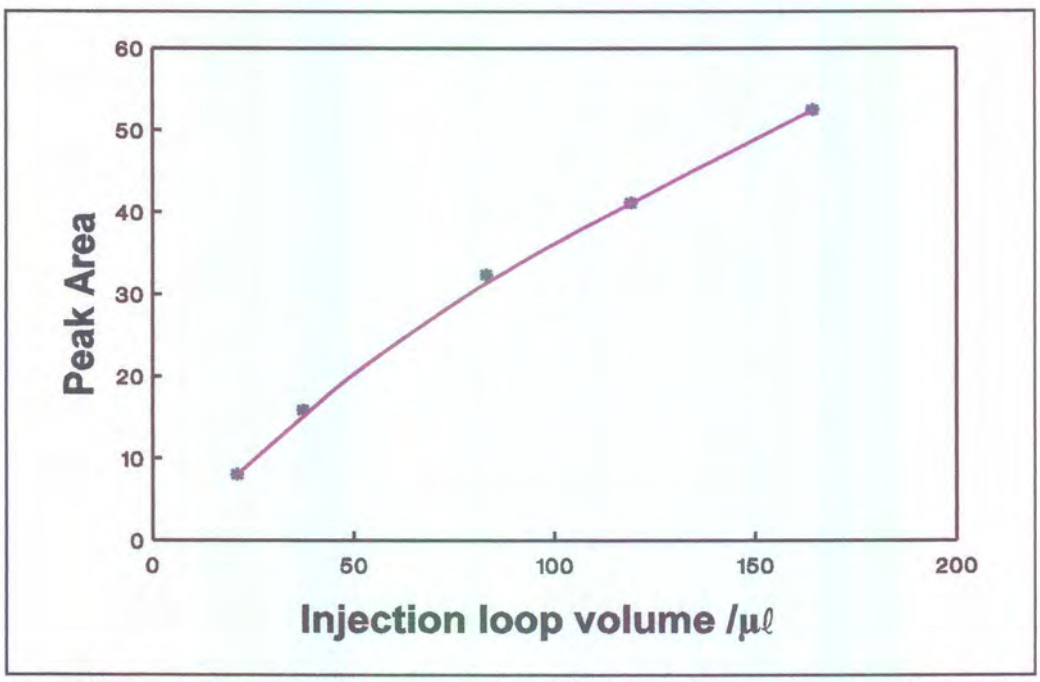

Figure 5.8 *The influence of the volume of the injector loop on the response of the system.*

5.3.4 Flow direction of the donor and acceptor channels

Under conventional FI-dialysis conditions, it was found that co-current movement of the donor and acceptor streams gave the best results. [17, 47 - 49] In this case it was found, however, that countercurrent movement of the donor and acceptor streams gave the best results, especially concerning RSD values. The moment the copper ions in the sample plug entered the electrodialyser in the donor channel, the majority of copper was immediately drawn as a narrow zone onto the cathode on the acceptor channel side as illustrate in Figure 5.9. Most of the plating occurred in the acceptor channel immediately opposite the entrance of the donor stream. After the electrodialysis mode, the acceptor channel was rinsed with nitric acid in the detection mode. (See Figure 5.3) If the acceptor channel was rinsed with the flow of the donor and acceptor streams counter currently, the dissolved copper ions would immediately be flushed out of the entrance of the acceptor channel as a plug with much less dispersion than would be the case with co-current rinsing as illustrate in Figure 5.9.

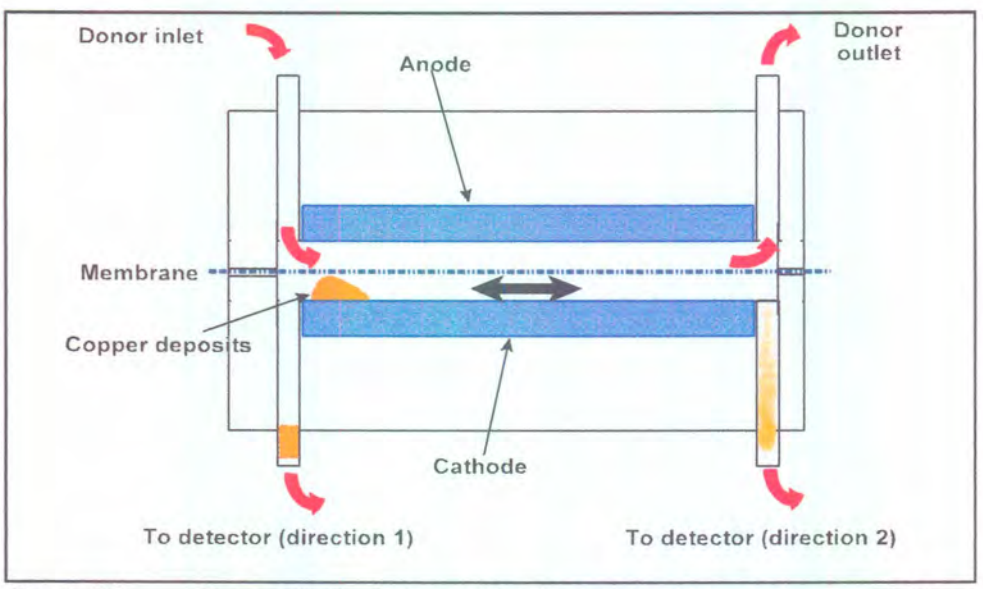

Figure 5.9 *Schematic illustration of the dispersion of the copper zone in the acceptor channel with countercurrent (direction 1) and co-current (direction 2) flow directions of the donor and the acceptor channels.*

5.3.5 Interferences

Interference could be divided into those interferences involving the electrodialysis system, the electrochemical system and those concerning the AAS detector. The main experimental work was concentrated on the interferences that may arise from the electrodialysis system. The interferences that could arise from the electrochemical system are those species that has a standard reduction potential of higher than 0.337 V. It was possible that these species could also plate onto the cathode. Chances however were very slim that they will interfere with the copper signal at the detector after it was solvated by the nitric acid solution. The interferences involving the electrodialysis process can be divided into two different categories, namely, the interferences of cations that may alter the flux of Cu^{2+} across the membrane due to competition and also chemical interference on the Cu^{2+} itself. These competitive interferences were evaluated by preparing the copper solutions in different brine solutions of known concentrations. It was found that at relatively low brine concentrations (ionic strength 20-200 mg ℓ^{-1}) there was no change in the sensitivity of the system or the peak profile. At concentrations of 100-10 000 mg ℓ^{-1}, there was some change in the peak profile, but no change in the total peak area. At concentrations above 10 000 mg ℓ^{-1}, the peak profiles became very uneven and the precision decreased. High concentrations of zinc ions in the samples interfered with the AAS detector. This interference was, however, circumvented by using a lean (oxidising) air-acetylene or a dinitrogen oxide-acetylene flame.

5.3.6 Data and calibration of the optimised system

The optimised parameters for the proposed electrodialysis-FI-AAS analyser for the determination of copper(II) ions in multivitamin tablets were as follows: donor flow rate, 0.32 mℓ min^{-1}; applied dc potential, 15 V; and injection loop volume, 80 $\mu\ell$.

The performance of the proposed analyser was critically evaluated under the

optimum conditions. The calibration graph was linear between 1 and 60 mg ℓ^{-1} with a relationship between peak area and copper(II) ion concentration given by the following equation:

$$y = 1.373x - 10.93 \qquad 5.1$$

where y is peak area and x is copper(II) ion concentration in mg ℓ^{-1}.

A linear regression coefficient (r^2) of 0.9975 (n = 11) was obtained over this concentration range. The percentage electrodialysis was found to be 94%. (Percentage dialysis was calculated by subtracting the percentage loss from the donor channel, when electrodialysis took place, from 100 %) The number of runs per hour for the proposed system was 14. The detection limit was calculated to be 1.44 mg ℓ^{-1}, and the sample interaction as 0.058%. (The purpose of sample interaction is to determine whether sample contamination takes place between successive samples. This is evaluated by doing the first determination with a low concentration of sample, followed by a sample with a 10 times larger concentration and then again followed by a sample containing the same amount of sample as the first). The detection limit and the sample interaction was calculated by using the following two equations:

$$\text{Detection limit} = \frac{3(S_b + I_b) - k}{m} \qquad 5.2$$

S_b: is the standard deviation of the background signal

I_b: is the relative peak area of the background signal

k: is the intercept of the calibration curve

m: is the slope of the calibration curve

$$\text{Interaction} = \left(\frac{A_3 - A_1}{A_2}\right) \times 100 \qquad 5.3$$

A_1: is the true peak area of the sample with low analyte concentration, or in

other words, the peak area obtained from a stable background.

A_2: is the true peak area of sample containing ten times more analyte than in A_1

A_3: is the peak area for the sample which will indicate the interaction with sample A_2. The concentration of A_1 is equal to A_3.

The mass of copper plated on the cathode, with a sample concentration of 20 mg ℓ^{-1}, was calculated to be 1.53 x 10^{-6} g, taking the percentage electrodialysis into account. The percentage electrodialysis was obtained by connecting the donor channel to the detector. Firstly the peak area was obtained when no dialysis or electrodialysis could take place (the acceptor channel was emptied beforehand). Hereafter the peak area was obtained from the donor channel after electrodialysis took place. The two peak areas obtained were then compared. The calculation of the percentage dialysis was done at optimised conditions.

5.3.7 Samples

The proposed system was applied to the determination of copper in a multivitamin and mineral supplement tablet. Tablets were dissolved in water and diluted to 100 mℓ. The need for membrane cleanup of the sample was illustrated once again due to the fact that the tables did not dissolve completely. Residues from the tablets could have block the nebulizer unit of the FAAS. The samples were analysed with the proposed electrodialyser-FI-AAS system by injecting them directly into the donor stream. The accuracy of the proposed system was evaluated by comparing the results obtained with those obtained by using a standard AAS procedure. In the standard method the samples were filtered manually before analysis. The results, as shown in table 5.1, revealed an excellent agreement between the two methods.

Table 5.1 Comparison of samples analysed by the proposed system and a standard AAS method

Sample	FAAS method mg ℓ^{-1}	Electrodialysis method	%RSD Proposed method
1	16.4	15.6	4.4
2	16.5	16.1	4.3
3	16.9	16.1	4.5
4	16.9	16.2	4.2
5	17.3	16.4	4.4

5.4 Conclusions

In chapter 4, it was found that the percentage dialysis of the analyte improved to a maximum of 37% (the chloride system). In this new proposed system, (the copper system) the percentage dialysis increased to a massive 94%. It was thus clear that the problems of the formation of gaseous products in the acceptor channel did not hamper the detection in this new system. The reasons for this is the following:

a: The detector used, the FAAS, was not as sensitive towards the formation of bubbles in the acceptor channel as was the case with the UV/Vis spectrophotometer.

b: In the newly developed copper method, the analyte could be plated onto the electrode in the acceptor channel which was not the case in chapter 4 with the chloride method. Due to the plating of the copper, the gas bubbles which did form, could be removed by rinsing the acceptor channel with de-ionised water before the HNO_3 was drawn into the acceptor channel for the solvation of the plated copper.

It was further possible, with larger injection volumes to preconcentrate the analyte even more and thus lower the detection limit. It would not be recommended to lower the flow rate or to increase the applied dc potential since the percentage dialysis is already 94%.

This system can also be applied for the analysis of very low concentrations of copper. In the preposed system, the use of the electroplating of the copper ions was not exploited to its full capacity. By increasing the injection volume, very low copper concentrations can be injected and copper trace enrichment can take place in the acceptor channel.

As is evident from the fact that the acceptor channel could be rinsed (to remove all the gaseous products formed at the cathode) before the copper was to be solvated in the HNO_3, this ED/FIA system can also be used with ease with detectors that are very sensitive towards the presence of bubbles (gaseous products in the acceptor channel) in the flow system. Also it will be possible to use an electrochemical detection system since the ED can switched off before the solvation and analysis of the Cu^{2+} ions.

The massive increase of the percentage dialysis from the chloride system to the copper system is mostly due to the much lower flow rate in the donor channel of the copper system. (2.0 mℓ min^{-1} in the chloride system to 0.32 mℓ min^{-1} in the copper system) It is further possible that the migration rate of the copper ions under the influence of an applied potential is higher for the copper ions than for the chloride ions. A possible explanation for this that the chloride ions may be more hydrated in solution than is the case with the copper ions. When this happens, the effective radius of the chloride ion will be much larger than that of the copper ion (both ions in solution). This enlarged effective radius of the chloride ions in solution will then in turn give rise to a lower drift speed of the chloride ions under in influence of the applied dc potential. (See paragraph 3.1)

The proposed electrodialyser-FI-AAS system is suitable for the analysis of samples containing solid particles in suspension. These particles were of such a nature that they continuously blocked the inlet path to the nebulizer of the AAS detector. The flexibility of the electrodialyser-FI system is not only the removal of the solid particles from the analyte, but also retaining the analyte concentration in an acceptor channel the same as it was originally in the donor channel.

5.5 References

1 Burguera, J.L., (**1989**) Flow Injection Atomic Spectroscopy, Marcel Dekker, New York.

2. Kuban V., Komarek J., Cajkova D., (**1989**) Collect. Czech. Chem. Commun. 54(10): 2683.

3. Hirata S., Honda K., Kumamaru T., (**1989**) Anal. Chim. Acta. 221(1): 65.

4. Purohit R., Devi S., (**1991**) Talanta. 38(7): 753.

5. Carbonell V., Mauri A.R., Salvador A., De La Guardia M., (**1991**) J. Anal. At. Spectrom. 6(7): 581.

6. Burguera J.L., Burguera M., Matousek de Abel de la Cruz A., Anez N., Alarcon O.M., (**1992**) At Sectrosc. 13(2): 67.

7. Naghmush A.M., Trojanowicz M., Olbrych-Sleszynska E., (**1992**) J. Anal. At. Spectrom. 7(2): 323.

8. Ma R., Van Mol W., Adams F., (**1994**) Anal. Chim. Acta. 285(1): 33.

9. Elmahadi H.A.M., Greenway G.M., (**1994**) J. Anal. At. Spectrom. 9(4): 547.

10. Maquieira A., Elmahadi H.A.M., Puchades R., (**1994**) Anal. Chem. 66(9): 1462.

11. Maquieira A., Elmahadi H.A.M., Puchades R., (**1994**) Anal. Chem. 66(21): 3632.

12. Burguera J.L., Burguera M., Carrero P., Marcano J., Rivas C., Brunetto M.R., (**!995**) J. Autom. Chem. 17(1): 25.

13. Van Staden J.F., Hattingh C.J., (**1995**) Anal. Chim. Acta. 308(1-3): 214.

14. Van Staden J.F., Hattingh C.J., (**1995**) J. Anal. At. Spectrom. 10(10): 727.

15. Ma R., Van Mol W., Adams F., (**1996**) At. Spectrosc. 17(4): 176.

16. Zhuang Z.X., Wang X.R., Yang P.Y., Huang B.L., (**1994**) Can. J. Appl. Spectrosc. 39(4): 101.

17. Azeredo L.C., Sturgeon R.E., Curtius R.J., (**1993**) Spectrochim. Acta. 48B(1): 91.

18. Ebdon L., Fisher A.S., Worsfold P.J., Crews H., Baxter M., (**1993**) J. Anal. At. Spectrom. 8(5):691.

19. Yang C.L., Zhuang Z.X., Wang X.R., Quin S.D., Yang P.Y., (**1994**) At. Spectrosc. 15(3) 135.

20. Bortoli A., Gerotto M., Marchiori M., Mariconti F., Polonta M., Troncon A., Microchem. J. 54(4): 402.
21. Hwang T., Jiang S.J., (**1996**) J. Anal. At. Spectrom. 11(5): 353.
22. Izquierdo A., Luque de Castro M.D., Valcarcel M., J. (**1993**) Autom. Chem. 15(4): 121.
23. Matysik F.M., Gerner G., (**1993**) Analyst. 118(12): 1523.
24. Izquierdo A., Luque de Castro M.D., Valcarcel M., J. (**1994**) Electroanalysis. 6(10): 894.
25. Chow C.W.K., Kolev S.D., Davey D.E., Mulcahy D.E., (**1996**) Anal. Chim. Acta. 330(1): 79.
26. Haj Hussein A.T., (**1996**) Talanta. 43(11): 1909.
27. Hattingh C.J., (**1994**) MSc. dissertation, University of Pretoria.
28. Chimpalee N., Chimpalee D., Srithawepoon S., Patjarut T., Thorburn Burns D., (**1995**) Anal. Chim. Acta. 304(1): 97.
29. Liu R.M. Liu D.J., Sun A.L., (**1993**) Talanta. 40(4): 511.
30. Barnes D.E., Jones E.A., (**1989**) Mintek report nr. M389. Council for mineral Technology.
31. Szpunar Lobinska J., Trojanowicz M., (**1990**) Anal. Sci. 6(3): 415.
32. Maquieira A., Elmahadi H.A.M., Puchades R., (**1996**) Analyst. 121(11): 1633.
33. Esmadi F.T., Khasawneh I.M., Kharoaf M.M., Attiyat A.S., (**1992**) Can. J. Appl. Spectrosc. 37(5): 119.
34. Cox J.A., Twardoski Z., (**1980**) Z. Anal. Chim. Acta. 119: 39.
35. Cox J.A., Carnahan J.W., (**1981**) Appl. Spectrosc. 35: 447.
36. Cox J.A., Dabek-Zlotorzynska E., Saari, R., and Tanaka, N., (**1988**) Analyst. 113: 1401.
37. Koropchak J.A., Allen L., (**1989**) Anal. Chem. 61: 1410.
38. Kasthurikrishnan, N., Koropchak J.A., (**1993**) Anal. Chem. 65: 857.
39. Kuban V., Komarek J., Chajkova D., (**1989**) Collect. Czech. Chem. Commun. 54: 2683.
40. Carbonell V., Salvador A., De la Guardia M., (**1992**) Fresenius' J. Anal. Chem.

324: 529.

41. Turnell D.C., Cooper J.D.H., (**1985**) Autom. Chem., 7: 177.
42. Turnell D.C., Cooper J.D.H., (**1985**) Autom. Chem. 7: 181.
43. Cox J.A., Carlson R., (**1981**) Anal. Chim. Acta. 130: 313.
44. Van Staden J.F., Hattingh C.J., unpublished work.
45. Van Staden J.F., Van Rensburg, A., (**1990**) Analyst. 115: 1049.
46. Marshall, G.D., Van Staden, J.F., (**1992**) Anal. Instrum.. 20: 79.
47. Schoeman, J.J., (**1992**) PhD Thesis, University of Pretoria.
48. Schoeman, J.J., Van Staden, J.F., (**1991**) Water SA, 1991, 17: 307.
49. Schoeman, J.J., Van Staden, J.F., (**1997**) J. Membr. Sci. 132: 1.

Chapter 6

Determination of zinc in pharmaceutical products using an electrodialyser incorporated into a flow injection system.

6.1 Introduction

The first studies linking zinc and growth were done in Iran and Egypt almost 3 decades ago. Zinc, as a trace mineral, is of utmost importance for normal human bodily functions. Minerals and vitamins are essential components of the diet. The body cannot synthesize minerals and the cells can generate only a small quantities of very few vitamins. [1] Minerals are inorganic ions released through the dissociation of electrolytes. Zinc is a trace mineral in the human body with a total body content of an adult human of 2 - 3 g. The highest concentrations are in the liver, kidneys, pancreas, bone, voluntary muscle, parts of the eyes, prostate gland, spermatozoa, skin and nails. [1,2] Zinc is known to participate in reactions involving either the syntheses or degradation of major metabolites such as carbohydrates, lipids, proteins and nucleic acids. More than 200 zinc enzymes have been isolated from different species. Zinc is also involved in the stabilization of protein and nucleic acid structure and the integrity of subcellular organelles and transport processes, immune function and expression of genetic information. Zinc acts as a cofactor of enzyme systems, notably carbonic anhydrase. Zinc deficiency can cause delayed wound healing, alopecia and diverse forms of skin lesions. [1, 2]

Atomic spectroscopy is one of the most sophisticated and elegant methods for direct assay of cations. [3,4] Atomic absorption spectrometry (AAS) allows no fewer than 70 metals to be determined directly, which makes it very suitable for many clinical and forensic analysis. Furthermore, indirect AAS methods allow many techniques to be extended to the analysis of a number of analytes besides metals (including anions and organic compounds). [5] Suspended solids, macromolecules and high salt

concentrations in samples, however, caused nebulizer clogging and ultimately blocked the nebulizer. This resulted in inaccurate results and low precision. To avoid this the nebulizer had to be removed and cleaned frequently, but the analysing process then became tedious and time consuming.

AAS in association with flow injection (FI) analysis is considered a very competent method for pharmaceutical sample analysis. The advantages of the FI-AAS association is matrix removal and analyte preconcentration. [5] Various means of matrix removal are possible in chemical analysis. According to Debrah *et al.* [6], precipitation is the oldest method of chemical separation. Precipitation methods are satisfactory for macro separations, although precipitates are usually contaminated with foreign ions present in the solution. Precipitation is useful to remove a major constituent of a sample if this constituent interferes with the subsequent determination of trace components. In an FI system it is possible to retain small quantities of precipitate on an in-line filter. It is even possible to retain the analyte element co-precipitated on the interior of an open knotted tube reactor. It is however not possible to use an in-line filter in an FI system for large amounts of precipitates. To overcome this problem, the use of a recirculating, closed-loop manifold for sample pretreatment was described by Debrah *et al.* [6] Solvent extraction is another very successful method of matrix removal. When analysing zinc (at the 213.856 nm line), a large excess of iron can interfere, originating from the weak 213.859 nm iron line. Removal of the iron interference by means of solvent extraction was done by Sweileh and Cantwell.[7] Similar work and the influence of a masking agent was illustrated by Ma *et al.* [8] The use of an ion-exchanger (eg. Chelex 100) has also been used extensively not only as a method for preconcentration, but also as a means to separate matrix interferences.[9] An alternative approach is to immobilise a micro-organism cell wall on an insoluble substrate. Living organisms have the ability to absorb trace metals from an aqueous solution.[10]

The problem of nebulizer clogging by high salt concentrations is not so severe when the AAS is interfaced to an FI system, but this is not the ultimate solution. Although the carryover is small, a gradual drop in the sensitivity was observed by Davey [11] when

analysing samples with high salt concentrations. The use of neutral dialysis membranes (passive dialysis) in flow-through dialysers as part of FI systems is an extremely powerful tool to remove suspended solids and macromolecules in order to let the analyte flow unhindered to the detector. Unlike filter systems, the part of the sample matrix containing suspended solids is continuously channelled via the donor stream to waste, while the clear dialysed analyte solution in the acceptor stream is flushed to the detector.

We successfully incorporated passive neutral membranes as part of various FI systems in our laboratory to remove interferences, before the determination of analytes. [12 - 18] We also included an electrodialyser (fitted with a passive neutral membrane) successfully as part of FI-AAS systems to enhance mass transfer together with the removal of interferences. [17, 18] A similar approach was used by Buschner *et al.* [19] during the on-line analysis of adenosine triphosphate and inositol phosphate with electrodialysis-capillary zone electrophoresis.

The main objective of this project was to develop a method that will be able to handle samples with high salt concentrations and at the same time remove the matrix interferences during the determination of zinc in pharmaceutical products.

6.2 Experimental

6.2.1 Reagents and Standards

All glassware and storage bottles were soaked in 10 % (v/v) nitric acid overnight and rinsed with de-ionised water prior to use. All reagents were of analytical grade and de-ionised water, obtained from a Modulab water system, was used for the preparation of all stock solutions and dilutions of standards. A 1000 mg ℓ^{-1} zinc(II) stock solution was prepared by dissolving 1.000 g zinc granules in 40 mℓ 1:1 hydrochloric acid, and dilute it to the mark in a 1ℓ volumetric flask. Electrolyte stock solution was prepared by dissolving 25.42 g of sodium chloride in a 1 ℓ volumetric flask and made up to the mark with de-ionised water. Suitable dilutions

of the stock solutions were made to prepare the zinc standards. The percentage nitric acid in the standard zinc solutions was also adjusted to be 1% (v/v) and the electrolyte concentration in all the zinc solutions was 0.31 mol ℓ^{-1} in sodium. Standard solutions were prepared daily. [20] The rinsing solution consisted of a 1 % (v/v) nitric acid solution and a 0.31 mol ℓ^{-1} sodium solution. (Sodium solution prepared from dried sodium chloride)

6.2.2 Instrumentation

The FI system (Figure 6.1) used was composed of the following components:

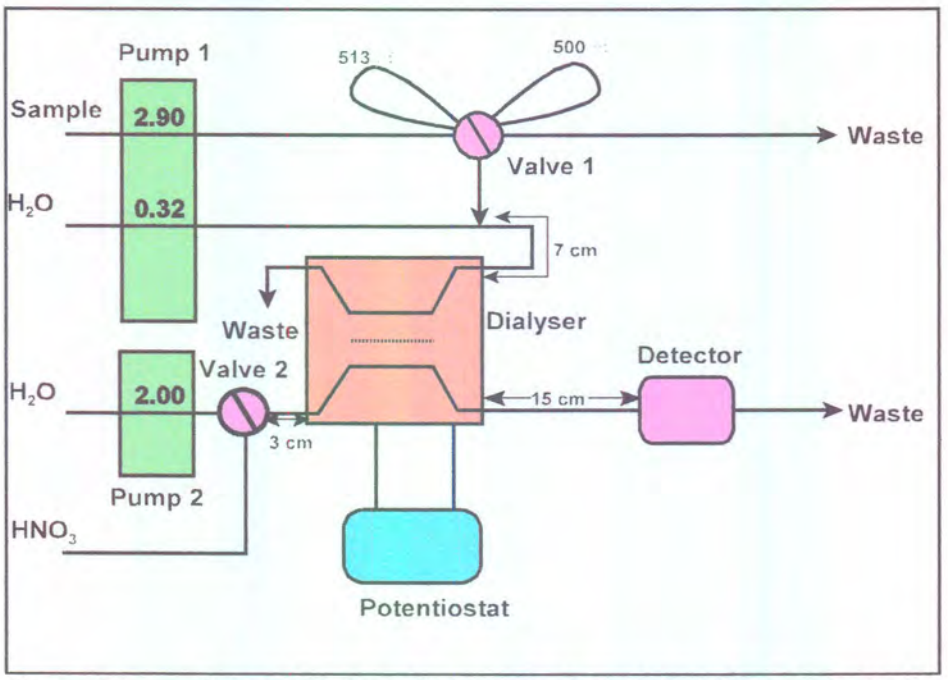

Figure 6.1 Schematic flow diagram of the ED-FI-AAS system for the determination of zinc.

1. A six-roller Cenco peristaltic pump (rotating at 10 rev min^{-1})
2. One Valco 10-port electrically actuated injection valve (Houston, TX, USA). The injection valve was configureured in such a way that it consisted of a sample loop of 513 $\mu\ell$ and a rinsing loop of 500 $\mu\ell$. These two loops were used to alternating inject the sample solution and the rinsing solution into the donor carrier stream of the electrodialyser (see

Figure 6.2).

3. The manifold consisted of Tygon tubing, with an internal diameter (id) of 0.76 mm, cut the required lengths and wound around Perspex rods with an outer diameter (od) of 10 mm. The electrodialyser unit used (Figure 6.2) was a slightly modified version of the dialyser previously described by van Staden and van Rensburg [12] It is similar to the one used in chapter 4 for the determination of chloride with the only difference that the polarity on the electrodes were swopped so that the anode was situated in the donor channel and the cathode in the acceptor channel. The dialyser unit consisted of two, mirror image, PVC blocks. Embedded into each of these blocks were graphite electrodes which acted as the anode (acceptor side) and the cathode (donor side) respectively. Placed onto each of the PVC blocks was a 0.6 mm thick Perspex spacer. Into each of the Perspex spacers, a groove of 0.6 mm diameter and 300 mm length was cut so as to form a channel when placed onto each of the PVC blocks respectively. The PVC blocks were then fitted onto each other in such a way that the Perspex spacers facing each other and the grooves in the respective Perspex blades coincided with each other. The membrane was then sandwiched between the two Perspex spacers as the only separation between the two tubes so formed. The walls of the tubes that were formed thus consisted of, at the far end, the graphite (which was embedded into the PVC blocks), the side walls of Perspex and the common wall, the membrane. A Technicon pre-mount membrane was used in the dialyser unit.
4. A Leader LPS 156 potentiostat was used to apply the dc potential.
5. A Prema 5000 integrating multimeter was used for current and potential measurements.
6. A Varian AA 1275 Atomic absorption spectrometer (Palo Alto, CA, USA) was used as the detector. A Varian Techtron Zn hollow cathode lamp, with a current of 7 mA, was used to give a monochromatic light ray in the detector. A wavelength of 213.9 nm and a spectral bandpass of 0.2 mm

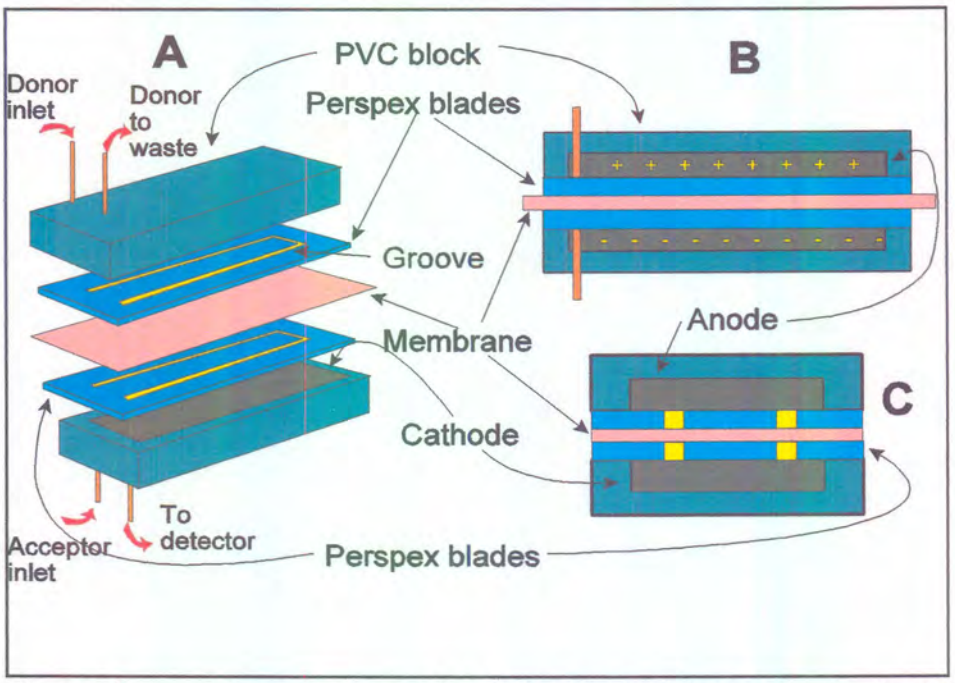

Figure 6.2 *Schematic presentation of the Electrodialyser unit. A - the 3D presentation, B - a longitudinal cross-section and C - a diagonal cross-section.*

was used. A lean (oxidising) air/acetylene flame was used.

7. The AAS detector, pump and valve were coupled to a personal computer equipped with the *FlowTEK* program. [21]

6.2.3 Flow system and Procedure

A single run consisted of the following procedures: (See Figure 6.3 for the timing diagram)

Operation of pump and valve

A timing diagram for the FI-AAS system is depicted in Figure. 6.3. The pump was never switched off during the analysis. The valve was switched between the "load" and the "inject" position. During the "load" position, the 513 $\mu\ell$ loop was filled with a sample, whilst the 500 $\mu\ell$ was connected to the donor channel. When

the valve was switched to the "inject" position, the 513 $\mu\ell$ loop was connected to the donor channel (thus injecting the sample into the donor channel), whilst the 500 $\mu\ell$ was filled with the rinsing solution.

The system was switched on and allowed to run for about 5 minutes in order to equilibrate the flow dynamics of all parts of the system. The computer was then actuated and the timing sequence started in the load position.

(i) Starting the system. (Loading)

Pump: The pump was switched on. Flow rates in the donor and acceptor channels were both 1.40 $m\ell\ min^{-1}$. The inlet tubing, connected to the donor channel, was removed from the water container so that air was pumped through the donor channel and de-ionized water was pumped through the acceptor channel.

Valve: The valve was switched to the load position. In the load position the 500 $\mu\ell$ loop was connected to the donor channel and the 513 $\mu\ell$ loop was filled with sample solution.

Potentiostat: The potentiostat was set to on position at 17.5 V.

(ii) Analysis

At time T = 0 s, the valve was switched to the "inject" position, thus

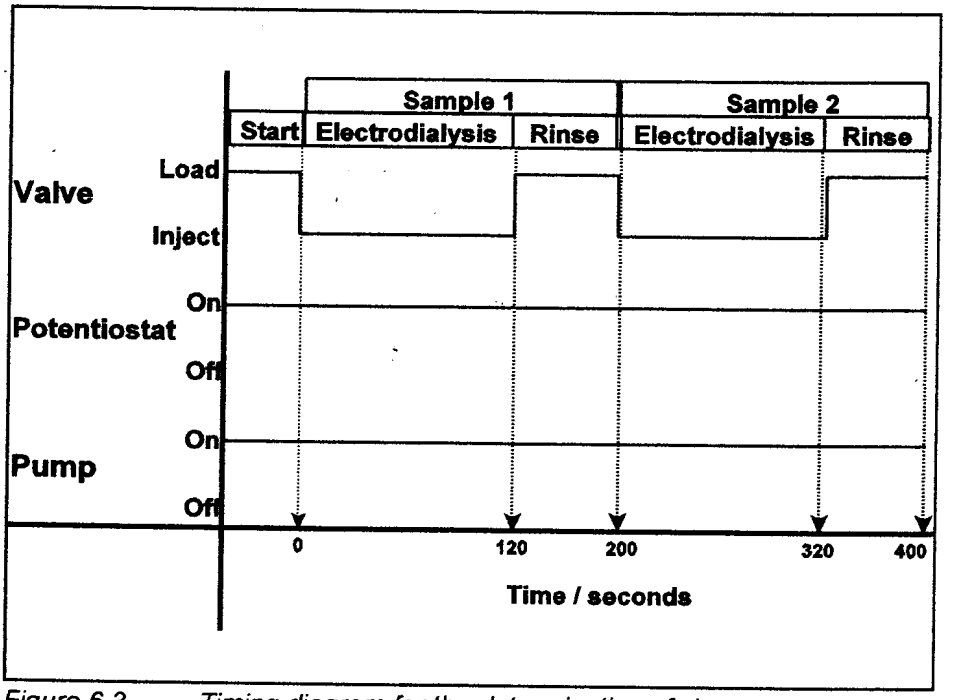

Figure 6.3 *Timing diagram for the determination of zinc*

directing the 513 $\mu\ell$ loop to the donor channel, whilst the 500 $\mu\ell$ loop was filled with rinsing solution. The sample plug was pumped through the donor channel at a rate of 1.40 mℓ min^{-1}. The applied potential over the membrane was kept constant at 17.5 V for the duration of the electrodialysis step. Analyte ions in the sample plug electrodialysed through the membrane into the acceptor channel. These analyte ions were then transported via the acceptor channel to the detector. At time T = 120 s, the valve was switched to the "load" position again to fill the 513 $\mu\ell$ loop for the next run and at the same time directing the 500 $\mu\ell$ rinsing solution into the donor channel.

Data acquisition and device control were achieved using a PC30-B interface board (Eagle Electric, Cape Town, South Africa) and an assembled distribution board (MINTEK, Randburg, South Africa). The *FlowTEK*[16,21] software package (obtainable from MINTEK) for computer-aided flow analysis was used throughout

for device control and data acquisition. All the data given (mean peak area values) are the average of 11 repetitions.

6.3 Results and discussion

In previous work done by van Staden and Hattingh [18], a similar approach was used for the analysis of copper(II). The zinc and the copper systems differ in the sense that in the latter system, copper metal was plated onto the cathode in the stagnant acceptor channel. It was however not possible to apply this procedure for the zinc determination since the reduction potential of zinc, at standard conditions, is much lower than 0 V The objective of this study was to introduce a zinc analyte plug from the FI system into the detector which was free from possible matrix interferences, but still have a high enough concentration so that preconcentration will not be necessary. To obtain this goal, it was imperative to ensure that the mass transfer across the membrane during the electrodialysing step was as high as possible (Figure 6.2). One of the disadvantages of a dialysis system is the fact that the dialyser has a double dilution effect on the analyte. Firstly, in the form of a massive increase in the dispersion of the analyte sample plug whilst passing through the dialyser and secondly, in the case of passive dialysis without the application of the electrical field across the membrane, the percentage dialysis varies between 0-7%. [16] Prevention of the dispersion in the donor channel was achieved by making use of air as the carrier (instead of de-ionised water). In the acceptor channel de-ionised water was pumped through continuously.

The FI-AAS system was optimised, according to achieved sensitivity and reproducibility, under the following headings:

6.3.1 Applied potential across the membrane

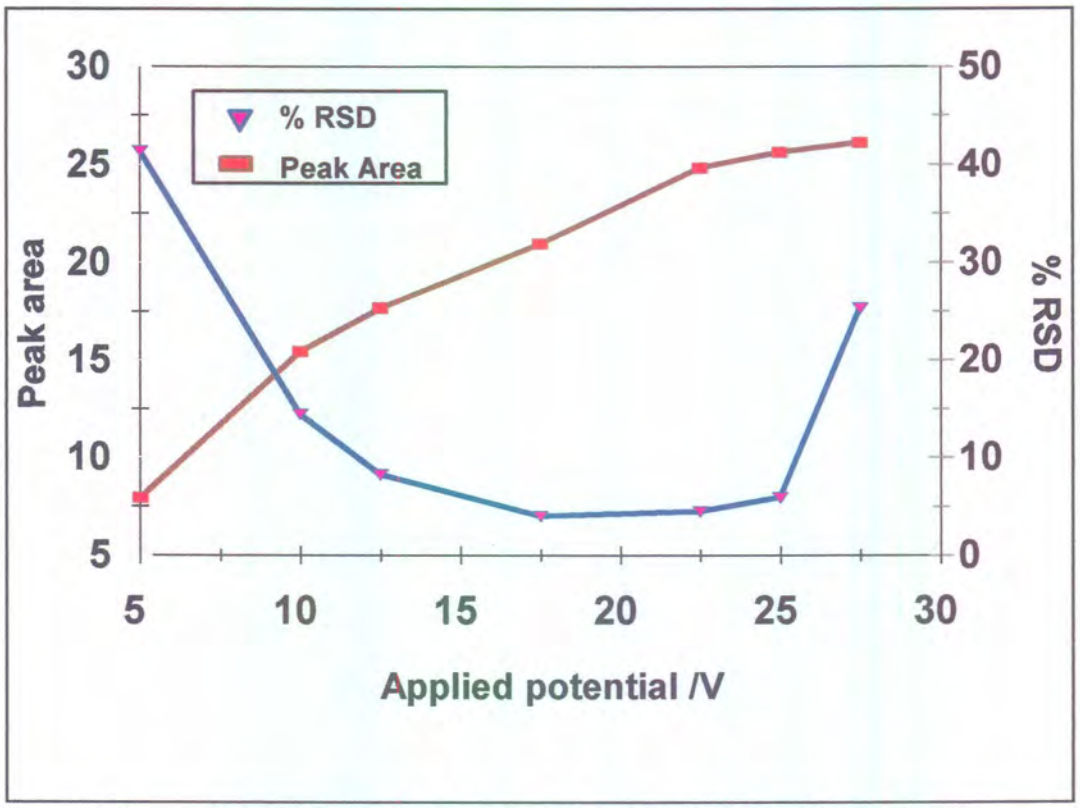

Figure 6.4 Effect of the applied dc potential on the % RSD and the peak area

Of all the parameters optimised (flow rate of the donor and acceptor streams, injection loop volume and electrolyte concentration), the applied potential had the largest influence on the migration rate of zinc ions across the membrane. The influence of the applied potential on the average peak area is illustrated in Figure 6.4. The flow rates of the donor- and acceptor channels were kept constant at 1.40 mℓ min^{-1} during the optimisation of the applied potential. It is clear from Figure 6.4 that the optimum potential in both the average peak area and the % RSD lies between 17.5 and 22.5 V. The optimum applied potential with the better sensitivity is at 22.5 V (Figure 6.4) with the reproducibility more or less the same. What is however not indicated on the graph in Figure 6.4 is the massive peak distortions which occurred at 22.5 V and to a much lesser extent at 17.5 V. These distortions were the result of gas formation at the cathode in the

acceptor channel. It is possible that these peak distortions can alter the analysis of real samples which may contain species that have high gas formation capabilities. It is clear that rather high RSD values occurred at the extremes of the measured applied potentials. At the higher potential (27.5 V), there was a very high rate of gas formation (and thus also a distortion of the peak) which in turn led to the higher RSD values. At the low applied voltages, the migration rate of the zinc across the membrane was so low that the reproducibility was increasingly influenced by the noise of the instrument. From Figure 6.5 it is evident that there is nearly a linear relationship between the applied dc potential and the electrical current across the membrane. It can be assumed that there will be a further increase in the current with increasing applied dc potential, but due to increased RSD values at higher applied potentials (see Figure 6.4), it was not recommended. The potential of 17.5 V was therefore chosen as the optimum applied potential.

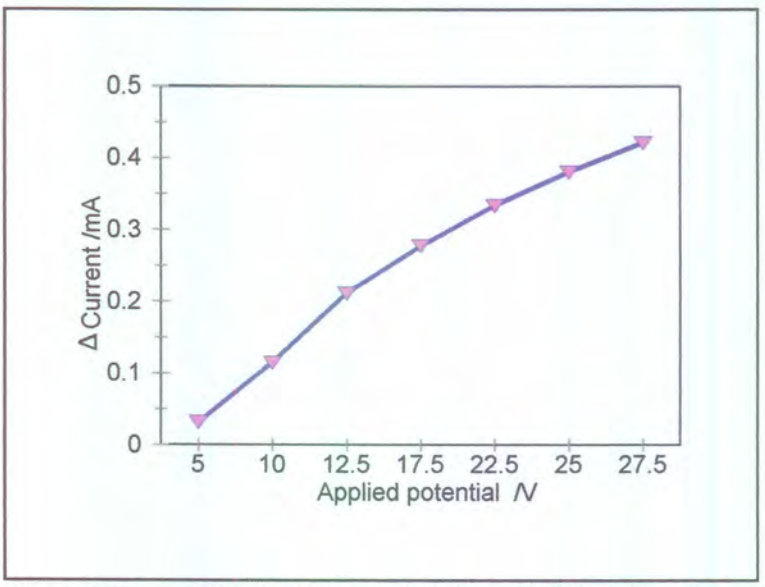

Figure 6.5 *Effect of the applied dc potential on the change of current in tie acceptor channel indicating the flux of ions through the passive neutral membrane*

6.3.2 Flow rates of the donor and the acceptor streams

The flow rates in the donor and the acceptor channels had the next largest influence on the diffusion rate of the analyte across the membrane. The flow rates of the donor and the acceptor streams were kept the same throughout the optimisation. Optimisation was done by injecting 10.0 mg ℓ^{-1} Zn^{2+} into the donor channel and keeping the applied potential across the membrane constant at 17.5 V. As can be seen from Figure 6.6, there was a steady decrease in the average peak area with the increase in the flow rate of the donor and the acceptor channels. The optimum flow rate was taken between 1.4 and 2 mℓ min^{-1}. At these flow rates the % RSD was also at its lowest. Too high flow rates prevented the transfer of the bulk of the zinc ions across the membrane to the acceptor channel, whereas too low flow rates led to unnecessary high analysis times.

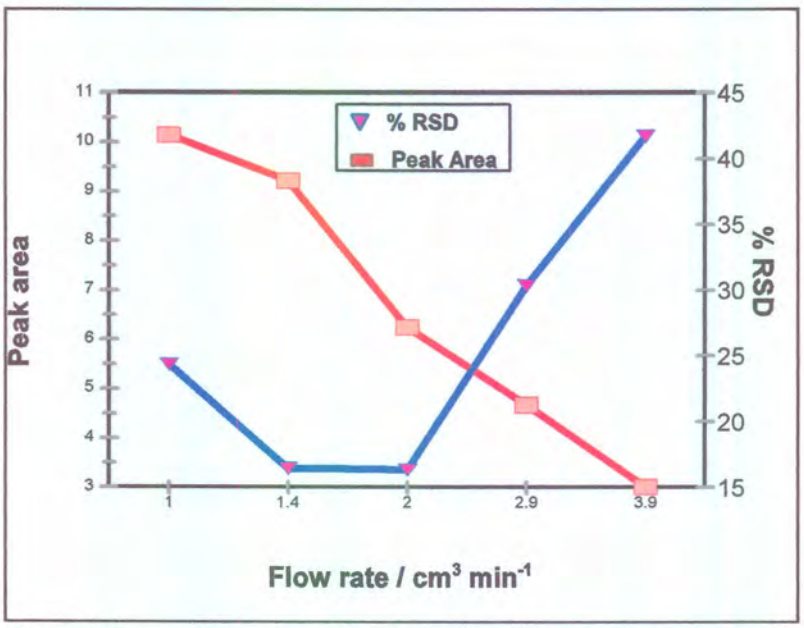

Figure 6.6 *Influence of the flow rate of the donor- and acceptor stream on the % RSD and the peak area.*

6.3.3 Injection loop volume

The flow rates of the donor and the acceptor streams were kept constant at 1.4 mℓ min^{-1} and the applied potential at 17.5 V during the optimisation of the injector loop volume. It can be seen from Figure 6.7 that there is a linear increase in the average peak area with increasing injection loop volume. The % RSD was rather low at most of the injection loop volumes with a slight elevation at the smaller injection loop volumes. The optimum injection loop volume was taken to be 513 $\mu\ell$. Even though larger injection loop volumes gave higher average peak areas with not much change in the % RSD, the higher injection loop volumes resulted in much longer experimental times and a lower throughput of samples.

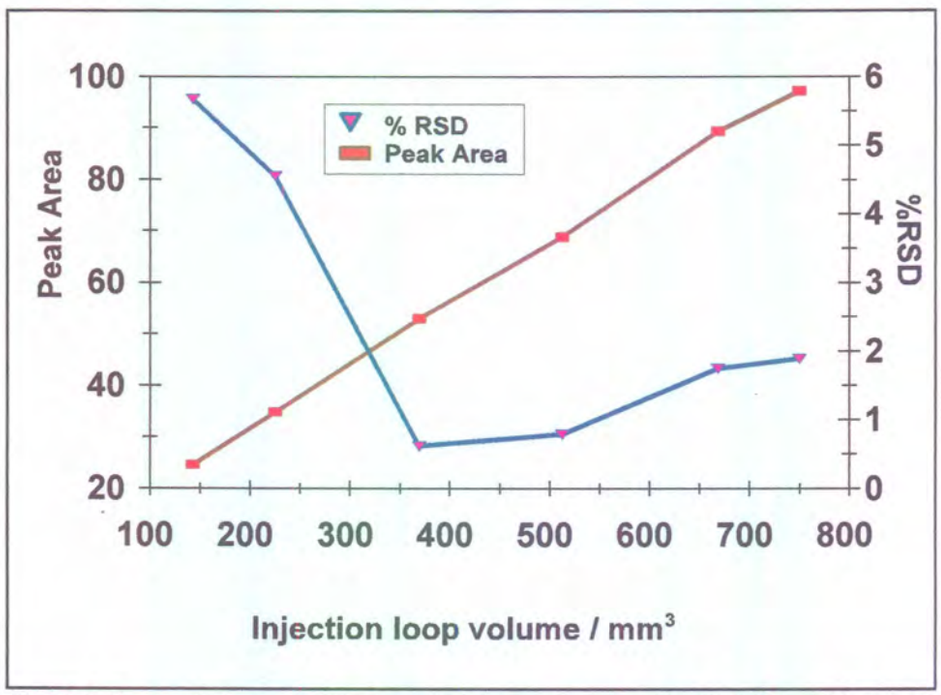

Figure 6.7 *Influence of the injection loop volume on the % RSD and the peak area*

6.3.4 Addition of an electrolyte

The migration rate of ions under the influence of an applied potential is altered by the addition of an electrolyte. With the addition of an electrolyte, the hydration of the analyte ion is changed and therefore also the effective ion radius of the ion in motion (the analyte). [22]. In addition to this, it was found that there was a slight retention of the analyte on the membrane. (After rinsing the donor channel with an electrolyte solution, traces of the analyte was found in the acceptor channel) To address both these situations, an electrolyte was added to all the solutions that were analysed. There was an increase in the zinc signal with the addition of the electrolyte. This phenomenon indicated that the migration of zinc across the membrane was enhanced with the addition of the electrolyte. The electrolyte concentration was increased up to the point where an increase in the electrolyte concentration did not further enhance (or alter) the zinc signal. An electrolyte solution (without zinc analyte) was used to rinse the dialyser between two consecutive runs to ensure that all the analyte ions were removed from the dialyser and the membrane. Sodium chloride at a concentration of 0.31 mol ℓ^{-1}, was used as the electrolyte. The counter anion, however, did not have an influence on the migration of zinc(II) ions across the membrane as long as it is neutral, but an anion with basic properties led to the precipitation of the zinc(II) ions.

6.3.5 Interferences

The electrodialyser was found to be an excellent means of sample cleanup. It is known that iron(III) can interfere with the 213.9 nm Zn line. The influence of iron(III) on the zinc analysis is depicted in Figure 6.8. It is clear from Figure 6.8 that iron in concentrations above 7.5 times the zinc concentration in the sample seriously altered the zinc signal. Masking agents like oxalate, phosphate, citrate, tartrate and fluoride can be used to eliminate the iron(III) interference. The use of these masking agents during the extraction of zinc was studied by Ma *et al.* [8]

Some of these masking agents had a negative influence on the zinc signal. The addition of fluoride ion to the zinc/iron mixture decreased the effect of the iron(III) to such an extent that the system could tolerate iron(III) concentrations up to ten times the zinc concentration in the samples before any alterations in the zinc signal was observed. Since all the fluoride ions migrated to the anode, the excess fluoride ions were perfectly removed from the zinc, which migrated across the membrane towards the cathode. It was thus possible to add a large excess of the masking anions without interferences with the zinc determination. It is thus clear that any anion or neutral species which interferes with the zinc can easily be separated from the zinc before analysis.

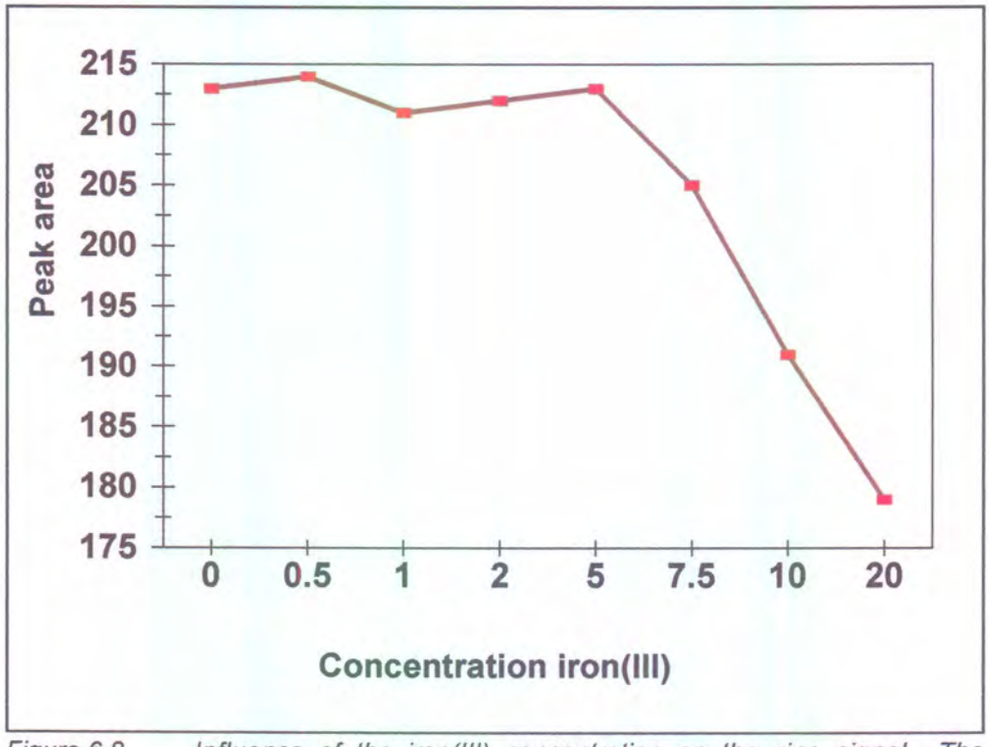

Figure 6.8 *Influence of the iron(III) concentration on the zinc signal. The concentration of the iron(III) is given as a multiple of the zinc concentration*

Anionic or neutral zinc complex formation would severely interfere with the analysis of zinc(II) ions. To prevent complex formation or to destroy any possible

zinc complexes, low pH's were maintained in all working solutions. In a strong acidic medium most of the zinc complexes will be destroyed. Apart from the simulated gastric fluid, nitric acid was added to the solutions so that the pH was < 1.0.

6.3.6 Data and calibration of the optimised system

The optimised parameters for the proposed electrodialysis-FI-AAS analyser for the determination of zinc(II) ions in multivitamin tablets are as follows:

Donor and acceptor flow rate:	1.40 mℓ min^{-1}
Applied potential:	17.5 V
Injection loop volume:	513 $\mu\ell$

The performance of the proposed analyser was critically evaluated under the optimum conditions. The calibration graph was linear between 1 and 20 mg ℓ^{-1} with the relationship between peak area and zinc(II) ion concentration given by the the following equation:

$$y = 7.14x + 12.17, \qquad 6.1$$

where y = peak area and x = zinc(II) concentration in mg ℓ^{-1}. A linear regression coefficient (r^2) of 0.9972 with n = 11 was obtained over this concentration range. The number of runs per hour for the proposed system was 18. The detection limit was calculated to be 0.998 mg ℓ^{-1} and the sample interaction as 0.0015 %. The detection limit and the sample interaction was calculated by using the following two equations:

$$\text{Detection limit} = \frac{3(S_b + I_b) - k}{m} \qquad 6.2$$

S_b: is the standard deviation of the background signal

I_b: is the relative peak area of the background signal

k: is the intercept of the calibration curve

m: is the slope of the calibration curve

$$\text{Interaction} = \left(\frac{A_3 - A_1}{A_2}\right) \times 100 \qquad 6.3$$

A_1: is the true peak area of the sample with low analyte concentration, or in other words, the peak area obtained from a stable background.

A_2: is the true peak area of sample containing ten times more analyte than in A_1

A_3: is the peak area for the interacted sample containing the same concentration of analyte as A_1

6.3.7 Samples

Multivitamin tablets were obtained from a local drug store. Three different tablets, referred to as follows, were analysed.

Sample tablet ST 1:	Vital Zinc
Sample tablet ST 2:	Extravite multivitamin tablets
Sample tablet ST 3:	Weigh less multivitamin tablets

All the sample tablets were dissolved in de-ionised water after which a simulated gastric fluid was added according to the United States Pharmacopeia guidelines. [23] After dissolution in the simulated gastric fluid, care was taken that the pH of the solutions was kept low during the dilutions of the samples. This was achieved by adding nitric acid in order to keep the acid concentration in the 1% (v/v) range. (Even though the simulated gastric fluid has a pH of about 1.2, it has no buffering capabilities leading to a pH increase with the dilution of the sample. It was further necessary to obtain a low pH so that all possible zinc complexes were destroyed). During the dilution of the sample, care was taken that the final sodium

concentration in the sample was at least 0.31 mol ℓ^{-1}. The accuracy of the proposed system was evaluated by comparing the results with those obtained using a standard AAS procedure. It is worthwhile to note that the samples used for the standard AAS method had to be filtered before analysis, since not all the constituents of the tablets were soluble. (We had great difficulties in cleaning the volumetric flasks in which the samples were prepared but no clogging of the dialyser unit or FIA system were observed. Nebulizer clogging would have occurred if the sample wasn't dialysed, since the grooves in the dialyser unit were considerably larger than that of the nebulizer.) The results, as shown in Table 6.1, revealed an excellent agreement between the two methods. The results were also in close agreement with the distributers note.

Table 6.1 *Comparison of the results of samples analysed by the proposed system, a standard AAS method and the distributors note. All concentrations are given in mg ℓ^{-1}. The subscript at each tablet's name indicate that three tablets of each kind were analysed*

Sample nr.	Proposed FIA/electrodialyser system	% RSD	FAAS	Distributers note
ST 1_1	14.67	2.39	14.98	15
ST 1_2	14.89	2.41	15.01	15
ST 1_3	14.77	3.09	14.07	15
ST 2_1	3.59	3.78	3.78	3.75
ST 2_2	3.80	3.85	3.67	3.75
ST 2_3	3.77	3.69	3.70	3.75
ST 3_1	7.59	3.51	7.62	7.5
ST 3_2	7.65	3.29	7.66	7.5
ST 3_3	7.55	3.44	7.60	7.5

6.4 Conclusions

The proposed FI-electrodialysis-AAS system proved itself to be a very useful tool for the removal of matrix interferences during the determination of zinc in pharmaceutical products. Iron interference was eliminated with the addition of an excess of fluoride ions and in the tablets that were analysed, where the iron concentration was very similar to that of the zinc, it did not really pose a problem during the determination of the zinc. This system can very easily be applied to the determination of zinc in practically any sample. The proposed system should be particularly attractive for pharmaceutical laboratories where solid particles, macromolecules and high salt concentrations in samples are problematic to analyse with conventional AAS instrumentation.

6.5 References

1. Martini, F. H., **(1995)** *Fundamentals of Anatomy and Physiology*, 3rd edition, Prentice-Hall.
2. Mahan, L. K., and Arlin, M. T., **(1992)** *Food, Nutrition and Diet Therapy*, 8th edition, WB Saunders Company.
3. Simonsen, K. W., Nielsen, B., Jensen, A. S., and Andersen, J. R., **(1986),** *Journal of Analytical Atomic Spectrometry*, **1**, 453.
4. Burguera, J. L., **(1989)** *Flow Injection Atomic Spectroscopy*, Marcel Dekker, New York,.
5. Sperling, M., Kościelniak, P., and Welz, B., **(1992)** *Anal. Chim. Acta.*, **261,** 115.
6. Debra, E., Tyson, J. F., and Hinds, M. W., **(1992)** *Talanta*, **39**, 1525.
7. Sweileh, J. A., and Cantwell, F. F, **(1985)** *Anal. Chem.*, **57**, 420.
8. Ma, R., Van Mol, W., Adams F., **(1995)** *Anal. Chim. Acta.*, **309**, 395.
9. Olsen, S., Pessenda, L. C. R., Růžička, J., and Hansen, E. H., **(1983)** *Analyst*, **108**, 905.
10. Maquieira, A., Elmahadi, H. A. M., and Puchades, R., **(1994)** *Anal. Chem.*, **66**, 3632.
11. Davey, D. E., **(1986)** *Anal. Lett.*,, **19**, 1537.
12. Van Staden, J. F., and van Rensburg, A., **(1990)** *Analyst*, **115,** 1049.
13. van Staden, J. F., and van Rensburg, A., **(1989)** *Fresenius Zeitschrift für Anal. Chem.*, **334,** 695.
14. van Staden, J. F., and van Rensburg, A., **(1990)** *Fresenius J. Anal. Chem.*, **337,** 393.
15. van Staden, J. F., **(1991)** *Fresenius' J. Anal. Chem.*, **340,** 415.
16. van Staden, J. F., **(1995)** *Fresenius' J. Anal. Chem.*, **352,** 271.
17. van Staden, J. F., and Hattingh, C. J., **(1998)** *Talanta*, **45**, 485.
18. van Staden, J. F., and Hattingh, C. J., **(1998)** *Journal of Analytical Atomic Spectrometry*, **13**, 23.
19. Buschner, B. A. P., Tjaden, U. R., van der Greef, J., **(1997)** *Journal of*

Chromatography A, **764**, 135.

20. von Loon, J. C., **(1982)** *Chemical Analysis of Inorganic constituents of Water,* CRC press.
21. Marshall, G. D., and van Staden, J. F., **(1992)** *Anal. Instrum.,* **20,** 79.
22. Bard, A. J., and Faulkner, L. R., **(1980)** *Electrochemical Methods, Fundamentals and Applications,* John Wiley & Sons.
23. The United States Pharmacopeia. **(1995)** The National Formulary, USP23 NF18.

Chapter 7

The determination of phosphate

7.1 Introduction

Phosphorus primary exists as phosphate in natural and water effluents. These phosphates include ortho-phosphate, condensed phosphates (pyro-, meta-, and other polyphosphates), and organically bonded phosphates. These phosphates exist in water as a solution, small particles or in living material. [1]

Ecologically phosphorus is an important compound due to the role it plays in a variety of cell processes. Phosphorus is one of the primary nutrients for normal growth of plants and animals. [2] Phosphorus in the human body consist mainly as phosphate (or orthophosphate). About 80 -85 % of the total phosphate is combined with calcium in bones and teeth. The remainder is combined with protein, lipid, carbohydrate and enzymes. Besides its structural importance in bones and teeth, phosphate also plays a major role in the absorption process of glucose and glycerol in the intestine, and in the formation of many enzymes essential to the intracellular oxidation process and production of energy. It also forms an active part of the buffer system in the body. [3,4]

Various analytical methods for the determination of orthophosphate are exploited so far in flow injection analysis. Two prominent methods made use of the reaction of phosphate with a colour reagent and measuring the coloured product with a spectrophotometer. The first of these methods was the phosphomolybdenum blue method. [5 - 12] The second was the molybdophosphate with malichite green method. [13, 14] Other methods included the use of high-performance liquid chromatography [15] and amperometric methods. [16] One other method was the indirect determination of phosphate by making use of a lead ion selective electrode (ISE). [17]

It came to mind that the only indirect method of analysis of phosphate in a flow injection system was the use of the lead ISE. [17] For the determination of sulphate however, various publications were found where sulphate was determined indirectly on the atomic absorption spectrophotometer (AAS). This was done by adding excess amounts of exactly known amounts of barium(II) ions to the sulphate solution. The barium signal was then used as an indirect indication of the sulphate concentration. The detection of the excess barium was usually done by filtering the precipitate and determine the barium on an AAS. [18 - 20]. Van Staden and Van Rensburg [21] had a different approach. This group used a dialyser equipped with a passive membrane instead of filtering the precipitate. The excess barium ions dialysed across the membrane to the acceptor channel while the precipitate was transported to waste. The barium dialysate was allowed to react with methylthymol blue to form a complex which was measured spectrophotometrically. The latter method had the advantage above the other methods in the sense than no maintenance of the dialyser was necessary whilst the methods using filters, the filters had to cleaned from time to time (that is if the system is not equipped with a modern self cleaning filter).

It was decided to investigate the applicability of both direct and indirect methods of determination. The major prerequisites for the method of choice for use was that it must be simple to use in a flow injection system with the minimum number of interferences. The use of the detection method was secondary to the process that took place in the electrodialyser. For this reason the phosphomolybdenum method for direct determination was chosen. For the indirect method the AAS detector was chosen for use in tandem with an electrodialysing unit.

7.2 Experimental

The experimental section is divided into two parts namely for the indirect determination of phosphate and the direct determination of phosphate.

7.2.1 Indirect determination of phosphate

7.2.1.1 Reagents and solutions

All reagents were prepared from analytical grade chemicals unless otherwise specified. Deionised water from a Modulab system (Continental Water Systems, San Antonio, TX) was used for dilution. All solutions were degassed before measurement with a water vacuum pump system. The main solutions were prepared as follows:

7.2.1.1.1 Standard barium solution

A standard stock barium solution containing 10 000 mg ℓ^{-1} (0.0728 mol ℓ^{-1} in Ba^{2+}) was prepared by dissolving 30.33 g of dried barium chloride in water and diluting to 2 ℓ with de-ionized water. Working standard solutions were prepared by appropriate dilutions to cover the working ranges as discussed in the text.

7.2.1.1.2 Standard phosphate solution

A standard stock phosphate solution containing 10 000 mg ℓ^{-1} (0.1053 mol ℓ^{-1} PO_4^{3-}) was prepared by dissolving 75.42 g of di sodium phosphate duodeca-hydrate ($Na_2HPO_4 \cdot 12\ H_2O$) in water and diluting to 2 ℓ with de-ionized water. Working standard solutions were prepared by appropriate dilutions to cover the working ranges as discussed in the text.

7.2.1.2 Instrumentation

The FIA system (Figure 7.1) used in this work, was composed from the following components: a six-roller Cenco peristaltic pump rotating at 10 rpm, two Valco (Houston, Texas) 10-port electrically actuated injection valves with sample loops

of 70 and 150 µℓ respectively, a reaction manifold system and a laboratory-made electrodialyser. The electrodialyser used (see Figure 7.2) was a slightly modified version of the dialyser unit as described by Van Staden [22, 23]. The dialyser unit consisted of two, mirror image, PVC blocks. Embedded into each of these blocks were graphite electrodes which acted as the cathode (acceptor side) and the anode (donor side) respectively. Placed onto each of the PVC blocks was a 0.6 mm thick Perspex blade. Into each of the Perspex spacer, a groove of 0.6 mm diameter and 300 mm length was cut so as to form a channel when placed onto each of the PVC blocks respectively. The PVC blocks were then fitted onto each other in such a way that the Perspex spacer facing each other and the grooves in the respective Perspex blades coincided with each other. The membrane was then sandwiched between the two Perspex spacer as the only separation between the two tubes so formed. The walls of the tubes that were formed thus consisted of, at the far end, the graphite (which was embedded into the PVC blocks), the side walls of Perspex and the common wall, the membrane. A Leader LPS 156 potentiostat was used to apply the d.c. potential. The passive membrane used was a Technicon pre-mount type C membrane (pore size 4-6 nm, thickness 0.015mm). Tygon tubing (0.76 mm id) was used to construct the manifold system. For current and potential measurements a Prema 5000 integrating multimeter was used. The detector used was a Varian (Palo Alto, CA, USA) AA-1275 atomic absorption spectrometer. A Varian Techtron Ba hollow cathode lamp, operating with a current of 8 mA, was used to give a monochromatic light ray in the detector. A wavelength of 554.0 nm and a spectral bandpass of 0.2 mm was used. A dinitrogen oxide-acetylene flame (reducing) was used. The spectrometer and the injection valve were coupled to a personal computer equipped with the FlowTEK program [24].

7.2.1.3 Flow system

The flow system used is depicted in Figure 7.1. Phosphate sample solutions were drawn up into a 70 µℓ sample loop of the Valco valve (valve 2 Figure 7.1) and barium standard solution was drawn up into a 150 µℓ loop of the Valco valve (valve 1 Figure 7.1) Both the phosphate and the barium were injected at the same time into two separate water streams. The two water streams then converged into one stream (forming the donor channel) where the following precipitation reaction between the phosphate and barium ions took place:

$3\ Ba^{2+}\ (aq) + 2\ PO_4^{3-}\ (aq) \rightleftharpoons Ba_3(PO_4)_2\ (s)$ with a K_{sp} at standard conditions for the reaction being 1×10^{-54}.

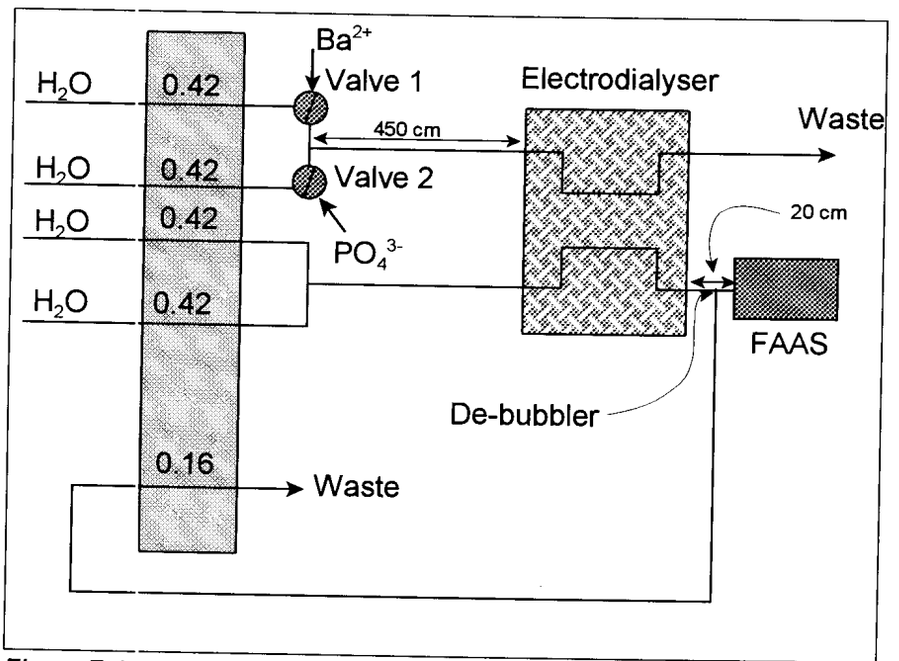

Figure 7.1 Flow system for the indirect determination of phosphate.

Barium ions were in excess. The barium/phosphate precipitate and barium ions which did not react with the phosphate ions were transported to the electrodialyser. In the electrodialyser the barium ions migrated (under the influence of an applied d.c. potential) across the membrane to the acceptor channel whereas the barium/phosphate precipitate was transported to waste. The electrodialysate barium ions were swept from the electrodialyser unit (acceptor channel) and transported to the spectrometer were the barium signal was measured as an indirect indication of the phosphate concentration.

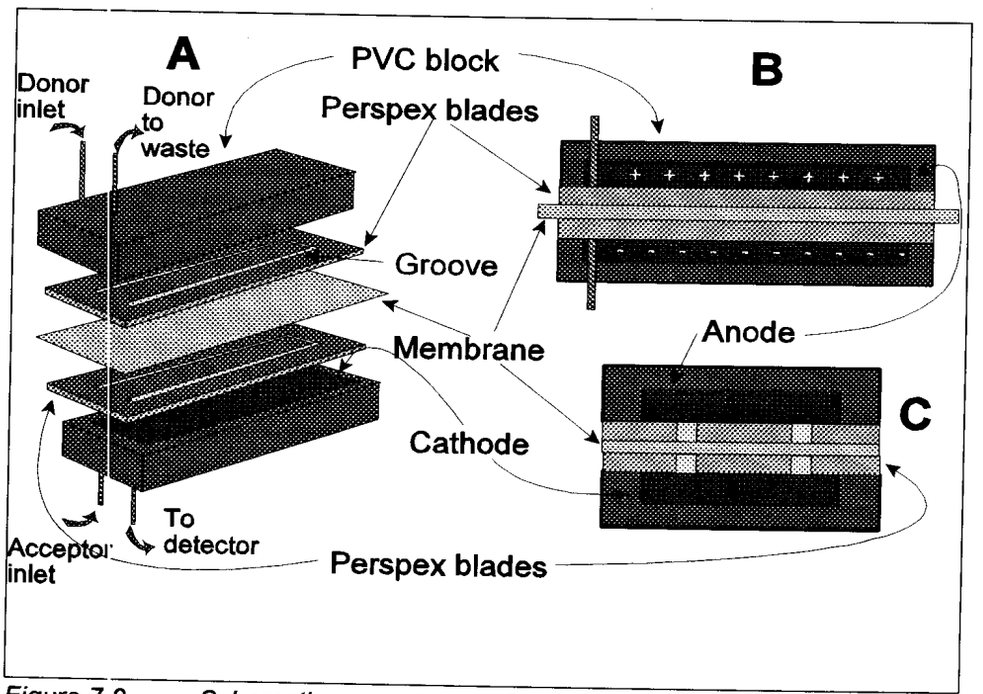

Figure 7.2 *Schematic presentation of the Electrodialyser unit. A - the 3D presentation, B - a longitudinal cross-section and C - a diagonal cross-section.*

Data acquisition and device control were achieved using a PC30-B interface board (Eagle Electric, Cape Town, South Africa) and an assembled distribution board (MINTEK, Randburg, South Africa). The FlowTEK [24] software package (obtainable from MINTEK) for computer aided flow-analysis was used throughout for device control and data acquisition. All the data given (mean peak area values) are the average of 11 replications.

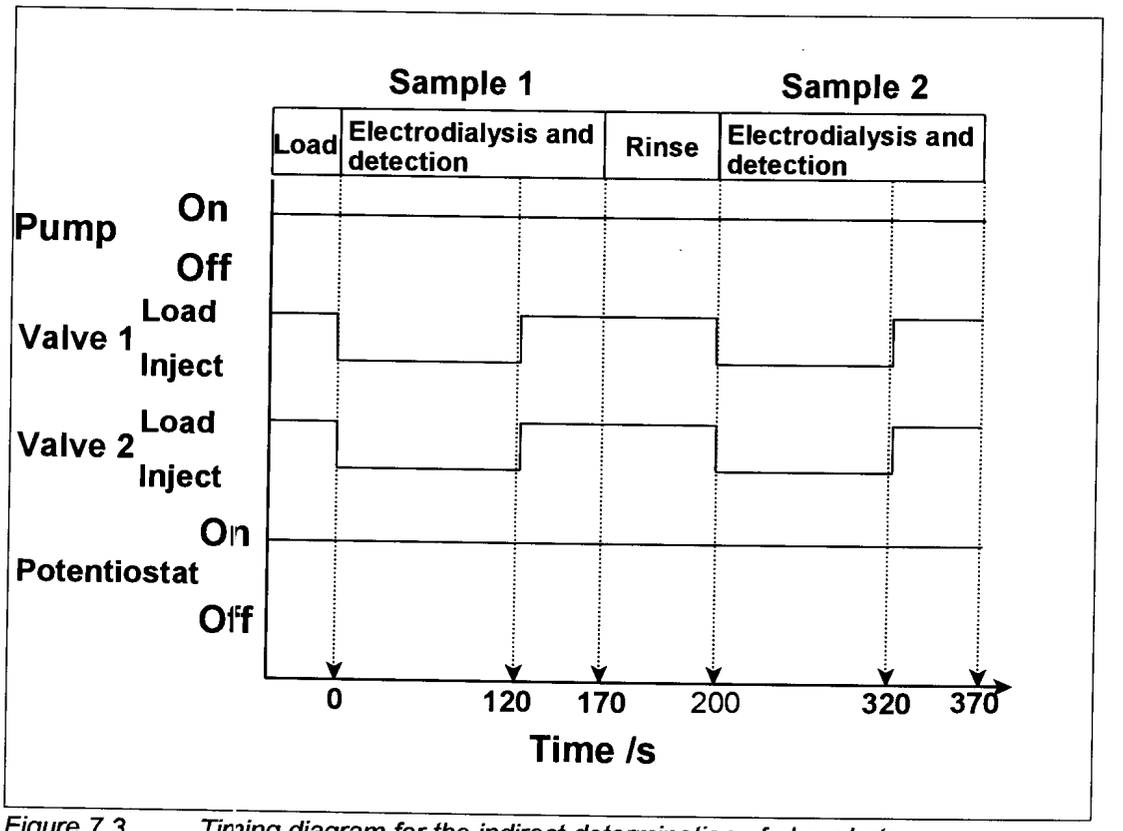

Figure 7.3 Timing diagram for the indirect determination of phosphate.

7.2.1.4 Procedure

The configuration of the FI system is shown in Figure 7.1. The pump and valves operated as described below:

5.2.1.4.1 Operation of pump and valves

The pump (Figure 7.1) was never switched to the "off" position during the analysis. Two Valco 10-port electrically actuated injection valves (valves 1 and 2 in Figure 7.1) were used to inject the barium standard solution and the phosphate sample solution at the same time. In the "load" position (on both valves), sample phosphate solution and barium standard solution were aspirated through the respective sample loops to waste, filling the whole sample loop (phosphate sample solution filled loop in valve 2 and barium standard solution

filled loop in valve 1). Upon switching both valves to the "inject" position, parts of the respective water streams were interrupted and the full sample loops were placed into the respective water streams.

The timing diagram for treating the samples is outlined in Figure 7.3. The system was switched on and allowed to run for about 10 min in order to equilibrate the flow dynamics of all parts of the system. The computer was then actuated and the timing sequence started in the "load" position which was only used at the beginning of the analysis. The following timing sequences were followed with time regulation from the FlowTEK [24] program:

i. *Starting of the system (Loading)*

Pump: Pump was switched to the "on" position. The individual water streams were pumped at a rate of 0.42 mℓ min^{-1} and after they merged, the flow rate of the donor stream through the electrodialyser was 0.84 mℓ min^{-1}. Aspiration of the sample and the standard solution into the injection loop was at a rate of 2.9 mℓ min^{-1}.

Valves: Both valves were in the "load" position.

Potentiostat: The potentiostat was set to "on" position at 20 V.

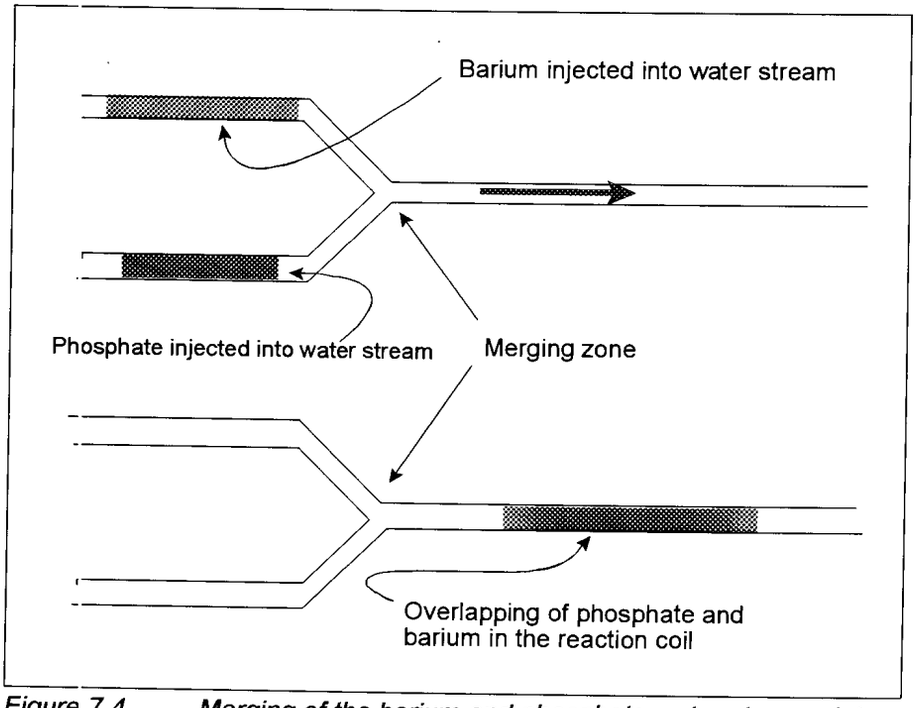

Figure 7.4 *Merging of the barium and phosphate water streams into the reaction coil.*

ii. *Electrodialysis and detection*

At time T = 0, the pump was kept in the "on" position. Both valves were switched to the "inject" position whereupon the whole sample and standard solution loops were placed into the two respective water streams. The sample and the standard plugs were then transported to the donor channel where they merged and the precipitation reaction occurred in the reaction coil. (See Figure 7.4) The precipitate was then transported via the electrodialyser's donor channel to waste whereas the excess barium ions migrated to the acceptor channel. The applied potential over the membrane was kept at 20 V for the duration of the electrodialysing and analysis steps. At time T = 50 s, the computer started reading the signal coming from the detector. The electrodialysed barium ions were pumped to the detector at rate a of 0.84 mℓ min^{-1}. (Flow rate was equal to two times 0.42 mℓ min^{-1} so as to obtain the same flow

rate as in the donor channel since there was not a pump tubing that could deliver 0.84 mℓ min^{-1}). Just prior to the detector a homemade de-bubbler was introduced to remove most of the gases formed at the cathode which interfered with the barium signal. At time T = 120 s, the valves were switched back to the "load" position so as to fill the loops again for the next run.

iii. *Completion of a run*

At time T = 170 s, the computer stopped measuring the signal from the detector. The donor and acceptor channels were rinsed and the next sample was aspirated into the sample loop. At T = 200 s, the two valves were switched to the "inject" position which marked the beginning of analysis of second sample.

7.2.1.5 Results and discussion

In the above mentioned flow system, the reaction of barium with the phosphate, the migration of the barium and the analysis of the barium were the most important considerations for the optimisation. Different from chapters 4, 5 and 6, in this electrodialyser system for indirect determination, it was not the analyte that was electrodialysed but the reactant (barium ions). It was however still very important to ensure the optimum and reproducible transport of the barium across the membrane. The system was thus optimised under the following headings:

i. Concentration of barium.
ii. Applied potential.
iii. Flow rate of the donor and acceptor channels.
iv. Reaction coil.

v. Injection loop volume.

7.2.1.5.1 Barium concentration

For maximum sensitivity of the system it was essential to obtain the optimum working conditions for the determination of the barium ions. For this reason the electrodialysis system was first optimised without the inclusion of any phosphate. The various barium ion concentrations were compared whilst other experimental parameters were kept constant at the following values:

- Concentration phosphate = 0 mg ℓ^{-1} .
- Injection loop volume (Barium) = 100 $\mu\ell$.
- Flow rate (donor and acceptor stream) = 0.84 mℓ min^{-1}.
- Applied d.c. potential = 15 V.

It is clear from Figure 7.5 that there is a steady increase in the peak area with

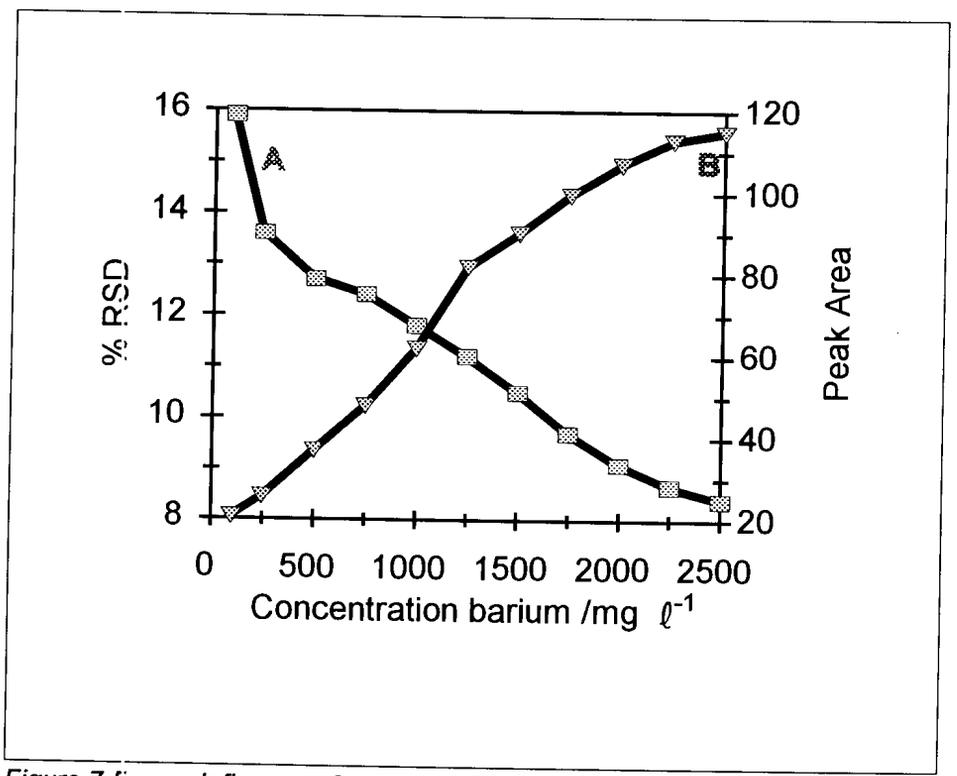

Figure 7.5 Influence of concentration of barium on % RSD (A) and peak area (B).

increasing barium concentration. On the other hand there was a steady decrease in the % RSD with increasing barium concentration. Since reproducibility was a problem in the experimental work a compromise was reached at 2000 mg ℓ^{-1}. At this concentration the reproducibility was relatively low and the sensitivity was acceptable.

7.2.1.5.2 Applied potential

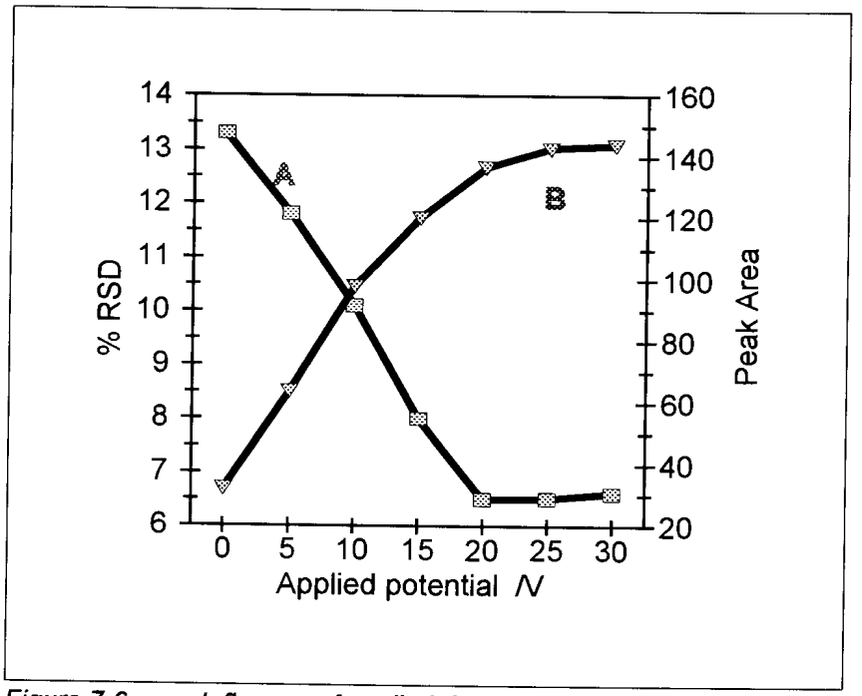

Figure 7.6 *Influence of applied dc potential on the % RSD (A) and the peak area (B).*

The sensitivity and reproducibility of the electrodialysed excess barium ions in the electrodialyser unit depended on the potential gradient applied on the system. The applied potential was therefore evaluated using the detector signal response and % RSD as indicators. The d.c. potential was varied between 0 and 30 V, while the flow rates in the donor and acceptor streams were kept constant at 0.84 mℓ min^{-1}, the injection loop volumes of the barium and the phosphate were respectively 100 and 80 $\mu\ell$ and the reaction coil was 300 cm.

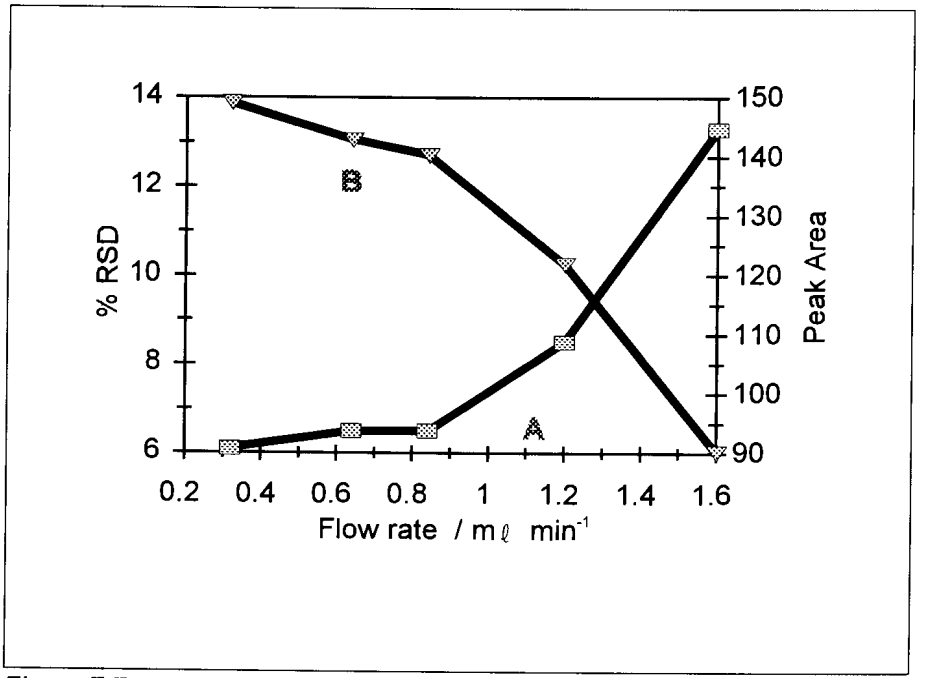

Figure 7.7 *Influence of flow rate on the % RSD (A) and peak area (B). (No phosphate added).*

It should be noted that during this part of the optimisation the concentration of the phosphate was zero so as to obtain the best conditions for the determination of barium. The results in Figure 7.6 revealed that the precision was poor at low applied potentials. This indicated that the contribution of detectable barium ions drawn through the neutral membrane was unstable. It is further clear that there was a steady increase in the peak area with increasing applied potential. This increase however did flatten off after potentials of higher than 20 V were applied. From the graph it is clear that the optimum applied potential was 20 V. With decreasing potential the precision decreased and with increasing potential the precision was constant (respective to 20 V). The sensitivity was also acceptable at 20 V.

7.2.1.5.3 Flow rates of the donor and acceptor streams

Evaluation of the flow rates of both the donor and acceptor streams revealed that the best results were obtained with the flow rates of both streams in the

same direction when applied in the continuous mode. Sensitivity and precision were used as indicators in the optimisation of the flow rates. During these experiments the following experimental parameters were kept constant:

- Phosphate concentration = 0
- Barium ion concentration = 2000 mg $m\ell^{-1}$
- Barium injection loop = 100 $\mu\ell$
- Applied potential = 20 V

The influence of the flow rates was first compared on the basis of %RSD and secondly on the basis of peak area as illustrated in Figure 7.7 It is clear from the results that the precision deteriorated remarkably for flow rates higher than 0.84 $m\ell$ min^{-1}. It is also clear that the sensitivity decreased with increasing flow rate. The reason for the increasing % RSD at higher flow rates is the fact that the barium ions had less time to migrate across the membrane which led to lower signal values and thus a low signal to noise ratio. A possible explanation for the decrease in sensitivity with higher flow rates was that although the flux of ions across the neutral membrane under the influence of the applied electric field remained the same, it could not match the influence of the higher flow rate with dilution effect on the dialysate cations in the acceptor channel of the FIA system. At this point in time it was not possible to make a clear cut decision on what the optimum flow rate will be. To further optimise the flow rate, phosphate was also injected whilst all other experimental parameters were kept constant. The concentration of the phosphate was chosen as it would react in a 2:3 ratio with the barium ions. Thus it was calculated that the concentration of the phosphate (PO_4^{3-}) must be 2075 mg ℓ^{-1}. The results can be seen in Figure 7.8. Considering the peak area, there was a slight increase in the peak area from 0.32 to 0.84 $m\ell$ min^{-1}. At these flow rates the peak areas were considerably lower than the corresponding peak areas in Figure 7.7. This indicated that the precipitation reaction took place and that the available barium ions to migrate across the membrane were considerably less. The increase peak area in

Figure 7.8 from 0.84 to 1.2 mℓ min^{-1} indicated that at the latter flow rate, the precipitation reaction was not complete. Reasons for this could be the fact that there was not enough time for the reaction to go to completion or that at the higher flow rate mixing of the reagents in the reaction coil was incomplete. At flow rates higher than 1.2 mℓ min^{-1}, there was a sharp decrease in the peak area. The reason for this was that even though there were more barium ions available in the donor channel, the ions hadn't had enough time in the donor channel to migrate across the membrane and there was also the higher dilution factor in the acceptor channel due to the increase in the flow rate. The best compromise between sensitivity and precision for employment of the proposed electrodialyser/FIA system was obtained with a flow rate of 0.84 mℓ min^{-1}.

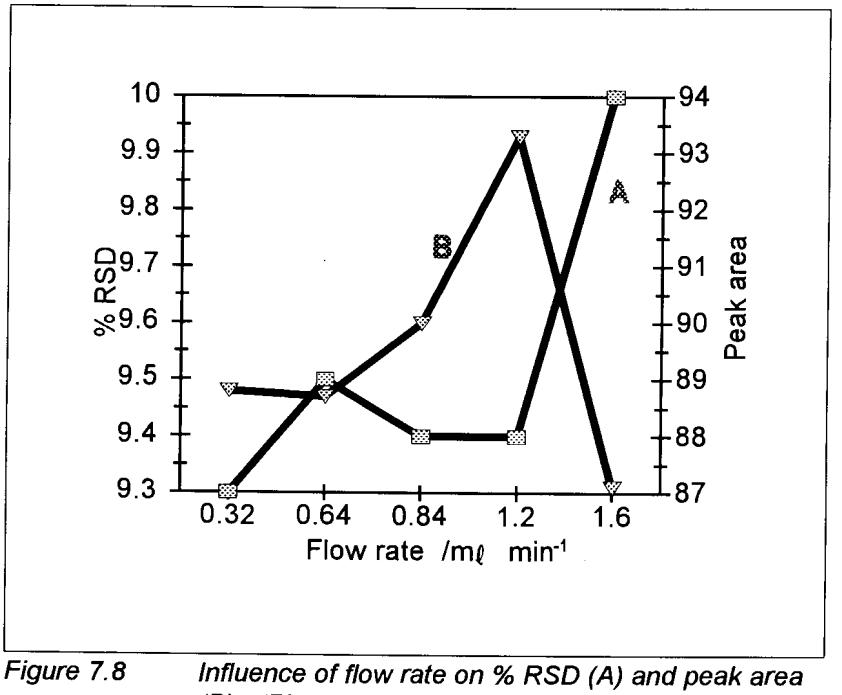

Figure 7.8 *Influence of flow rate on % RSD (A) and peak area (B). (Phosphate added).*

7.2.1.5.4 Reaction coil

As can be seen from the previous paragraph, the reaction time and mixing efficiency was of utmost importance (which was influenced by the flow rate in the previous paragraph). All experimental parameters were kept constant at the following values while the reaction coil length was varied:

- Barium injection loop = 100 $\mu\ell$.
- Phosphate injection loop = 80 $\mu\ell$.
- Barium ion concentration = 2000 mg ℓ^{-1}.
- Phosphate concentration = 2075 mg ℓ^{-1}.
- Flow rate = 0.84 mℓ min^{-1}
- Applied d.c. potential = 20 V

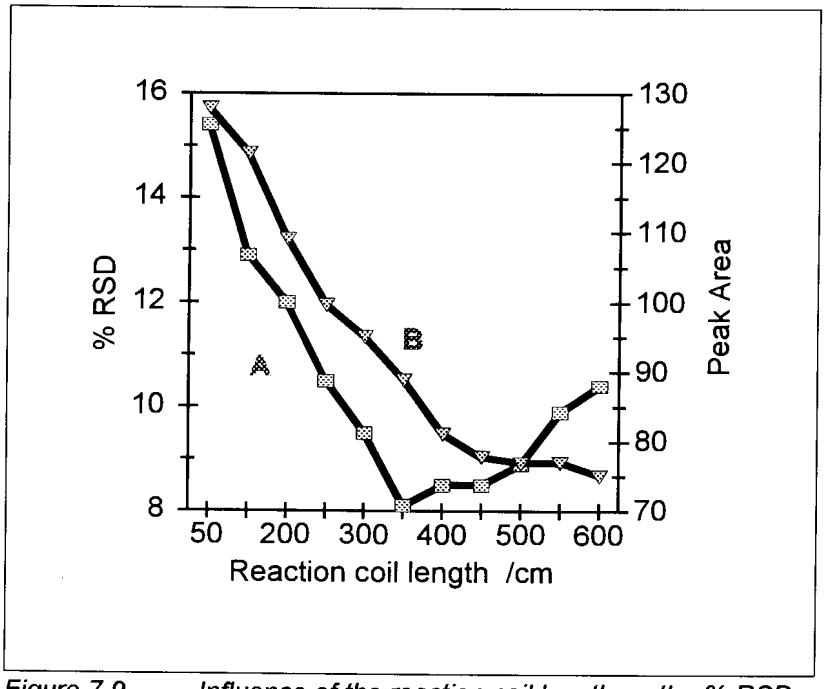

Figure 7.9 *Influence of the reaction coil length on the % RSD (A) and the peak area (B).*

The results can be seen in Figure 7.9. As is evident from Figure 7.9, there was a definite decrease in the barium signal with increasing coil length. This is due

to the better mixing of the reagents and more time for the precipitation reaction to take place with increasing coil length. At lengths longer than 450 cm, there was no significant decrease in the barium signal indicating that the reaction went to completion at a length of 450 cm. The % RSD also showed a steady decrease with increasing coil length up to 350 cm whereafter there was a slight increase in % RSD with increasing coil length. The initial decrease was due to the fact that there was better mixing between the two reagents which led to a more homogeneous mixture and therefore more stable peaks. The increase in the % RSD after 350 cm was due to the fact that there was more time for the excess barium ions to disperse and so very flat and stretched-out peaks were observed. These type of peaks in turn then led to the increase in the % RSD. The optimum length was taken as 450 cm. At 450 cm the barium signal was better than at 350 cm even though the % RSD at 350 cm were slightly better than at 450 cm.

7.2.1.5.5 Injection loop volumes

For the optimisation of the injection loops it was firstly important once again to obtain the optimum barium signal. For this reason the injection loop volume of the barium ions was optimised independently from the phosphate and then afterwards the injection loop volume of the phosphate was optimised at the optimised barium injection loop volume.

For the optimisation of the barium injection loop volume, all the previous experimental parameters were kept constant at their individual optimised values and the concentration of the phosphate was zero. The results can be seen in Figure 7.10. As was expected, there was an increase in the barium signal with increasing injection loop volume. Furthermore it is evident that there is definite decrease in the % RSD at larger injection loop volumes. This is due to the fact

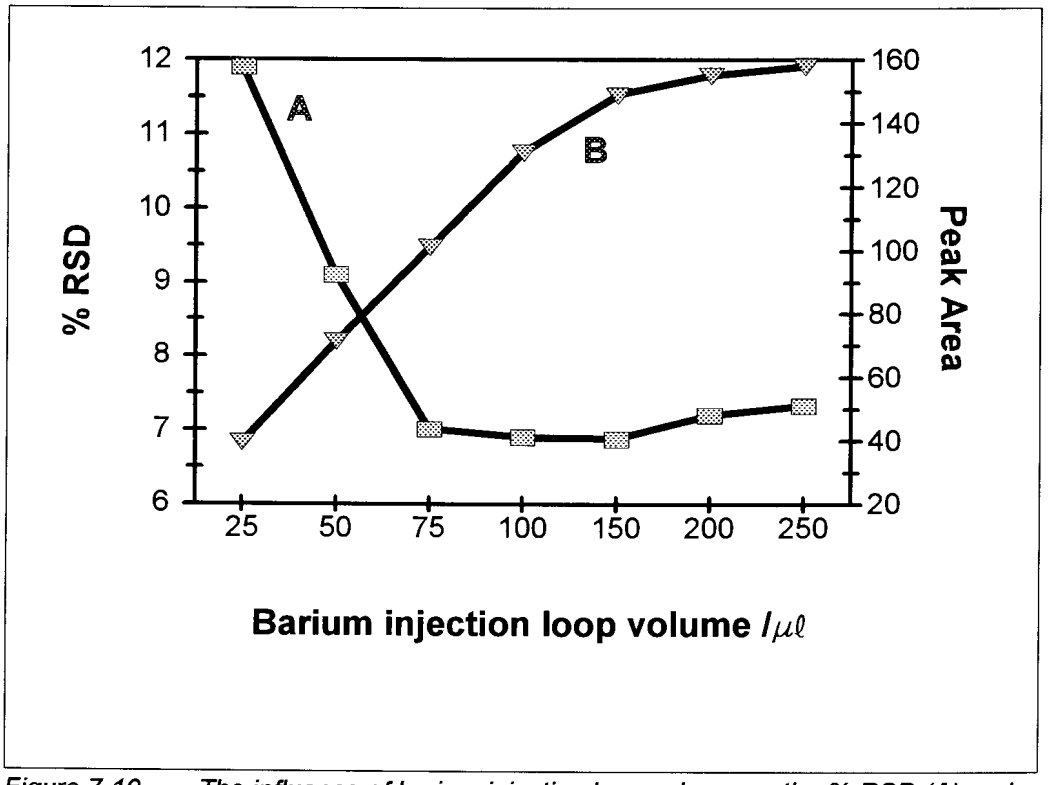

Figure 7.10 *The influence of barium injection loop volume on the % RSD (A) and the peak area (B). Concentration of phosphate was zero.*

that the greater the barium signal, the better the signal to noise ratio will be. The optimum was taken at 150 $\mu\ell$.

During the optimisation of the phosphate injection loop, all experimental parameters were kept constant as with the optimisation of the barium injection loop volume. The barium injection loop volume was kept constant at 150 $\mu\ell$ and the phosphate (PO_4^{3-}) concentration was 2075 mg ℓ^{-1}. From Figure 7.11 it is clear that the barium signal decreased sharply with increasing phosphate injection loop volume up to a volume of 70 $\mu\ell$. Thereafter there was only a gradual decrease in the barium signal. It is further clear from Figure 7.11 that the % RSD increased with increasing injection loop volume. This increase in the % RSD was once again due to the of the barium signal to noise ratio.

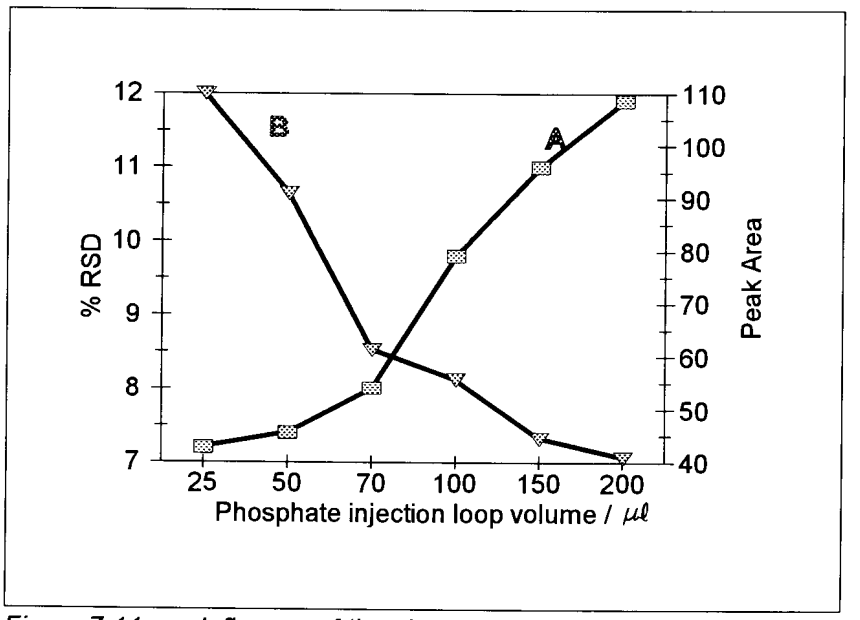

Figure 7.11 *Influence of the phosphate injection loop volume on the % RSD (A) and the peak area (B).*

Other experiments were also done to investigate the influence of the overlapping of the barium and the phosphate zones in the reaction coil. This was done by changing the respective injection loop volumes and changing the concentrations of the barium and the phosphate such that the barium was always in excess. The configurations used are depicted in Figure 7.12. When the overlapping configuration was as indicated in Figure 7.12 C (phosphate zones overlap those of the barium), lower detection values were obtained but the resolution between two different phosphate concentrations were very bad. For this reason the configuration as shown in Figure 7.12 A was preferred.

7.2.1.5 Data and calibration of the optimised system

The optimised parameters for the proposed electrodialysis-FI-AAS analyser for the indirect determination of phosphate were as follows:

- Barium ion concentration: 2000 mg ℓ^{-1}
- Flow rates of donor and acceptor channel: 0.84 mℓ min^{-1}
- Applied d.c. potential: 20 V
- Barium injection loop volume: 150 $\mu\ell$
- Phosphate injection loop volume: 70 $\mu\ell$
- Reaction coil length: 450 cm

The performance of the proposed analyser was critically evaluated under the optimum conditions. The calibration graph was linear between 450 and

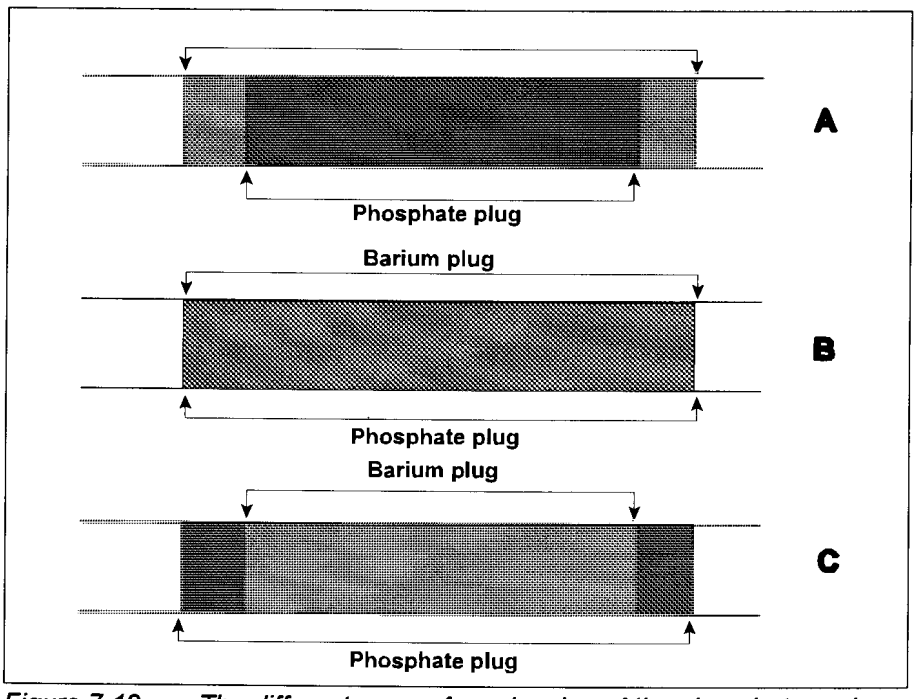

Figure 7.12 The different ways of overlapping of the phosphate and barium zones in the reaction coil.

1750 mg ℓ^{-1} with a relationship between peak area and phosphate concentration given by the following equation:

$$y = -0.9778x + 230.1,$$

where y = peak area and x = phosphate ion concentration in mg ℓ^{-1}. A linear regression coefficient, the variance (r^2) of 0.9778 (n=11) was obtained over this concentration range. The number of runs per hour for the proposed system was 18. The detection limit was calculated to be 413.5 mg ℓ^{-1}, and the sample interaction as 0.98%. The detection limit and the sample interaction was calculated by using the following two equations:

$$\text{Detection limit} = \frac{3(S_b + I_b) - k}{m} \qquad 7.2$$

S_b: is the standard deviation of the background signal

I_b: is the relative peak area of the background signal

k: is the intercept of the calibration curve

m: is the slope of the calibration curve

$$\text{Interaction} = \left(\frac{A_3 - A_1}{A_2}\right) \times 100 \qquad 7.3$$

A_1: is the true peak area of the sample with low analyte concentration, or in other words, the peak area obtained from a stable background.

A_2: is the true peak area of sample containing ten times more analyte than in A_1

A_3: is the peak area for the interacted sample containing the same concentration of analyte as A_1

7.2.2 Direct determination of phosphate

7.2.2.1 Reagents and solutions

All reagents were prepared from analytical grade chemicals unless otherwise specified. Deionised water from a Modulab system (Continental Water Systems, San Antonio, TX) was used for dilution. All solutions were degassed before measurement with a water vacuum pump system. The solutions were prepared as follows:

7.2.2.1.1 Standard phosphate solution

A standard stock phosphate solution containing 10 000 mg ℓ^{-1} (0.1053 mol ℓ^{-1} PO_4^{3-}) was prepared by dissolving 37.71 g of di-sodium phosphate duodeca-hydrate ($Na_2HPO_4 \cdot 12\ H_2O$) in water and diluting to 1 ℓ with de-ionized water. Working standard solutions were prepared by appropriate dilutions to cover the working ranges as discussed in the text.

7.2.2.1.2 Colour reagent

The colour reagent consisted of two solutions namely the reducing agent and the molybdenum solution.

i. Reducing agent solution.

0.1061 g Tin chloride di-hydrate ($SnCl_2 \cdot 2\ H_2O$) and 2.60 g $N_2H_6SO_4$ (hydrazine sulphate) were dissolved in one litre of 0.5 mol ℓ^{-1} sulphuric acid. Sulphuric acid solution was prepared by diluting 27.6 mℓ concentrated sulphuric acid (98 %) to 1 ℓ.

ii. Molybdenum reagent solution.

14.6 g of $(NH_4)_6Mo_7O_{24} \cdot 4\ H_2O$ was dissolved in 1 ℓ of a 0.63 mol ℓ^{-1} sulphuric acid solution (35 mℓ of 98 % sulphuric acid solution diluted to 1 ℓ). To this solution was added 2 mℓ of a sodium laurel sulphate solution. The sodium laurel sulphate solution was prepared by dissolving 17.6 g of sodium laurel sulphate into 100 mℓ water.

7.2.2.1.3 Electrolyte solution

A 4 mol ℓ^{-1} potassium nitrate electrolyte solution was prepared by dissolving 404.44 g of dried potassium nitrate(KNO_3) in water and diluting to 5ℓ with de-ionized water. Working solutions were prepared by appropriate dilutions to cover the working ranges as discussed in the text.

7.2.2.2 Instrumentation

The FIA system (Figure 7.13) used in this work, was composed from the following components: a six-roller Cenco peristaltic pump rotating at 10 rpm, one Valco (Houston, Texas) 10-port electrically actuated injection valve with a sample loop of 80 μℓ, a reaction manifold system (with an i.d. of 0.76 mm) and a laboratory-made electrodialyser. The electrodialyser used was similar to the one used for the indirect determination of phosphate (see Figure 7.2) with the only difference that the cathode was situated in the donor channel and the anode in the acceptor channel. A Leader LPS 156 potentiostat was used to apply the d.c. potential. The passive membrane used was a Technicon pre-mount type C membrane (pore size 4-6 nm, thickness 0.015mm). Tygon tubing (0.76 mm i.d.) was used to construct the manifold system. For current and potential measurements a Prema 5000 integrating multimeter was used. The detector used was a Unicam 8625 UV/VIS spectrophotometer equipped with a 10 mm Hellma-type flow-through cell (volume 80 μℓ). The wavelength of

operation was 660 nm. The spectrometer and the injection valve were coupled to a personal computer equipped with the FlowTEK program [24].

7.2.2.3 Flow system

The flow system used is depicted in Figure 7.13. Sample solutions were drawn up into a 90 μℓ sample loop of the Valco valve from where it was injected into the carrier donor stream and transported into the electrodialyser. Analytes in the sample donor stream were electrodialysed under the influence of an applied d.c. potential through the passive neutral membrane to the acceptor channel. The electrodialysate ions were swept from the electrodialyser unit and mixed with molybdenum chromogenic reagent in the reaction manifold system. The following reactions took place:

Phosphate in an acidic medium and excess molybdate reacts to form molybdophosphoric acid. During a selective reduction of this acid a product with an intense blue colour is formed. The intensity of this colour is proportional to the phosphate concentration. This method is based on the following reactions: [25]

$$H_3PO_4 + 12\ H_2MoO_4 \rightarrow H_3P(MoO_{40}) + 12\ H_2O$$

$$Mo(VI) + \text{reducing agent} \rightarrow Mo(V)\ \text{(slow reaction)}$$

The second reaction is the rate determining step.[1] There was a choice of two reducing agents for use namely ascorbic acid and $SnCl_2$. Even though the ascorbic acid forms a more stable reduction product [26] (leading to a higher reproducibility) and the ascorbic acid itself is more stable than the Sn(II). (Sn(II)

[1] This coloured reaction product was transported to the spectrophotometer for measurement at a wavelength of 660 nm. Experimental work done by the author on a diode array spectrophotometer indicated that the peak maximum shifted to longer wavelengths with time. The shift with time was very slow however and all the analysis were done at the abovementioned wavelength.

is easily oxidised by atmospheric oxygen). The Sn(II) was preferred to the ascorbic acid. The reason for this choice was the fact that the reduction reaction rate for the Sn(II) is much higher than for the ascorbic acid which led to better sensitivity and a higher sampling rate. [27]

Data acquisition and device control were achieved using a PC30-B interface board (Eagle Electric, Cape Town, South Africa) and an assembled distribution board (MINTEK, Randburg, South Africa). The FlowTEK [24] software package (obtainable from MINTEK) for computer aided flow-analysis was used throughout for device control and data acquisition. All the data given (mean height values) are the average of 10 replications.

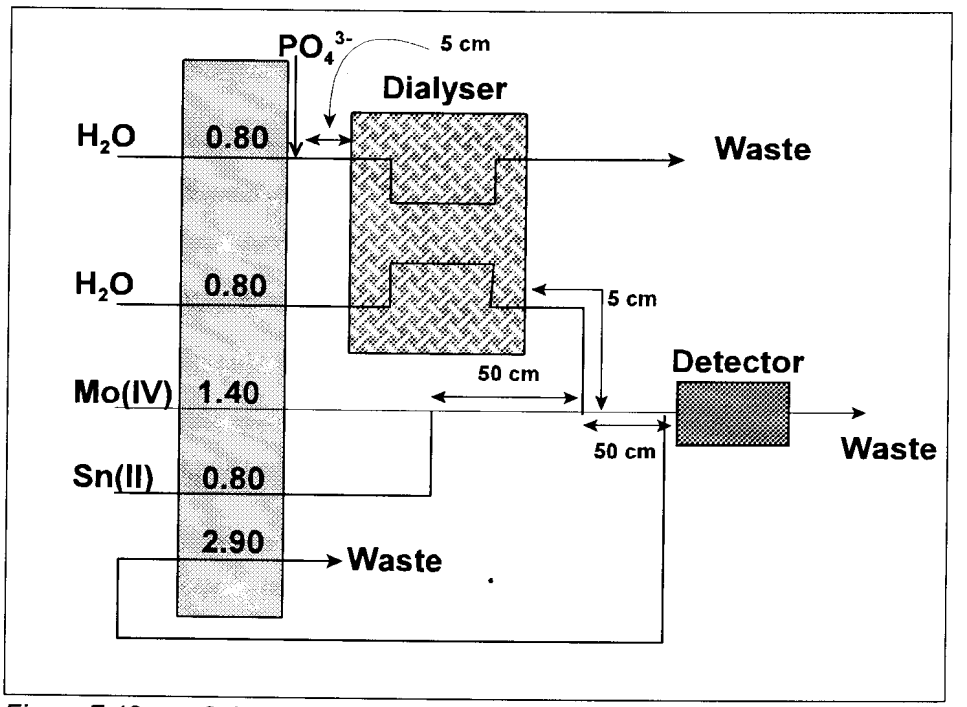

Figure 7.13 *Schematic presentation of the flow/electrodialysis system for the determination of phosphate based on the molybdenum colour reaction.*

7.2.2.4 Procedure

The configuration of the FI system is shown in Figure 7.1. The pump and valves operated as described below.

7.2.2.4.1 Operation of pump and valves

The pump (Figure 7.13) was never switched to the "off" position during the analysis. The Valco 10-port electrically actuated injection valve was used to inject the phosphate sample solution into the water carrier stream. In the "load" position, sample phosphate solution was aspirated through the respective sample loops to waste, filling the whole sample loop. Upon switching the valve to the "inject" position, part of the respective water carrier stream was interrupted and the full sample loop was placed into the water carrier stream.

The timing diagram for treating the samples is outlined in Figure 7.14. The system was switched on and allowed to run for about 10 min in order to equilibrate the flow dynamics of all parts of the system. The computer was then actuated and the timing sequence started in the "load" position which was only used at the beginning of the analysis. The following timing sequences were followed with time regulation from the FlowTEK [24] program:

i. *Starting of the system (Loading)*

Pump: Pump was switched to the "on" position. The carrier donor and acceptor water streams were pumped at a rate of 0.80 mℓ min^{-1}. Aspiration of the sample solution into the injection loop was at a rate of 2.9 mℓ min^{-1}.

Valve: The valve was in the "load" position.

Potentiostat: The potentiostat was set to "on" position at 20 V.

ii. *Electrodialysis and detection*

At time T = 0, the pump was kept in the "on" position. The valve was switched to the "inject" position whereupon the whole sample solution loop was placed into the carrier water stream. The sample plug was then transported to the donor channel of the electrodialyser. In the electrodialyser, under the influence of an applied d.c. potential, the phosphate ions migrated towards the anode in the acceptor channel. The applied potential over the membrane was kept at 20 V for the duration of the electrodialysing and analysis steps. At time T = 45 s, the computer started reading the signal coming from the detector. The electrodialysed phosphate ions were pumped to the detector at rate of 0.80 mℓ min^{-1}. Just prior to the detector a homemade de- bubbler was introduced (operating at a flow rate of 0.16 mℓ min^{-1}) to remove most of the gaseous products formed at the anode which interfered with the phosphate colour product signal. At time T = 100 s, the valve was switched back to the "load" position so as to fill the loop again for the next run.

iii. *Completion of a run*

At time T = 200 s, the computer stopped measuring the signal from the detector. The donor and acceptor channels were rinsed and the next sample was aspirated into the sample loop. At T = 250 s, the valve was switched to the "inject" position which marked the beginning of analysis of second sample.

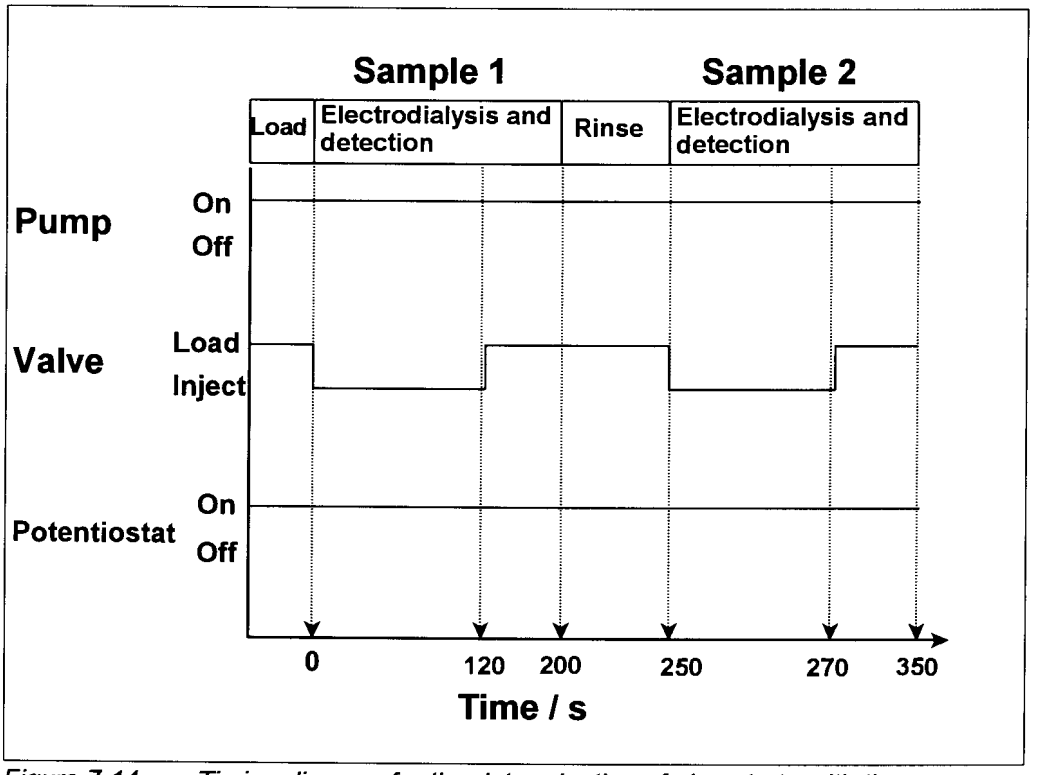

Figure 7.14 *Timing diagram for the determination of phosphate with the molybdenum blue colour reaction.*

7.2.2.5 Results and discussion

Different from the aim of investigation in paragraph 7.2.1, in this section it was the aim to obtain the maximum migration for phosphate through the membrane. The optimisation of this system was for that reason also built round this aim. The determination of the phosphate after dialysis was secondary to the dialysis of the phosphate. For this reason the optimisation and evaluation of the proposed flow system was based upon the factors influencing the phosphate dialysis in the electrodialyser. The following parameters were optimised:

- Flow rate of donor and acceptor channels.
- Applied d.c. potential.
- Injection loop volume.
- Addition of electrolytes to the sample.

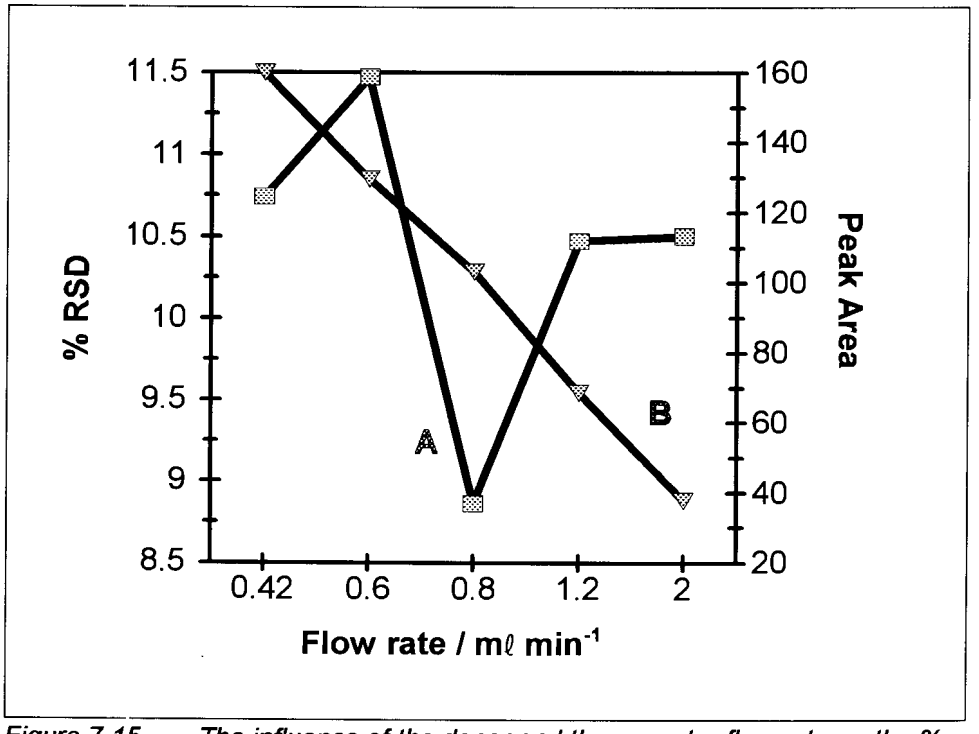

Figure 7.15 *The influence of the donor and the acceptor flow rate on the % RSD (A) and the peak area (B).*

All experimental parameters were evaluated on the basis of % RSD (reproducibility) and peak area (sensitivity).

7.2.2.5.1 Flow rate of the donor and acceptor channels

During the optimisation of the flow rate in the donor and acceptor channels the other experimental parameters were kept constant at the following values:

- Applied d.c. potential: 15 V
- Injection loop volume: 90 $\mu\ell$

The concentration of the phosphate ions was kept constant at 50.0 mg ℓ^{-1}. The donor and the acceptor channels were always flowing at the same rate and it was varied between 0.42 and 2.00 mℓ min^{-1}. The results can be seen in Figure 7.15.

As was expected there was a decrease in peak area with increasing flow rate. The reasons for this is that due to the higher flow rate, less time is available for the phosphate ions to migrate across the membrane. Furthermore, even if the number of phosphate ions that did migrate, the higher flow rate in the acceptor channel led to a higher dilution factor of the dialysate ions. The % RSD also did increase with an increase in the flow rate due to the lowering of the signal to noise ratio. Even though the peak areas at low flow rates compared very favourably with those at the higher flow rates but high % RSD values were obtained at these low flow rates. The high % RSD was due to unstable flow patterns at too low flow rates. (Different from the copper system discussed in Chapter 5, unstable flow will influence zinc system since the zinc will not be plated under these low flow rates. Thus, in the zinc system detection took place during the low flow rates whereas in the copper system plating took place under low flow rate conditions) A flow rate of 0.80 mℓ min^{-1} was a good compromise between too high % RSD values and too low peak areas.

7.2.2.5.2 Applied potential

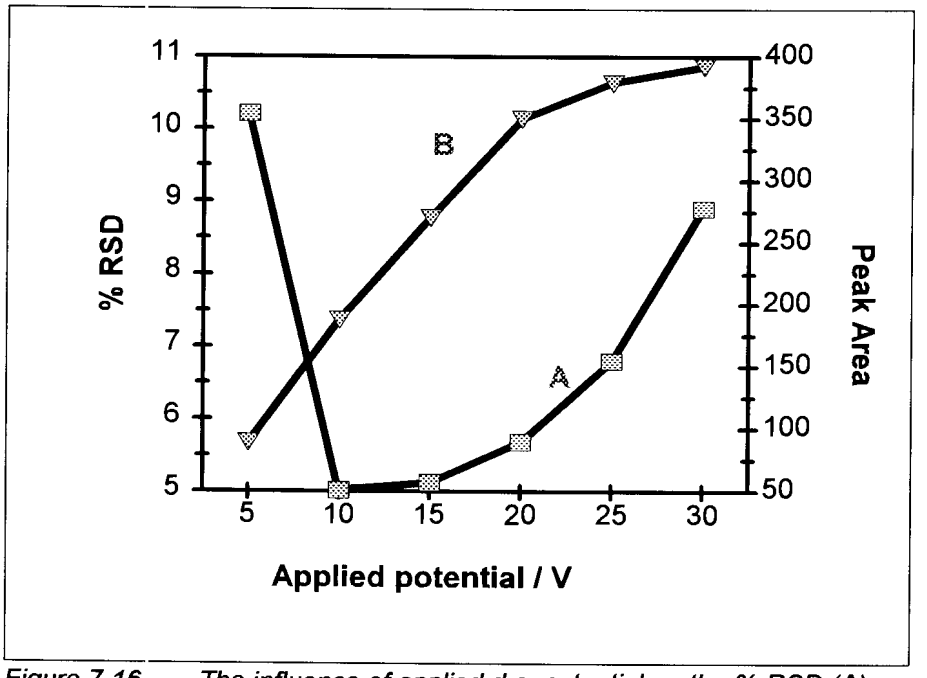

Figure 7.16 *The influence of applied d.c. potential on the % RSD (A) and the peak area(B) for the proposed molybdenum blue colour reaction.*

The applied d.c. potential was proven to be the single most important parameter for an increase in the signal peak area. During the optimisation of the applied d.c. potential all other experimental parameters were kept constant at the following values:

- Flow rate of donor and acceptor channel: 0.80 mℓ min^{-1}.
- Injection loop volume: 80 $\mu\ell$.

The concentration of the phosphate sample was 50 mg ℓ^{-1}. The applied potential was varied between 0 and 30 V. The results can be seen in Figure 7.16. A sharp increase in the peak area was observed with increasing applied potential from 0 to 20 V. After 20 V the increase somewhat flattened off. The reason for this flattening in the peak after 20 V is that it can be assumed that at 20 V most of the phosphate ions will migrate to the acceptor channel. Even though not as obvious as in Figure 7.16, the same can be derived from Figure 7.17. With increasing potential, the number of phosphate ions that migrate will not increase accordingly. The high % RSD value at 5 V is due to the low signal to noise ratio. The increase in the % RSD from 20 V and higher is due to the formation of more gaseous products at the anode than the de- bubbler can

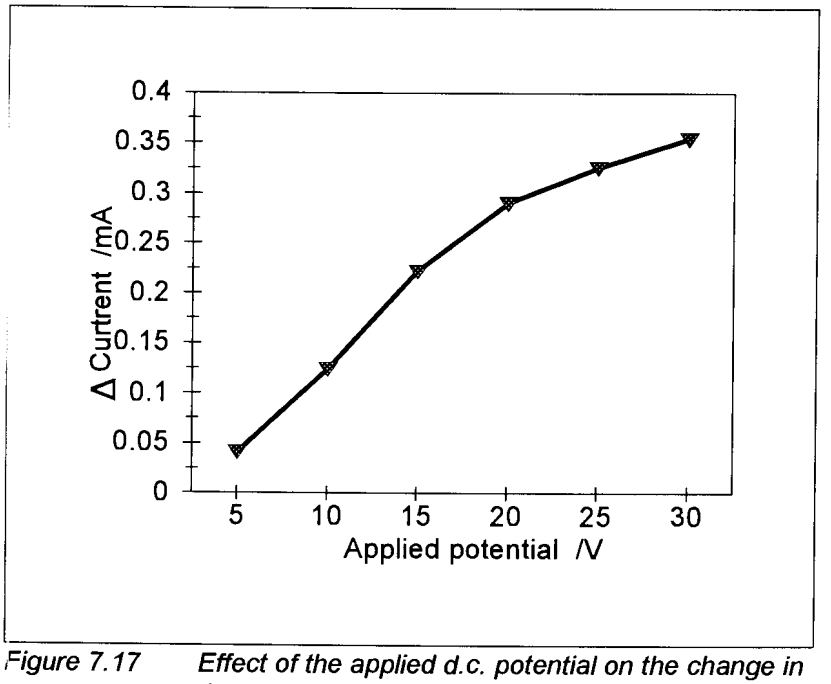

Figure 7.17 *Effect of the applied d.c. potential on the change in the acceptor channel indicating the flux of ions through the passive neutral membrane*

handle. The optimum applied d.c. potential was taken at 20 V.

7.2.2.5.3 Injection loop volume

For the optimisation of the injection loop volume the other experimental parameters were kept constant at the following values:

- Flow rate of donor and acceptor channel: 0.80 mℓ min^{-1}.
- Applied d.c. potential: 20 V.

The concentration of the phosphate sample was 20.0 mg ℓ^{-1}. The results are depicted in Figure 7.18. The optimum volume was taken at 80 $\mu\ell$. Even though the sensitivity was not as high as with the larger volumes, the precision was much better

7.2.2.5.4 Influence of added electrolyte

During the optimisation of the proposed flow/electrodialysis system, perfect

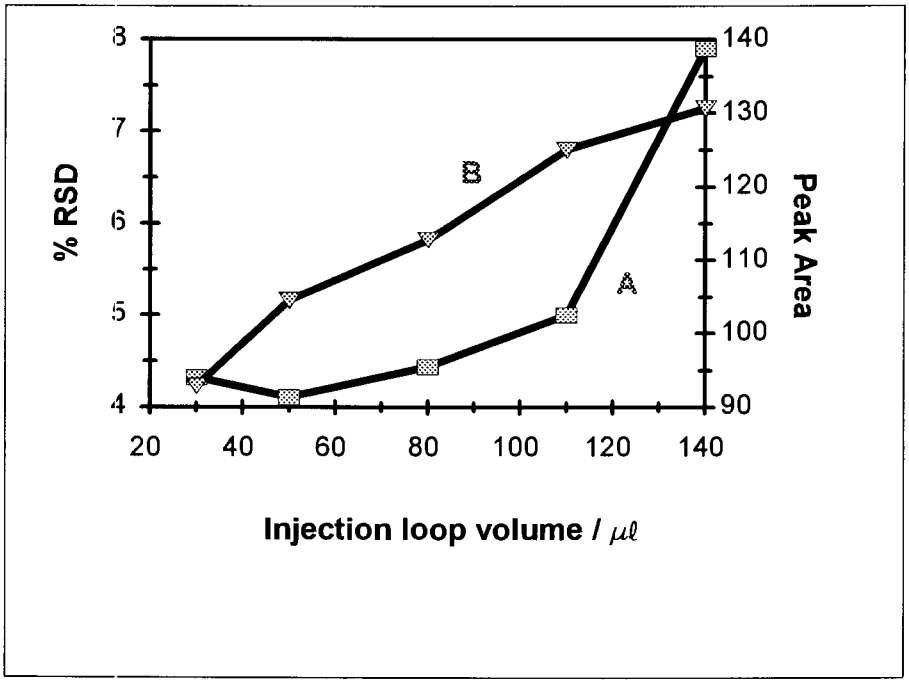

Figure 7.18 Influence of injection loop volume on % RSD (A) and peak area (B).

conditions availed during the optimisation of each experimental parameter. Under normal circumstances when analysing real samples, other electrolytes may also be present in the sample solution. It was therefore of utmost importance to evaluate the influence of electrolyte concentrations on the proposed system. Potassium nitrate was added, in different concentrations, to the sample solution (sample solution phosphate concentration were kept constant at 30 mg ℓ^{-1}). All the experimental parameters was kept at the optimised values. The results are depicted in Figure 7.19. It is clear that electrolyte does have a large influence on the migration of the phosphate ions. As can be seen in Figure 7.19, the peak area increased with increasing electrolyte concentration up to a concentration of 1 mol ℓ^{-1}. After 1 mol ℓ^{-1}, there was no further increase in the peak area with increasing electrolyte concentration. This increase in peak area with increasing electrolyte concentration was due to the fact the phosphate ion was less hydrated and thus the effective radius decreased leading to a smaller viscous drag (implying a higher migration rate across the membrane, see chapter 3). For real samples, electrolyte was added to the samples so that the final electrolyte concentration in the sample was at least 1 mol ℓ^{-1}.

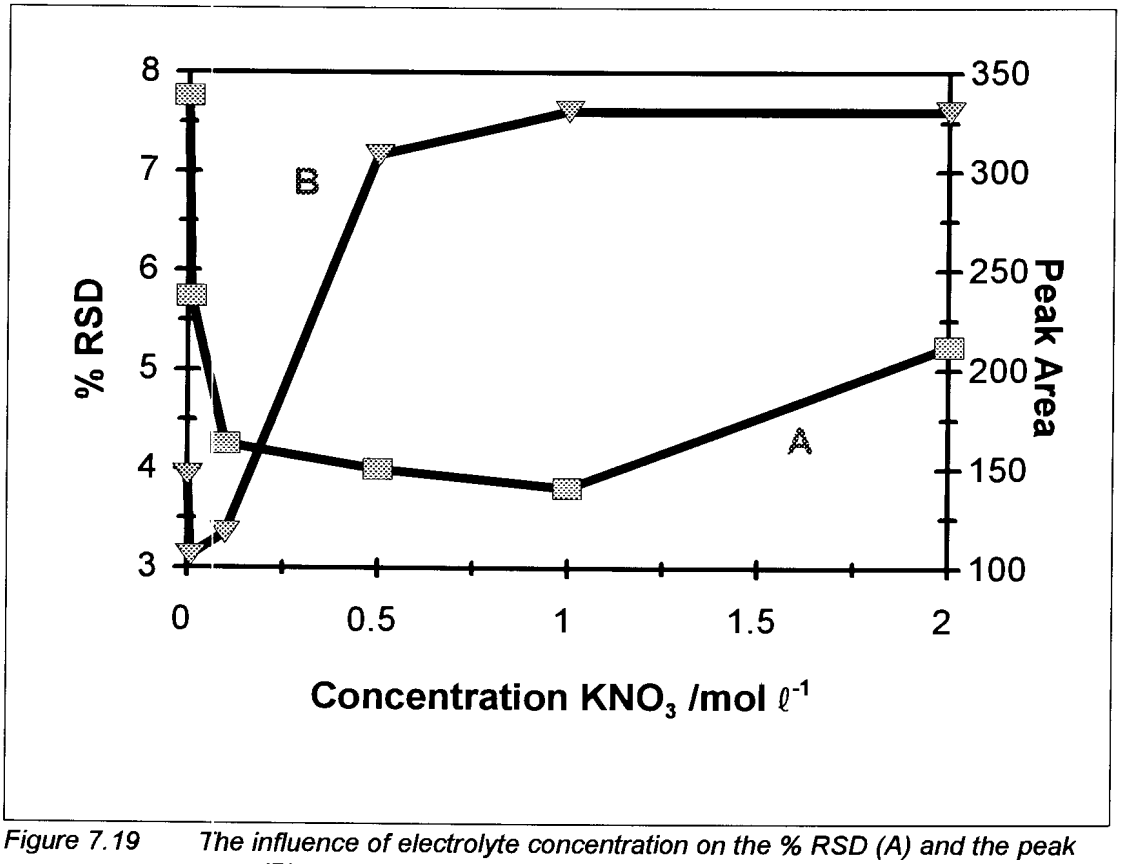

Figure 7.19 *The influence of electrolyte concentration on the % RSD (A) and the peak area (B).*

7.2.2.5.5 Interferences

The most common interferences in the determination of phosphate is Si(IV), Fe(III), Cu(II) and arsenate (AsO_4^{3-}) . [11, 25] What is of interest, was that by making use of the electrodialyser, all cationic interferences were removed. This only left us with the arsenate which was not present in the samples that were analysed.

7.2.2.5.6 Data and calibration of the optimised system

The optimised parameters for the proposed electrodialysis-FI-AAS analyser for the direct determination of phosphate with the molybdenum blue colour reaction were as follows:

- Flow rates of donor and acceptor channel: 0.80 mℓ min^{-1}
- Applied d.c. potential: 20 V
- Injection loop volume: 80 $\mu\ell$
- Minimum electrolyte concentration: 1 mol ℓ^{-1}

The performance of the proposed analyser was critically evaluated under the optimum conditions. The calibration graph was linear between 15 and 200 mg ℓ^{-1} with a relationship between peak area and phosphate concentration given by the equation;

$$y = 1.021x + 102.4, \qquad 7.4$$

where y = peak area and x = phosphate ion concentration in mg ℓ^{-1}.

A linear regression coefficient, the variance (r^2) of 0.997 (n = 11) was obtained over this concentration range. The number of runs per hour for the proposed system was 14. The detection limit was calculated to be 10.27 mg ℓ^{-1}, and the sample interaction as 0.0887%. The detection limit and the sample interaction was determined by making use of equations 7.2 and 7.3 respectively.

7.2.2.5.7 Samples

All samples were prepared in a 1 mol ℓ^{-1} KNO_3 solution. The following samples were analysed:

Sample 1	Shake 'n Grow Fern Food
Sample 2	Grokon Potplant Food
Sample 3	Wonder 3:2:1 (22)
Sample 4	Wonder African Violet Food

The results are depicted in Table 7.1. The fertilisers were dissolved in the electrolyte solution. The amount of fertiliser dissolved depended on the

distributer's note. The phosphate concentration after preparation was ca 70 mg ℓ^{-1}. The distributer's note only indicated the concentration of phosphorus. It can be seen from table 7.1, that all the concentrations obtained with the proposed method corresponded very well with the concentrations obtained with the standard method. For sample 2, it was found that the concentration of phosphate was far to low. The reason for this might be that the phosphorus was not in the ortho-phosphate form.

Table 7.1 *comparison of samples analysed by the proposed system and a standard method of analysis for phosphate.*

Sample	Phosphate concentration / mg ℓ^{-1} (Proposed method)	% RSD	Phosphate concentration / mg ℓ^{-1} (Standard method)
1_a	65.7	5.2	69.9
1_b	67.8	4.9	70.2
2_a	17.3	5.6	17.2
2_b	15.6	5.1	16.9
3_a	72.2	4.5	69.9
3_b	70.9	4.5	70.1
4_a	70.1	4.6	70.7
4_b	69.5	4.7	70.1

7.3 Conclusions

The direct method completely overshadowed the indirect method of phosphate analysis. It is very obvious that the direct determination of phosphate is much more liable for general use than the indirect method of analysis. Very high detection limit for the indirect method made it very difficult to defend this analysis method. High % RSD values for such high concentrations were unacceptable. Thus the sensitivity, precision and the sample throughput of the direct method was much more acceptable. The ease

of use and compatibility of the direct method was also much better than the indirect method.

Concerning the direct method, it was proven to be a very effective way for the determination of phosphate in water solutions. It exhibited a very wide linear response for the peak area versus concentration of phosphate. For this reason a wide range of phosphate concentrations could be analysed without prior dilution or pre-concentration of the sample.

In this Chapter it was also shown that the phosphate ion's drift speed can be changed by adding an electrolyte. By the addition of the electrolyte, the drift speed of the phosphate ion under the influence of the applied d.c. potential increased tremendously due to the fact that the viscous drag caused by the water molecules which encapsulated the phosphate ion. The addition of the electrolyte led to the partial decapsulation of the phosphate ion which led to lower viscous drag and higher drift speeds and thus also a better percentage dialysis.

By comparing the anions analysed with the electrodialyser, it can be seen that the phosphate system was far more superior to the chloride system (Chapter 4). The main reason for this lay in the development of the homemade de-bubbler. As is evident from the results from Chapter 4, the main problem that hampered the detection of the chloride was the gaseous products that were produced at the anode. For this reason it was not possible to work at optimum flow rates for the chloride as was the case with the phosphate.

7.4 References

a: Standard Methods (**1985**) Standard methods for the examination of water and wastewater. 16th ed. American Health Association, Washington.

b: Boolootain R.B., Stiles K.A., (**1981**) College Zoology, Macmillan Publishing Co., Inc., New York

c: Jeannette E., Watson R.N., (**1979**) Medical-Surgical Nursing and related physiology, W.B Saunders Company.

d: Bohinski R.C., (**1987**) Modern Concepts in Biochemistry, 5th ed., Allyn and Bacon Inc.

e: MacLaurin P., Worsfold P.J., Norman P. Crane M., (**1993**) Anal. Proc. 30(3): 134.

f: Shan Y., McKelvie I.D., Hart B.T., (**1993**) Anal. Chem. 65(21): 3053.

g: Spvakov B.Ya., Maryutina T.A., Shipigun L.K., Shkinev V.M., Zolotov Y. A., Ruseva E., Havezov I., (**1990**) Talanta. 37(10): 889.

h: Daykin R.N.C., Haswell S.J. (**1995**) Anal. Chim. Acta. 313(3): 155.

i: Carrer I., Cusmai P., Zanzottera E., Martinotti W., Realini F., (**1995**) Anal. Chim. Acta. 308(1-3): 20.

j: Benson R.L., McKelvie I.D., Hart B.T., (**1994**) Anal. Chim. Acta. 291(3) 233.

k: Benson R.L., McKelvie I.D., Hart B.T., Truong Y.B., Hamilton I.C., (**1996**) Anal. Chim. Acta. 326(1-3): 29.

l: Peat D.M.W., McKelvie I.D., Mathews G.P., Haygarth P.M., Worsfold P.J., (**1997**) Talanta. 45(1): 47.

m: Oshima M., Goto N., Susanto J.P., Motomiza S., (**1996**) Analyst. 121(8): 1085.

n: Motomiza s., Oshima M., (**1987**) Analyst. 112(3): 295.

o: Baba Y., Yosa N., Ohashi S., (**1985**) J. Chromatogr. 318(2): 319.

p: Harden S.M., Nonidez W.K., (**1984**) Anal. Chem. 56(12): 2218.

q: Coetzee J.F., Gardner C.W., (**1986**) Anal. Chem. 58(3): 608.

r: Stock D.J., (**1987**) At. Spectrosc. 8(1): 1.

s: Kokkonen P., Palko M., Lajunen L.H.J., (**1987**) At. Spectrosc. 8(3): 98.

t: Yakuta K., Sagra F., Yoshida I., Ueno K., (**1990**) Anal. Sci. 6(5): 711.

u: Van Staden J.F., Van Rensburg A., (**1990**) S. Afr. J. Chem. 43(3-4): 78.

v: Van Staden J.F., (**1991**) Talanta. 38(9): 1033.

w: Van Staden J.F., (**1995**) Frezenius'. Z. Anal. Chem. 352: 271.

x: Marshall G.D., Van Staden J.F., (**1992**) Anal. Instr. 20 79.

y: Pauer J.J., (**1989**) Die vloei-inspuitanalise van sekere determinante in oppervlak- en grondwater. MSc. dessertation. University of Pretoria.

z: Murphy J., Riley J.P., (**1962**) Anal. Chim. Acta. 27: 1431.

aa: Janse J.A.H.M., Van der Wiel P.F.A., Kateman G., (**1983**) Anal. Chim. Acta. 155: 89.

Chapter 8

Conclusions

As was indicated in Chapter 1, there is an ever increasing demand for better accuracy, lower detection limits, higher sample throughput and the need for automation. Flow injection analysis (FIA) lend itself perfectly to the fulfilment of these demands due to its versatility. FIA were used extensively with a variety of different detectors to fulfil some of the abovementioned requirements. To further improve the performance of FIA it was used in tandem with numerous sample modifying methods. Modifying in the sense of preconcentration, dilution, derivitisations, conversions and sample cleanup so that the detector is able to respond accurately in an acceptable response time. One of these in tandem methods was the use of a dialyser equipped with a passive neutral membrane. This FIA/dialysis tandem system was applied very successfully in automated sample dilution and cleanup systems. Dialysis, however, was found to be a very slow process which gave rise to unacceptably high detection limits. This then led to a tremendous decrease in the applications of passive dialysis systems in tandem with FIA. Since passive dialysis were so easily incorporated into FIA systems, means of circumventing the massive dilution factor, accompanied with passive dialysis, had to be found without reducing the extent of its advantages.

The proposed system kept the dialyser intact and only introduced electrodes in the donor and acceptor channel respectively. By applying a d.c. electrical potential across the membrane then increased the movement of ions from the donor to the acceptor channel. The reasons for the increase in the percentage dialysis from the passive dialyser to the electrodialyser were two fold.

The first reason was the increased concentration on the donor side of the passive membrane (in the case of the electrodialyser. This was due to the migration of ions under the influence of the applied d.c. electrical potential from the bulk of the donor

channel to the surface of the membrane (donor side). The ions accumulated as a thin, highly concentrated analyte layer which of course gave rise to a higher concentration gradient for diffusion across the membrane. In the case of the passive dialyser, the concentration gradient across the membrane was only due to the concentration of the analyte in the sample bolus. Thus the electrodialyser acted as a preconcentration method of the analyte in the acceptor stream which led to a higher concentration gradient across the membrane.

The second reason was the increased movement of ions across the membrane. The movement of ions across the membrane took place due to not only one force, but to two separate forces. The first force for the transport across the passive membrane was the concentration gradient whereas the second force was the electrical potential applied across the membrane.

It was found that the percentage dialysis increased from ca 7% in passive dialysis to over 90% in some applications (the proposed electrodialysis system). The dilution factor was reduced to a large extent. In the electrodialysis system it was possible to introduce controllable dilution without changing the surface area of the membrane. This was accomplished by changing the applied d.c. electrical potential to suit the specific need.

The advantage in the passive dialysis system of sample cleanup was retained in the proposed electrodialysis system. It was found that the electrodialyser was capable of discriminating against opposite charge (opposite in charge to the analyte) and neutral interferences. Interferences of opposite charge to the analyte migrated away from the membrane and were then kept in the donor channel. The interference from neutral species were diminished to a very large extent. Since the neutral species did not migrate under the influence of the applied d.c. electrical potential, the transfer of these species to the acceptor channel were minimal. Even though some neutral species could have diffuse to the acceptor channel due to the concentration gradient, the

transfer of analyte ions was far more superior to the transfer of neutral interfering species.

Comparison of the passive dialysis system to that of the electrodialysis system can be taken a step further. In passive dialysis, preconcentration of the analyte can be done only outside the dialyser unit. On the other hand, in the case of the electrodialyser, it was possible to preconcentrate the analyte in the dialyser unit itself. (The electrodialyser unit could thus be used as an analyte preconcentration tool). The reduction of a metal analyte ion made it possible to preconcentrate the analyte on the cathode in the acceptor channel. This led to a tremendous decrease in the detection limit of the system in which it was possible to reduce the metal analyte cation.

Unfortunately we are not living in the perfect world. Many problems arose with the development of the electrodialyser system, many of which we were able to reduce to certain extents.

The introduction of the electrodialyser unit into the FIA system was very troublesome. Tremendous problems were experienced with the initial development of the electrodialyser unit and the initial introduction thereof into the FIA system. Choices were to be made of types of electrode- and electrodialyser unit materials. Experiments were done on the physical dimensions of the electrodialyser unit. Changing and fitting of the membranes and the cleaning of the electrodialyser unit took very long periods of time. Due to reactions that took place at the electrodes during analysis, erosion of the electrodes took place. Small particles of the electrodes led to blockages of the FIA system and sometimes also interfered in the detector. The blockage problem forced the use of larger than necessary couplings to the electrodialyser unit which led to increased dispersion.

One of the first problems encountered was in the use of electrochemical detectors with the electrodialyser unit. The use of electrochemical detectors showed very poor

results. No matter how well the electrodialyser unit was grounded, interferences occurred in these type of detectors. Low precision and large baseline drift was experienced. This reduced the versatility of the FIA/electrodialysis system to a large extent.

Another problem encountered was the formation of gaseous products at the electrode in the acceptor channel. These gaseous products caused major problems in the UV/Vis spectrophotometric detectors and to a lesser extent in the Flame atomic absorption spectrometer. This necessitated for higher than optimum flow rates in the dialyser unit which led to higher dilution of the dialysate in the acceptor channel, lower mass transfer rates and in the long run higher detection limits and a poor precision. Even though the homemade de-bubbler used, removed much of the gaseous products, it did not solve the problem completely. The de-bubbler had a slow-moving stream area (to allow the gas bubbles to separate from the liquid) which increased the dead volume and of course led to an increased dispersion.

In conclusion one can make the following comments: The newly developed electrodialysis system can be introduced into a laboratory for routine analysis. Full advantage must be taken of its superior application (superior to passive dialysis) in FIA systems. Care must however be taken to minimise factors leading to dispersion of analyte samples. Time must also be allowed for the development of each individual application.

Addendum A

Method Construction

Automisation and automatic instrumental development is of utmost importance in analytical chemistry. For this reason all experimental work done in this project was fully or partially run by a computer. The software package used was the FlowTEK programe which was specifically developed for flow injection analysis and sequential injection analysis by Marshall. [1] To explain the use of the FlowTEK program, as it was used in the experimental work of this flow injection project, experimental setup for the determination of copper in multivitamins (described in Chapter 5) was chosen. All technical data concerning the FlowTEK program can be obtained from the operation manual. [2]

As is evident from Figure 5.3, each run (or analytical sample measurement), consisted of an electrodialysing and a detecting step. The runs were separated from each other by a rinsing period of 60 seconds. The devices operated from the FlowTEK program was one peristaltic pump, two injection valves and a flame atomic absorption spectrophotometer (FAAS). (Even though two pumps were used in the experimental setup, the one pump (Pump 1, Figure 5.3) was never switched off and therefore there was no need to couple it to the computer) Following are the steps taken for the setup of the FlowTEK program before use in the experimental work.

A1 Setup of the FlowTEK program for device control and data collection

A1.1 Detector

The FAAS detector used gave maximum output at zero absorbance. For this reason the detector setup, in the FlowTEK program had to be changed from the default setting. (Default setting converts the peak directly as the signal is received from the detector, thus maximum output from the instrument will be at a peak maximum). The setting was done

as follows:

From the main menu select *Setup* (S). From the *Setup* menu select *Detectors* (D). The questions and demands which follow must be answered in the following way:

Enter number of detectors:	1	
Enter signal transformation for detector:	I	For inversion of the signal.
Enter analog input point for detector:	1	Indicate the position where the detector is coupled to the distribution box.

In the distribution box, the signal from the detector was set to be amplified 100x and the baseline was set by using the adjusting screw. Direct conversion of the signal could be monitored by using the hotkey F4.

A1.2 Pump and injection valves

The operation of the pump and the injection valves were managed by making use of a method. The detection electrodialysis and the detection step both were incorporated into the method constructed.. The method was constructed in the following way:

From the main menu select *Method* (M). First the devices used in the construction of the method must be identified. From the *Method* menu select *Type device* (T). Answer the following questions and commands:

Enter number of devices:	3	The pump and the two injection valves.
Enter type device 1:	GP	Gilson pump.
Enter digital output point for GP:	1	Indicates the position of connection of GP on the

		distribution box.
Enter type device 2:	IV	Injection valve.
Enter digital output point for IV:	3	
Enter type device 3:	IV	
Enter digital output point for IV	5	

After entering the above mentioned, the screen will divide itself into three horizontal columns, each representing one of the devices in the method of construction. At this moment there is a yellow straight line in each of the columns. At present this yellow line indicates that the Gilson pump is in the "off" position and the two injection valves are in the "load" position. At this point in time the experiment time has to be specified. To do this, in the *Method* menu, select *Expt time* (E) and answer the questions following:

Enter time to start data collection:	120
Enter experiment time:	190

Now only can the specific actions of the devices be entered. There are two ways by which it can be done. In the first way, by making use of the curser, the **Num Lock** key must be deactivated. At this stage a small green coloured square will be flashing in the bottom right corner of the screen. Hit any one of the arrow keys and the cursor will appear. Use the cursor to the column of the device in question and align it with the time for the change of a specific event. Example: Move the cursor to the top column (indicated GP on the right hand side of the screen). Align it with time 0 and enter. This time is now marked. From the *Method* select *Insert* (I) and answer the question to follow:

Enter event (FRO):	F	F indicates forward, R indicates reverse, O indicates off.

An event that was introduced previously can also be deleted in the same way. Instead of selecting *Insert* from the menu, one has to select *Delete*.

A better way of introducing and deleting events is to activate the **Num Lock** key. At this point a red square will flash in the bottom right hand corner of the screen. To insert an event select *Insert* (I) from the *Method* menu and answer the following questions: (The example to follow is for the insertion of an injection command for the first injection valve)

Enter device No:	2	
Enter time of event:	0	
Enter event (IL)	I	I indicates inject and L indicates load.

Various events were inserted to fulfill the requirements of the experiment in question. After the construction of a method, the method has to be saved. This is done by selecting the *File* (F) on the *Method* menu and answer the question:

Save, Retrieve or Erase (SRE):	S
Enter method file name:	c:\Temp1\data\Cuopt1.met (.met indicating a method file)

The method is now finished and the screen for the constructed method should look like Figure A.1

This method can now be used either directly or in a "procedure". (The creation and use of a procedure will be discussed)

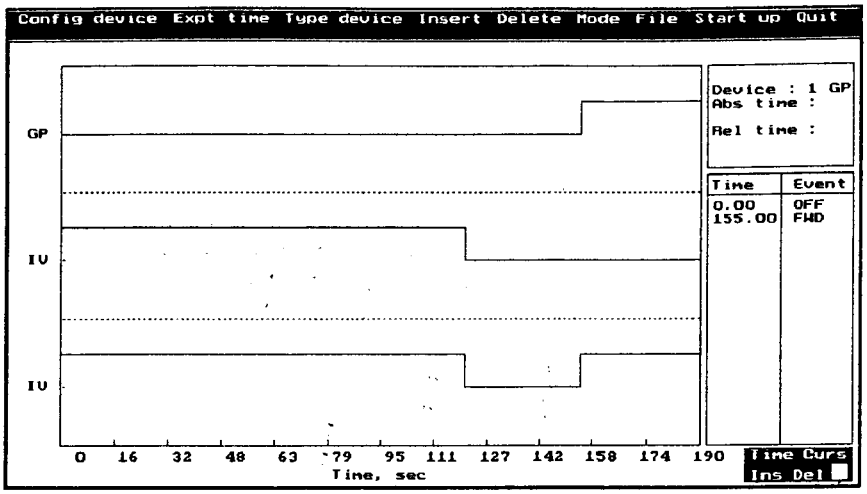

Figure A.1 *Method screen after the completion of a method.*

A2 The use of the FlowTEK program for device control and data collection

The method constructed in paragraph A1, can be applied directly or can be build into a procedure. For the direct application press *Once* (O) on the *Main* menu and the program shall run the method once. The method can be build into a procedure for repetitions of the same method or use it in conjunction with other methods. The procedure used was build as follows:

From the *Main* menu select *Repeated* (R). From the *Repeated* menu select *Build Proc* (B) and answer the following questions and commands:

Enter procedure file name:	c:\Temp1\data\Cuopt1.pdr (.pdr indicates a procedure file)
Enter procedure or method file name:	c:\Temp1\data\Cuopt1.met
Enter number of repetitions:	1
Enter procedure or method file name:	Wait
Enter time to wait (in sec)	60
Enter procedure or method file name:	c:\Temp1\data\Cuopt1.met

Enter number of repetitions: 1

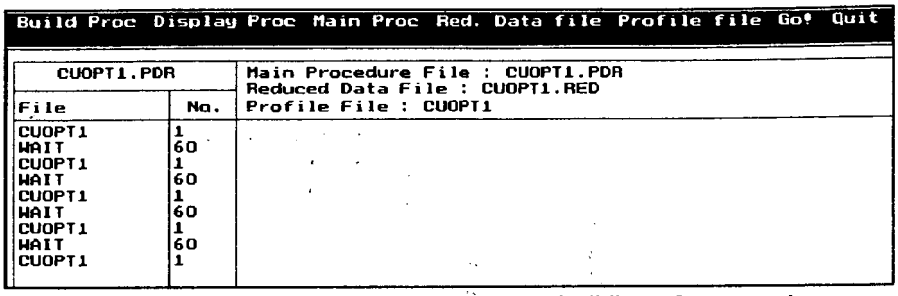

Figure A.2 *Repeated screen after of the building of a procedure was completed.*

This procedure can be build as to the number of repetitions of the above cycle required. The procedure indicated in Figure A.2 consisted of fife repetitions of the method, each separated by a 60 second rinsing period.

To terminate the definition of a procedure, use the **ESC** key. Hereafter the main procedure must be selected. This is the file that will be used to execute the experiment (that is the procedure just built). In the *Repeated* menu, select *Main Proc* (M) and answer the following command:

Enter main procedure file name: c:\Temp1\data\Cuopt1.pdr

The option *Red. Data file* on the *Repeated* menu selects a reduced data file for saving all the experimental information. Select *Red. Data file* (R) on the *Repeated* menu and answer the following command:

Enter reduced data file name: c:\Temp1\data\Cuopt1.red

The option *Profile file* on the *Repeated* menu selects the file root name for storing the profile data. The name extension gives the number of the experiment number.

To execute the main procedure select the option *Go!* (G) on the *Repeated* menu. To abort the main procedure press **ESC**.

After the optimisation of the experimental parameters, use can be made of the calibration function of the FlowTEK program. (This option was not used in the experiment and therefore imaginary values are used) This can be done as follows:

On the *Main* menu select *Calib* (C). On the *Calib* menu select *Setup* (S) and answer the questions following:

Enter no of calibration standards:	5
Enter no of replicates for each standard:	1
Enter concentration units:	mg/l
Now enter the different concentrations	
Enter reduced data file name (ESC for manual input):	ESC

On the *Calib* menu select *Pk param* (P) and answer the commands or questions to follow:

Enter peak parameter (H A W T):	A
Std to edit (1-5; 0 for all; ESC):	0

Enter the responses. In this case the responses were manually entered but it is also possible to do it via the reduced data file. It was found to be easier to do it manually since the program cannot discriminate against any shooters out.

Enter the calibration model (L Q T E H A):	L

The calibration file was saved by selecting *File* (F) on the *Calib* menu.

Save, Retrieve or Erase (S R E):	S

Enter calibration file name: c:\Temp1\data\Cuopt1.cal

Figure A.3 is an indication on how the screen will look like after the setup of the calibration file.

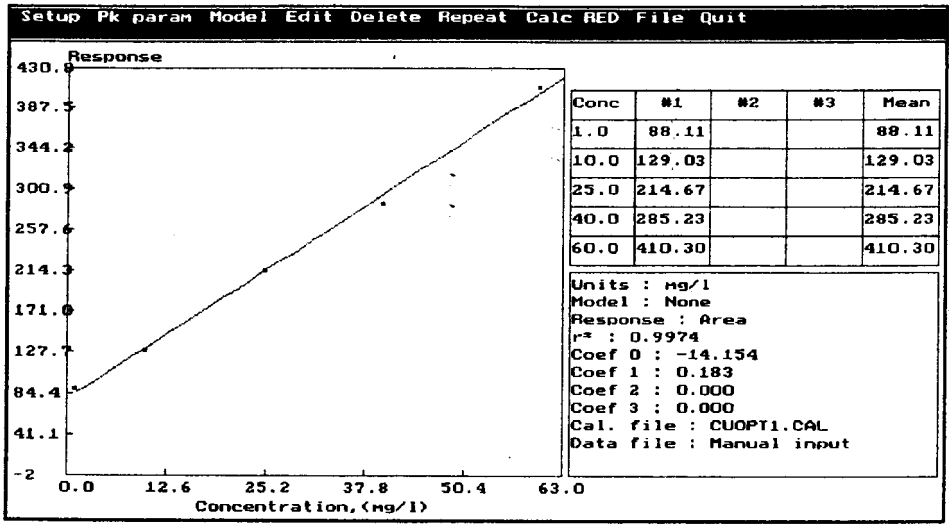

Figure A.3 Calib screen after setup of calibration.

All device descriptions can be viewed under the *Notepad* menu. This menu can be obtained from the *Main* menu by selecting *Notepad* (N). The notepad consist of two pages. For the purposes of the experimental work done, the second page was not needed. If needed however, type **N** on the *Notepad* menu. Figure A.4 is the *notepad* screen for the experiment done.

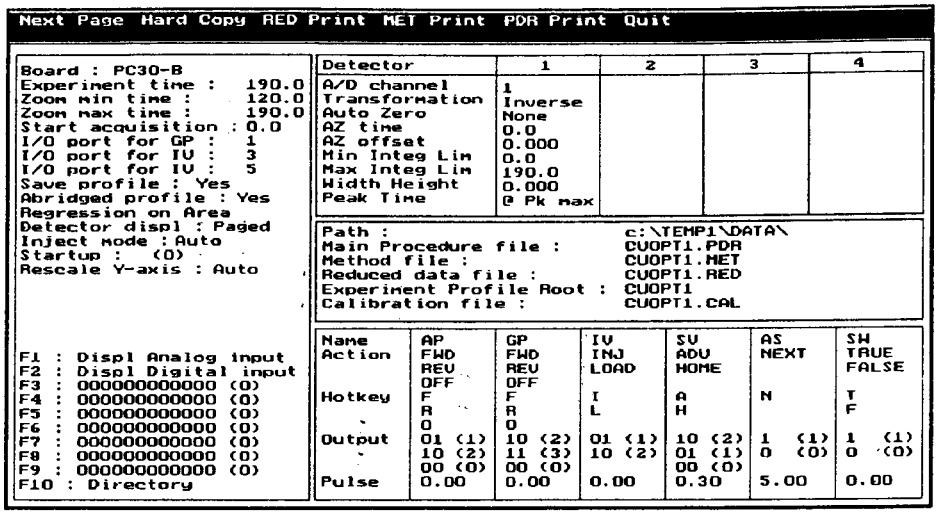

Next Page Hard Copy RED Print MET Print PDR Print Quit

Board : PC30-B
Experiment time : 190.0
Zoom min time : 120.0
Zoom max time : 190.0
Start acquisition : 0.0
I/O port for GP : 1
I/O port for IV : 3
I/O port for IV : 5
Save profile : Yes
Abridged profile : Yes
Regression on Area
Detector displ : Paged
Inject mode : Auto
Startup : (0)
Rescale Y-axis : Auto

F1 : Displ Analog input
F2 : Displ Digital input
F3 : 000000000000 (0)
F4 : 000000000000 (0)
F5 : 000000000000 (0)
F6 : 000000000000 (0)
F7 : 000000000000 (0)
F8 : 000000000000 (0)
F9 : 000000000000 (0)
F10 : Directory

Detector	1	2	3	4
A/D channel	1			
Transformation	Inverse			
Auto Zero	None			
AZ time	0.0			
AZ offset	0.000			
Min Integ Lim	0.0			
Max Integ Lim	190.0			
Width Height	0.000			
Peak Time	@ Pk max			

Path : c:\TEMP1\DATA\
Main Procedure file : CUOPT1.PDR
Method file : CUOPT1.MET
Reduced data file : CUOPT1.RED
Experiment Profile Root : CUOPT1
Calibration file : CUOPT1.CAL

Name	AP	GP	IV	SV	AS	SW
Action	FWD	FWD	INJ	ADV	NEXT	TRUE
	REV	REV	LOAD	HOME		FALSE
	OFF	OFF				
Hotkey	F	F	I	A	N	T
	R	R	L	H		F
	O	O				
Output	01 (1)	10 (2)	01 (1)	10 (2)	1 (1)	1 (1)
	10 (2)	11 (3)	10 (2)	01 (1)	0 (0)	0 (0)
	00 (0)	00 (0)		00 (0)		
Pulse	0.00	0.00	0.00	0.30	5.00	0.00

Figure A.4 Notepad screen.

A3 References

1. Marshall G.D., Van Staden J.F. (**1992**) Anal. Instrum. 20: 79.
2. FlowTEK Reference Manual,(**1993**) Device Control and Data Acquisition software. Version 1.1. Mintek.

Addendum B

Correspondence resulting from this project

Publications:

1. Incorporation of electrodialysers into the conduits of FIA systems. Enhancement of the mass transport of chloride anions through passive neutral membranes. **Talanta** 45 (1998) 485-492.
2. Incorporation of electrodialysers into the conduits of FI/AAS systems . Determination of copper(II) ions in multivitamin tablets after enhancement of mass transfer through a passive neutral membrane. **Journal of Analytical Atomic Spectrometry** 13 (1998) 23-28.
3. The determination of zinc in pharmaceutical products using an electrodialyser incorporated into a flow injection system. **Fresenius' Journal of Analytical Chemistry**. (In press)
4. The direct determination of phosphate in fertilisers. (Submitted)
5. The indirect determination of phosphate (Submitted)

Conference proceedings:

1. SACI, Cape Town, South Africa (January 1996) One poster.
2. Euroanalysis (IX), Bologna, Italy (September 1996) One poster.
3. ICFIA'97, Orlando, Florida, USA (January 1997) One poster.
4. Flow Analysis (VII), Piracicaba, Brazil (August 1997) One poster.
5. Euroanalysis (X), in Basel, Switzerland (September 1998) Oral presentation.
6. SCAR (Romanian Society of Analytical Chemistry) (XIV), Pietra Niamţ, Romania (September 1998) One poster.
7. Analytica' 98, Midrand, South Africa (October 1998) One oral presentation and one poster.

Addendum C

Legend of Symbols

R	resistance / membrane mass transfer resistance / gas constant
A	area
ρ	resistivity
κ	conductivity
S	reciprocal ohm
Λ_m	molar conductivity
c	molar concentration
Λ_m^0	limiting molar conductivity
ν	number of ions per formula unit
λ	molar conductivity of either cat- or anions
α	degree of ionisation
J	Flux
D	diffusion coefficient
N	number density
$\Delta\phi$	potential difference
E	uniform electric field
ℓ	length or distance
Γ	frictional force / force
f	friction coefficient
s	speed
η	viscosity
a	radius / activity
u	mobility of an ion / convective flow
z	sign of the charge

e	elementary charge
t	time interval or transport number
N	Avogadro's number
F	Faraday's constant
I	current
V	volume
ε	electric permittivity / surface porosity / fraction of pores/pore area ratio
T	temperature
w	work required
D	diffusion coefficient
v	velocity or diffusional flow
P	probability / permeability
d	distance
ΔX	gradient potential across a membrane
n_p	number of pores
τ	pore tortuosity
A_m	membrane area
x_i	mole fraction
Δx or ℓ	membrane thickness
S	solubility
k_d	Henry's law constant
b	hole affinity constant
c'_h	saturation constant
m	reciprocal friction
D_T	thermodynamic diffusion coefficient
N_0	number of particles at time t = 0
v	velocity/diffusional flow
K_i	solubility constant

P	pressure
$\Delta\mu$	chemical potential difference
ΔF	electrical potential difference
γ	activity coefficient
k_d	Henry's law constant
m	mobility coefficient
D_T	diffusion coefficient